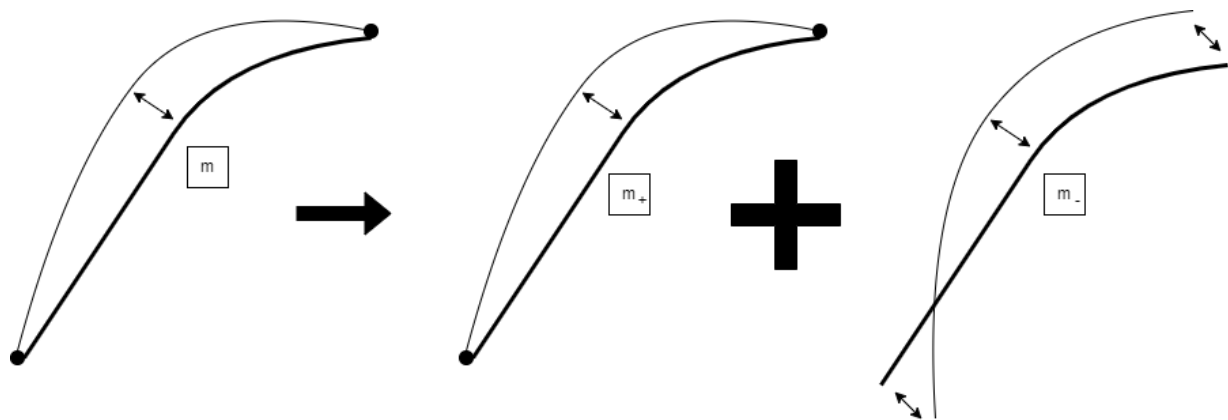# Mimicking of Non-conservative Systems

Demonstration of a generalized method for applying the mimetic spectral element method to non-conservative systems

Ibrahim Ouerghi

TUDelft

Mimicking of Non-conservative Systems

Demonstration of a generalized method for applying the mimetic spectral element method to non-conservative systems

by

Ibrahim Ouerghi

to obtain the degree of Master of Science
at the Delft University of Technology
to be defended publicly on Friday November 24, 2023 at 2:00 PM

Studentnumber:	4019598
Thesis committee:	
Chair:	Dr. R. P. Dwight
Supervisor:	Dr. ir. M. I. Gerritsma
External examiners:	Dr. A. Jamshidnejad
	Dr. A. Palha
Place:	Faculty of Aerospace Engineering, Delft

An electronic version of this thesis is available at http://repository.tudelft.nl/.

Faculty of Aerospace Engineering · Delft University of Technology

Acknowledgements

"... My success comes only through Allah. In Him I trust and to Him I turn." Surah Hud:88.

"He who does not thank people, does not thank Allah." Prophet Muhammad peace be upon him

Abstract

The mimetic spectral element method is a relatively young method in numerical solutions of partial differential equations and actions that describe physical systems. Its advantage is that it takes the geometrical structure of the problem into account which guarantees consistency of the numerical scheme and the conservation of relevant quantities. This prohibits the solution to diverge into non-physical states since the discretization mimics the physical behaviour of the problem. With relation to physics the mimetic method makes use of the stationary action principle which contains all information about the system and reduces the continuous variables to discrete ones that become ready for computation. The stationary action principle requires a formulation of the Lagrangian such that it implies Newton's laws of motion or equivalent physical laws. However these Lagrangians are only easily formulated for monogenic systems. This work investigates the class of (discrete) non-monogenic physical systems. The goal is to present a general method to numerically mimic non-conservative systems such that energy (loss) is exact. This is done by modifying a newly introduced systematic method that transforms the non-conservative problem to a system with a doubled degrees of freedom that makes it a conservative or monogenic one. In this modification process new degrees of freedom are introduced which are allowed to have arbitrary variations at the initial and final states of the new action. The system can than be mimicked with the spectral element method where algebraic dual polynomials are used as both approximating polynomials and as test functions that serve as arbitrary variations. Furthermore a gauge transformation is introduced by the modified action such that it contains the initial and final states of the system to make the solution unique. The introduced method is generally applicable to Lagrangian mechanics of discrete systems with holonomic constraints. The method is applied to the damped harmonic oscillator (DHO) as a test case. The computational results are clearly accurate and converging. However they deviate with one order from the h-refinement spectral element theory of Gauss-Lobatto-Legendre interpolation basis polynomials. Theoretical analysis of the equations of the mimicked (single and doubled) DHO show that energy (loss) is exact. Nevertheless, the computations show an oscillation in energy that remains closely around the conserved value. This oscillation in energy in time was observed in earlier works that applied the mimetic spectral element method to conservative systems. The reason behind this behavior of energy remains a topic for further research. Furthermore, in a follow up research the method can be extended to the Lagrangian field theory and tested with simplified non-conservative fluid problems to verify it for fields.

Contents

List of Figures

1

Introduction

Listening to Andrés Segovia's guitar play or enjoying a piano solo by Martha Argerich fills our spirit with energy and pleasure. We can hear the sound of the vibrating strings freely fade away after they are hit masterfully by the old hand. This nice feeling of "spiritual" energy that we experience is caused by the behaviour of physical energy in the musical instruments. The musical characteristics of the sound waves decide how the energy dissipates out of the strings. Small amplitude vibrations have a rate of change of energy that is proportional to the energy that is entered into the string [1]. Mainly due to frictional forces in the instrument these chosen sounds die away to give other ones a new life that we can enjoy again. This is an example of energy dissipation effects which occur practically in every macro physical system. Whenever the configuration of a macro system changes, some of the energy gets dissipated out from kinetic energy to heat. Energy dissipation is itself an example of a non-conservative effect in classical mechanics. To know the state of a non-conservative system the information of what happened during the path must be known, it is not solely the initial and final configurations that determine the state of the system. This thesis will investigate a way of numerically describing non-conservative systems such that the conservation laws are exactly maintained.

1.1. Motivation and Objective

It comes without a need for explanation how important numerical simulations are in engineering practices. These numerical simulations are generally lower in cost compared to experiments and so are used extensively along side them in the design process. However a major problem with the current widely used numerical methods is that they do not take over the structure of the continuous physical equations exactly. This creates fundamental errors such that the energy will not be exactly conserved. To make up for this discrepancy, recently new methods have been introduced that try to preserve the structure of the physics as much as possible. One of these is the mimetic method which relies on mimicking the geometry of the continuous system with a discrete one that is numerically solvable. By taking the geometry of the physical variables into account the physical laws can be faithfully represented at the discrete level. By doing this the consistency of the discrete system is ensured whenever the partial differential problem is well defined. Furthermore in classical numerical methods stability of solutions, such that they does not diverge over a longer time period, can be related to the geometry of the variables in the system of equations.

To apply the mimetic method to a physical system the principle of stationary action can be used. The action contains all the information that is to be known about the system. However the classical conservative theory of this principle does not account for many of the processes that occur in practice. These processes are called non-conservative processes where for instance energy dissipates due to damping in a vibrating string or due to viscous friction in a fluid. Furthermore non-conservative systems are time related and time related methods are barley implemented in the mimetic method. Since the mimetic method aims to preserve the physical conservation laws, it can be now put to the test where physical systems are characterized by their energy dissipating behaviour. Thus by this work the main aim is to find and investigate a method that systematically obtains actions of non-conservative systems which are compatible with the mimetic spectral element method that uses algebraic dual polynomials. This procedure will be applied to the damped harmonic oscillator as a test case. The main question that this thesis answers is:

”**Can we find a systematic procedure to apply the mimetic spectral element method using algebraic dual polynomials to non-conservative systems such that energy conservation is exactly satisfied?**”

To answer this main question it is reformulated in the following sub questions that need to be answered:

- What is a systematic method for obtaining Lagrangians of non-conservative systems for the formulation of actions that are suitable for the mimetic method with algebraic dual polynomials?

- Does this method give accurate results when applied to the case of a damped harmonic oscillator?

- Does this method satisfy the law of energy conservation exactly?

The following section will give a flow overview that describes the steps of how this thesis answers the posed questions.

1.2. A Road Map of the Thesis

Below in Fig. 1.1 is an overview the road map of the thesis.
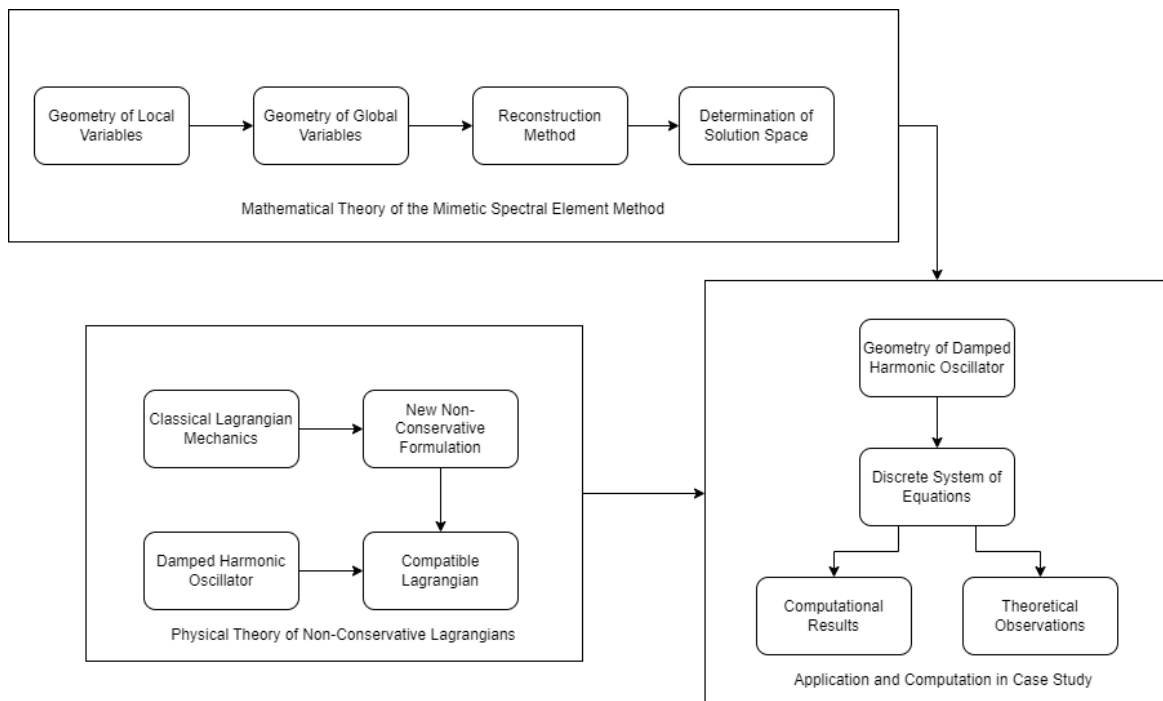
Figure 1.1: The layout of the thesis

<div align="right">

2

</div>

Mathematical and Physical Background

This chapter presents the existing mathematical background that this thesis is built on to obtain the numerical simulation required for answering the research questions. The chapters of this part start with a historical overview of how the mimetic method came to be in 2.1. An introductory Section 2.2 gives reasons for looking at the geometry of the problem. This is followed by a preliminary treatment in Section 2.3 of the mathematical formalism for describing geometry that will be used when addressing the physical problems. Section 2.4.2 explains the mathematics behind discretization of the the domain and of the physical variables for the mimetic method. The approximation polynomials are treated in Section 2.5 introduces the approximation functions and what there roll is in the discretization process. This is followed by Section 2.6 on how to formulate Lagrangians, energy and actions in classical monogenic mechanics and a section on generalization of to non-conservative mechanics in Section 2.7. This is followed by chapter on the theory of calculus of variations which is used to obtain the formulation of the stationary solution. It includes a part on the identification of the solution spaces and how to measure the error of the approximate solution with respect to the exact one. Finally the theory of harmonic oscillators is then summarized in Section 2.9.

2.1. History of the Method

Due to the use of classical vector calculus, numerical simulations that are obtained through to classical discretization techniques do not (necessarily) specify the geometric structure of the field variables. Also, and oftentimes as a consequence, the balance laws from the local description of continuous partial differential equations are not carried over in the discretization and approximation. The mimetic method has as an advantage that it relates the variables to geometric forms that mimic the actual observed laws over any subspace in the computational domain. This requires mainly the introduction of the use of two mathematical fields: exterior calculus (from differential geometry) and algebraic topology. Exterior calculus associates geometry to the physical variables so that the continuous functions can be integrated on a discretized domain. Algebraic topology is the tool that expresses the relation between the discretized (integrated) physical objects such that the local relations between the forms in exterior calculus remain maintained between the discrete chains.

The algebraic relations in exterior calculus, i.e. exterior algebra, were introduced as a subfield in linear algebra by Hermann Grassman in his 1844 book. After the introduction of the exterior derivative by Elie Cartan, together with Grassman's exterior algebra, this so called exterior calculus has become an advantageous alternative to the standard formalism of vector calculus. In 1895 Henrie Poincaré started algebraic topology through the introduction of homology and homotopy. These above were the fundamental mathematical groundwork that eventually characterized the mimetic method.

As mentioned the mimetic method applies results from the above disciplines to numerically solve differential equations. Enzo Tonti [2] decomposed the equations of physical theories in definition equations, balance equations and constitutive relations. Important conclusions on the structure of the operators of the balance equations resulted from this. Furthermore, Josef Dodziuk [3], by looking at the relations between the objects in a discretized domain, noticed the existence of a discrete Hodge that is an approximation

of Hodge's theory of continuous forms. The importance of the Hodge is that it represents the place of constitutive relations in the physical theories.

A pioneering work in setting up and defining the required operators for the scheme of this framework was an unpublished paper by Hyman and Scovel [4]. Furthermore in his Japanese papers [5] Bossavit showed the importance and advantage of the geometrical method through theoretical application to electromagnetism. In another paper Bossavit et al.[6], showed that discrete operators following from the partial differential equations by using the geometrical method can be separated in exact topological and approximate metric ones. Amongst other works these results gave the method a jump forward where-after many works appeared that progressed the method. A number of these, but definitely inexhaustive, are Arnold et al. [7], Kreeft and Gerritsma [8] and Robidoux and Steinberg [9]. The method has been applied to different cases and proved its reliability. In this thesis a specific way of interpolation, with algebraic dual polynomials [10], within this method is used. (Some of) these polynomials have been applied to multiple studies. Amongst many, cases like Stokes flow [8], potential flow [11], diffusion [12], Hamiltonian and time related systems have already been studied [13]. Generally however, cases where the process are non-conservative have not been fully investigated yet.

2.2. Why Bother About Geometry?

When we go about constructing models for the behaviour of physical phenomena we often look at two kinds of limits. We conceptualize physical variables and their rate of change at a local point. A simple example of a local physical variable and a local rate of change are the pressure and the velocity respectively. This mathematical limit formulation is a standard manner of describing the physical phenomena, even when the measurement values themselves are global and not infinitesimal in nature. That means that we measure pressure from force distributed over some finite measurable area and velocity as the global displacement over some finite measurable time change. So these measurements are performed in a finite domain where physical variables are related to observable geometrical objects, like areas and lines, instead of limits that are only related to local points. Actually, from these observed measurements we come up with the physical laws. The relations found in these measurements are later transformed to the familiar partial differential equations (PDEs) where the limiting appears. However these can only be analytically solved for specific or simplified cases. The complicated situations can only be approached using numerical computational schemes of the PDEs. Tonti [14] suggests to directly construct discrete mathematical relations since these reflect the way we observe physical reality (which seams to be a consistent reality). This is because we only measure global variables, and additionally our measurements are never exact in their precision.

The different conservation laws that dominate the physics and are formulated in the language of the limit process in mathematics are abstractions of the laws extracted from global and discrete physical observations. Thus formulations like divergence or curl of a field yielding zero are actually limiting processes of some integral value on a volume or surface under regularity conditions. These global physical variables are thus associated with geometric spaces that have an orientation. In a later section, 2.4.2, the geometry of these objects and their orientations will be explained. Besides this essential observation, Tonti [14] mentions some other important notions that must be considered when working in the discrete setting. They can be found in the aforementioned source and are all geometric in nature. This highlights the importance of understanding the geometry behind the PDEs construction.

Global variables can be related to each other through exact topological relations. This can be done through the coboundary operator as will be shown in Section 2.4.2. Naturally geometric objects have dual objects that have a dual orientation. When the orientation of a physical variable is changed in the discrete setting from an explicit primal form to an implicit dual form, a metric operation is introduced that relates them to each other. The relation involved has a constitutive relation combined with it where the approximation of the material properties can be implemented [9]. The transformed physical variables are than associated to a different lay out of the domain, also known as a dual (or primal) grid. Robidoux [9] shows how this can follow from standard vector calculus if the geometries are properly tracked. Mimetic numerical methods do this naturally through the tools of exterior calculus. Besides looking for approximation in the right function vector spaces they mimic the geometry of the physics behind the differential equation [8]. This is exactly like the idea of Tonti because it starts with a geometrical approach that mimics the geometry of physical measurement.

As mentioned before early work by Tonti [2] shows that equations of a large chunk of physical theories can be divided in three fundamental parts. These are divided in the constitutive, definition and balance equations parts. It can be shown that the balance parts and definition parts, when in the discrete setting, are also exact through the topological relations. This follows from the use of exterior calculus which keeps track of the geometry and from algebraic topology which translates this track keeping to the global discrete variables. This results in keeping the structure of the differential equation and this preserves its convergence properties [7]. Furthermore, this geometry mimicking procedure maintains the conservation properties both pointwise and over every cell in the computational domain.

2.3. The Geometry Behind the Physics

As discussed previously the physical quantities that are measured are not local but are associated with a variety of geometric objects. Geometrical objects are classified by having dimensions, absolute values, directions and orientations. These concepts are captured in the language of exterior calculus. In contrast to classical vector calculus, exterior calculus always keeps track of the geometry involved in the different mathematical operations. It holds also that the operators of exterior calculus are more convenient in their use. For instance expressions don't change depending on the coordinate systems, cartesian or curvilinear, and the associativity holds for wedge product in contrast to the cross product [15, p. 42]. The following section gives an overview of where forms that discribe physical variables come from and an introductory description of exterior calculus as the tool that works with them. For more exhaustive works look for instance at [16]. Furthermore the De Rham complex, which is a tool from algebraic topology that classifies the relations between these forms, is introduced.

2.3.1. Origins of the Geometrical Objects

Exterior calculus makes use of forms and tangent vectors. These objects, also known as (exterior) co-vectors and vectors, follow from the definition of a smooth manifold. A manifold consists of patches of spaces that are similar to an n-dimensional Euclidean space [17]. In the Euclidean setting a metric gives the notion of length and angels [15]. Even though manifolds can be embedded in a larger Euclidean space [18], there is no need for a metric to be defined on the manifold itself since it can be defined intrinsically. Since forms are defined on manifolds with no metric structure it is possible to have relations between the forms, like the exterior derivative, that are only topological in nature [15, p. 43].

By defining locally smooth curves on a manifold $\mathcal{M}$, tangent vectors can be assigned to the manifold's points. The set of all tangent vectors at a point spans a tangent space $T_p\mathcal{M}$ out of the point. The union of all tangent spaces on the manifold is the tangent bundle $T\mathcal{M}$. A famous result from linear algebra is that any vector space has a dual vector space. The union of these co-vector spaces $T_p^*\mathcal{M}$ over all points is the fibre bundle of co-vectors, also known as the cotangent bundle $T^*\mathcal{M}$. A cotangent space can actually be constructed from a basis consisting of derivatives of functions that map the manifold patches to Euclidean spaces, namely derivatives of the charts. These derivatives act as functionals on the tangent vectors such that they form a homomorphism from the intrinsic tangent space to the identity on real values [19]:

$$T_p^*\mathcal{M} \equiv Hom(T_p\mathcal{M}, \mathbb{R})$$

Suppose $x^i(p)$ is the component of a coordinate chart, i.e. a map that assigns the i-th coordinate in Euclidean space to a selected point on the manifold. A derivative of this map, with respect to a coordinate chart component, is a functional from the tangent vector space to real values. When the derivative of a coordinate coordinate chart component, $dx^i(p)$, acts on a tangent vector along a coordinate component, $\alpha^j \frac{\partial}{\partial x^j}(p)$, it gives α^j and else zero. Also every tangent vector can be formed by a linear combination of basis vectors along $(n-1)$-constant coordinate curves and and to every basis vector there belongs a corresponding chart derivative. From this we conclude that there is a basis of the tangent vector space, namely vectors along the coordinates lines, and a basis of its dual co-vector space which consists of the chart derivatives. They are both canonical and have n-dimensions. These canonical basis vectors thus satisfy the Kronecker delta property [19]:

$$dx^i(p)\frac{\partial}{\partial x^j}(p) = \delta_j^i \quad \forall i,j \in 1,\ldots,n$$

An amount of co-vector spaces at a point, say r, can be joined together with Cartesian products to form a new space. The same can be done for s tangent vector spaces. The Cartesian product of these two again forms a new space shown in equation (2.1). The union of these spaces $T_r^s\mathcal{M}$ on all points of the manifold is a again fibre bundle.

$$T_{rp}^s\mathcal{M} = (T_p^*\mathcal{M} \times \ldots \times T_p^*\mathcal{M}) \times (T_p\mathcal{M} \times \ldots \times T_p\mathcal{M}) \tag{2.1}$$

A section of a bundle is a smooth selection of co-vectors at all points of the manifold. When a section, $\Gamma T^s_{rp}\mathcal{M}$, of a bundle is selected it is called an r-covariant and s-contravariant type tensor field. This field acts on a set of vectors and co-vectors to give a real number. So a tuple of r co-vectors, specifically an element of the r-covariant section, contracts with a tuple of r vectors, and a tuple of s vectors, specifically an element of the s-contravariant section, contracts with a tuple of s co-vectors all joined by a tensor product multiplication:

$$\Gamma T^s_r \mathcal{M}(p) : T^r_{sp}\mathcal{M} \longrightarrow \mathbb{R}$$

Different kinds of (up to) r-covariant fiber bundles can be constructed from cotangent spaces. There may exist a specific fiber bundle on a manifold called the exterior bundle $\Lambda^r\mathcal{M}$. It has the property that its sections are totally anti-symmetric with respect to tuples of tangent vectors they contract with. These sections are the so-called differential forms [19]. When this section is evaluated at some point of the manifold we get a so called exterior form, an object that possess the properties of an alternating algebraic form [7]. The alternating algebraic form is a multi-linear form that can be generated through series of wedge (exterior) products [20]. More about this and other operators follow in Section 2.3.2. The differential forms mentioned above that live on manifolds are actually the descriptions of physical variables which are used as replacement for the standard vector formulation. The operations that are used in vector calculus will be replaced by other operations on differential forms that retain the related geometries and there consequences. The required operators for this thesis are introduced in the next Section 2.3.2.

2.3.2. Some Essential Operators in Exterior Calculus

Different operators can be applied on and between the differential forms introduced in the earlier section. A wedge product, symbolized by $\wedge$, can be defined as the determinant of the contraction of the individual forms with the vectors, where the vectors are in the columns and forms are in the rows. The following equation below shows how this is clearly an alternating relation since transposition of columns or rows changes the sign of the determinant of a matrix [20]:

$$\alpha^1 \wedge \alpha^2 \wedge \ldots \wedge \alpha^n (X_1, X_2, \ldots, X_n) = \begin{vmatrix} \alpha^1(X_1) & \alpha^2(X_1) & \ldots & \alpha^n(X_1) \\ \alpha^1(X_2) & \alpha^2(X_2) & \ldots & \alpha^n(X_2) \\ \vdots & \vdots & & \vdots \\ \alpha^1(X_n) & \alpha^2(X_n) & \ldots & \alpha^n(X_n) \end{vmatrix}$$

This operation thus can build a higher dimensional exterior form as (2.2) displays. Besides this multiplicative operator addition and subtraction are also possible and behave like the operations in linear algebra.

$$\wedge : \Lambda^k \mathcal{M} \times \Lambda^l \mathcal{M} \longrightarrow \Lambda^{(k+l)}\mathcal{M} \tag{2.2}$$

It is possible to operate on two exterior forms with an inner product which is simply a point-wise multi-linear multiplication that behaves exactly as the familiar tangent vector space inner product [8]:

$$\langle \cdot\, , \cdot \rangle : \Lambda^k \mathcal{M} \times \Lambda^k \mathcal{M} \longrightarrow \mathbb{R}$$

Carrying this out in the familiar 3D geometry by using the exterior product and canonical basis definition the 0-forms, 1-forms, 2-forms and 3-forms may than be formulated respectively as equations (2.3), (2.4), (2.5) and (2.6) show. The zero form can be naturally understood as a scalar valued function. Since having two equal columns vanishes the determinant, the dimension of the space in which a k-form on a n-manifold lives is consequently equal to choosing k from n as in combinatorics which is the binomial function $\binom{k}{n}$ [20] [7]. This can be appreciated for a 3-manifold in the equations below:

$$\alpha^{(0)} = \alpha(x^1, x^2, x^3) \tag{2.3}$$

$$\alpha^{(1)} = \alpha_1(x^1, x^2, x^3)dx^1 + \alpha_2(x^1, x^2, x^3)dx^2 + \alpha_3(x^1, x^2, x^3)dx^3 \tag{2.4}$$

$$\alpha^{(2)} = \alpha_1(x^1, x^2, x^3)dx^2 \wedge dx^3 + \alpha_2(x^1, x^2, x^3)dx^3 \wedge dx^1 + \alpha_3(x^1, x^2, x^3)dx^1 \wedge dx^2 \tag{2.5}$$

$$\alpha^{(3)} = \alpha(x^1, x^2, x^3)dx^1 \wedge dx^2 \wedge dx^3 \tag{2.6}$$

Integration on a metric Euclidean space is an analytical process which requires the notion of a limit on a Euclidean space where metric is already defined. However integration only requires a measure and no metric on the (co)domain space. Exterior forms naturally induce a standard measure on differential manifolds where no metric is defined [21]. A $(k + 1)$-form can than be integrated over a $k + 1$-submanifold, $\Omega_{k+1} \subset \mathcal{M}$, of the m-manifold $\mathcal{M}$ where the integration is equivalent to a duality pairing between the differential form and the sub manifold [8, 7]. With the introduction of exterior calculus on topological manifolds this operation is thus metric free and requires no resorting to any additional structure [7].

Integration brings us at the core of the mimetic method; here is where the generalized Stokes theorem lies. It is also known as the "*Newton-Leibniz-Gauss-Green-Ostrogradskii-Stokes-Poincaré*" theorem because it generalizes all the fundamental theorems of calculus [22]. The generalized Stokes theorem concludes that the pairing of a form with the boundary of a (sub)manifold is equal to pairing its exterior derivative with the (sub)manifold [15, 22, 8]. Equation (2.7) shows these relations where d represents the exterior derivative and where tr is a specific pull-back operator. tr pulls the forms back to the inclusion of the boundary. Furthermore here ∂ is the boundary operator which defines the differential operator d by these formulae in (2.7)[8].

$$\int_{\Omega_{k+1}} da^{(k)} = \int_{\partial\Omega_{k+1}} tr\ a^{(k)} \quad \Leftrightarrow \quad \langle da^{(k)}, \Omega_{k+1} \rangle = \langle tr\ a^{(k)}, \partial\Omega_{k+1} \rangle \tag{2.7}$$

The overview in equation (2.8) puts standard vector analysis' differential operators in comparison with the exterior derivative. Here we see how the gradient, curl and divergence, depending on the dimension of the geometrical objects, are in comparison with the exterior derivative [15].

$$d\alpha^{(0)} \Leftrightarrow \nabla\alpha \cdot \vec{\mathbf{dx}}, \quad d\alpha^{(1)} \Leftrightarrow \nabla \times \alpha \cdot \vec{\mathbf{dS}}, \quad d\alpha^{(2)} \Leftrightarrow \nabla \cdot \alpha\ dV \tag{2.8}$$

The two main properties of this exterior derivative is that it is a differential for which the Leibniz rule holds when it is applied to a wedge product [7]. These rules are formalized in equations (2.9) and (2.10). Secondly, applying the exterior derivative to a zero form gives a one form derived in all basis vector direction as shown in (2.11) for a zero form on an m-manifold.

$$d \circ d = 0 \tag{2.9}$$

$$d(\alpha \wedge \beta) = d\alpha \wedge \beta + (-1)^j \alpha \wedge d\beta, \quad \alpha \in \Lambda^j \mathcal{M}, \quad \beta \in \Lambda^k \mathcal{M} \tag{2.10}$$

$$d\alpha^{(0)}(x_1, x_2, \ldots, x_m) = \frac{\partial\alpha^{(0)}}{\partial x_1}dx^1 + \frac{\partial\alpha^{(0)}}{\partial x_2}dx^2 + \ldots + \frac{\partial\alpha^{(0)}}{\partial x_m}dx^m \tag{2.11}$$

Forms with different orientations can be related to each other with the Hodge operator. The Hodge operator is an exterior calculus representation that can carry with it the constitutive relations [23]. This operator is induced by the inner and wedge product [8]. It is easy to show that a space of exterior forms has a dual space of dual forms. Here the exterior product of a form with its Hodge dual can be seen as a point wise inner product between the two original forms having a geometry. This affirms the existence of this dual space. The result of a wedge product with a Hodge than has the form of a volume than can act on the argument vectors. Since every form has remaining unused basis vectors in the wedge notation, or

at least a scalar which it can be wedged with, this remainder classifies the dual form. For a 3-manifold the Hodges of the basis 1-forms are shown in the set of equations in (2.12). The Hodge relations for all 1-manifold basis forms are shown in equations (2.13). The dual forms are said to have an outer orientation compared to the inner orientation of the primal forms. This can be symbolized with a tilde: $\star\alpha^{(k)} = \tilde{\alpha}^{(n-k)}$. Also from combinatorics it is easy to affirm that the dimension of the space of outer forms is equal to that of the inner forms [20].

$$\star dx^1 = dx^2 \wedge dx^3, \quad \star dx^2 = dx^3 \wedge dx^1, \quad dx^3 = dx^1 \wedge dx^2 \tag{2.12}$$

$$\star 1 = dx, \quad \star dx = 1 \tag{2.13}$$

An inner orientation can be intuitively understood as having a direction along the geometry of the sub-manifold while the outer orientation is "directed" out of it in an ambient space.

2.3.3. De Rham Complex in Exterior Calculus

The exterior derivative, which as shown is the exterior calculus counterpart of classical vector differential operators, allows for exact relations between the differential forms. All of these relations between the differential forms on an m-manifold M can be grouped using a so called de Rham complex. The De Rham Complex has in it a sequence of modules that are connected by homomorphisms [24]. The modules can be either closed or exact. The meaning is that a closed module is null-valued after applying the homomorphism to its predecessor and an exact module is topologically exact in this application [25]. Exactness of a module means that a module is a result of applying the homomorphism to another module. Both concepts are visualised in Fig. 2.1. Whenever there are holes in the manifold, non-zero genus, exact sequences cannot be satisfied, meaning that not every module stems from another one through the homomorphism [20]. The condition for being able to form an exact sequence is slightly stronger for the domain must actually be contractible [8]. Points, straight lines, rectangles and their smooth deformations are contractible since they can be deformed continuously to one point [26, 15]. This is the case for the GLL-domains, see Section 2.4.1, considered in this thesis. Thus in case of differential forms a sequence of them under the exterior derivative can form a branch of a De Rham complex [8]. This is because the exterior derivative is an exact topological operator due to its differential property and the cohomology spaces are null due to the contractibility of the domain [7]. This first sequence is shown below in relations (2.14).
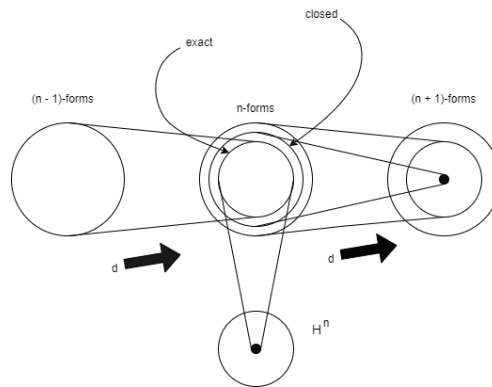
Figure 2.1: Exactness and closedness of form relations and their relation to the genus of a manifold, adopted from [16].

$$\mathbb{R} \hookrightarrow \Lambda^0 \mathcal{M} \xrightarrow{\mathrm{d}} \Lambda^1 \mathcal{M} \xrightarrow{\mathrm{d}} \cdots \xrightarrow{\mathrm{d}} \Lambda^n \mathcal{M} \xrightarrow{\mathrm{d}} 0 \tag{2.14}$$

Since all forms have a dual counterpart and the exterior derivative operation is also exact on them, a second sequence can also be generated for the outer-orientation. The two sequences can then be connected with the Hodge operator which yields a complete De Rham complex as is visualized in Figure

2.15 below. The different vector calculus operators (and identities) that occur in partial differential equations can be constructed starting with a k-form and following the operators to a specific form via the obtained routes below:

$$
\begin{array}{ccccccccc}
\mathbb{R} & \hookrightarrow & \Lambda^0\mathcal{M} & \xrightarrow{\ \mathrm{d}\ } & \Lambda^1\mathcal{M} & \xrightarrow{\ \mathrm{d}\ } & \cdots & \xrightarrow{\ \mathrm{d}\ } & \Lambda^n\mathcal{M} & \xrightarrow{\ \mathrm{d}\ } & 0 \\
& & \star\updownarrow & & \star\updownarrow & & & & \star\updownarrow & & \\
0 & \xleftarrow{\ \mathrm{d}\ } & \tilde{\Lambda}^n\mathcal{M} & \xleftarrow{\ \mathrm{d}\ } & \tilde{\Lambda}^{n-1}\mathcal{M} & \xleftarrow{\ \mathrm{d}\ } & \cdots & \xleftarrow{\ \mathrm{d}\ } & \tilde{\Lambda}^0\mathcal{M} & \hookleftarrow & \mathbb{R}
\end{array}
$$

2.3.4. Summary of the Introduced Geometry

First it was discussed that the actual observations that lead to discovering the physical laws are described with variables that are global in nature and thus are related to geometrical objects. It is the limiting process in mathematical analysis that reduces these variables to point wise values. By the introduction of differential manifolds, which are spaces that contain geometrical objects that are infinitesimal in nature, we can relate these objects to dual objects called forms. These forms are mathematical models of the physical variables and they display the same mathematical behaviour with their related formalism, namely exterior calculus, as the standard differential vector calculus while still keeping track of the infinitesimal geometrical objects to which the forms are related to. The different vector calculus operators have an exterior calculus counterpart that can be found in the De Rham complex. In this way we can formulate the differential equation, the Lagrangian and actions in terms exterior calculus and use these formulations to obtain solvable discrete systems for numerical computations as can be seen in the next chapter.

2.4. Discretization in the Mimetic Method

Mimetic discretization must respect the required topologically exact and closed relations on the forms that are in the local setting of exterior calculus. Furthermore the conservation and definition relations between the forms must be maintained exactly [2]. All of these local relations are formulated in terms of integrals, derivatives and products [27]. The approximate constitutive relations must be separated in a different part of the discretization process where the inexactness needs to be introduced. A step-by-step process to achieve this discretization can be found for instance in [27].

This chapter gives the main results and the understanding behind them. The overall idea is that we can pick a(n approximation) function for a physical variable over a manifold and implement it in the equations of the physical theory and integrate this over any relevant sub manifold in the grid. In this way we reduce the local values to discrete values on the grid cells. The values in the discrete setting are co-chains defined on the chains of cells. These values have discrete relations with each other in term of discrete operators that mimic the local relations, such that when these discrete values are used to reconstruct the exact solution the reconstructed solution satisfies the exact relations' mathematical structure. Because this new system of equations is finite and has the required initial or boundary conditions it becomes computationally solvable and the obtained coefficients are used to reconstruct the solution.

The following section will introduce the grid used to which the forms are reduced to. Afterwards the discrete geometric objects are introduced. The way to reduce local forms to global discrete forms is shown. This is supplemented by the operators that arise between these reduced forms (co-chains).

2.4.1. The Grid Considered

The manifold is divided and labeled using a grid construction. This work uses the Gauss-Lobatto-Legendre (GLL) grid. The points (on a vertical, horizontal or depth line) of the grid are determined by roots of the polynomial given in (2.15). Here L_N is the Legendre polynomial of degree N that solves Legendre's differential equation. The domain of the reference grid is $[-1, 1]$. A grid with an arbitrary interval can be constructed which is simply the reference grid after being appropriately linearly stretched and translated.

$$\phi_{GLL} = (1 - \tau)\frac{dL_N(\tau)}{d\tau}, \quad \forall \tau \in [-1, 1] \tag{2.15}$$

The discretized domain in this thesis is a time 1-manifold. As mentioned the domain can be chosen to be an arbitrary interval $[a, b]$. This means that any domain can be subdivided in a number of K_{el} elements where each element is itself an arbitrary domain $[k_{j-1}, k_j]$ that discretized with a GLL-grid. Thus in each element a GLL-grid is constructed where solutions are found. Solutions at the final time, b_{j-1}, of the previous element, k_{j-1}, than become initial conditions at the initial time, a_j, of the next element k_j. An elaborate treatment of the construction of the grid can be found in [28].

Integration of an N-degree polynomial can be done using the Lobatto-quadrature as shown in equation (2.16). Here w_i are the Lobatto weights at the abscissas τ_i which are the roots of the derivative of the Legendre polynomial with order $(N - 1)$. The remaining error term R_n is a multiple of the $(2N - 2)$-th derivative of the integrated polynomial. This means that this quadrature is exact for integration of polynomials up to a degree of $(2N - 1)$ [29]. More details on the evaluation of this quadrature can be found in [30].

$$\int_{-1}^{1} f(\tau) \, d\tau = w_0 f(-1) + w_N f(1) + \sum_{i=1}^{N-1} w_i f(\tau_i) + R_N \tag{2.16}$$

2.4.2. Discretization of Differential Forms with Algebraic Topology

Classical numerical methods generally require only the points of a grid to associate the discrete coefficients with them. This is because classical numerical methods don't start from the perspective of the physical measurement as a model for the computation as Tonti [14] suggests. They discretize the partial differential

equations formulated in classical vector calculus whose vectors don't show clear association with the underlying geometry. However the geometry of a manifold is richer and can be classified by the types of its submanifolds. For a three dimensional manifold there are points, lines, surfaces and volumes as sub-manifolds. These sub-manifolds can have an inner orientation or an outer orientation [8]. The global variables, later shown to be integrated differential forms, that can be measured, as is discussed by Tonti [14], are associated with these sub manifolds. Some sub-manifolds are visualized in Fig. 2.2 for 2-submanifolds embedded in a 2-manifold and in Fig. 2.3 for 1-sub-manifold embedded in a 2-dimensional manifold.
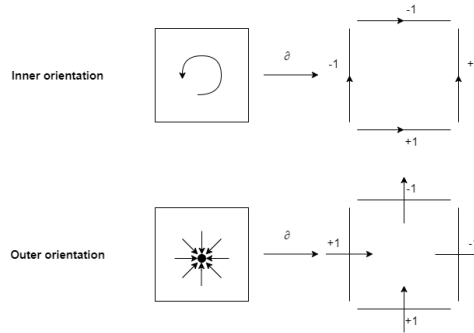
Figure 2.2: Boundary operator acting on 2-submanifold embeddeb in a 2-manifold.
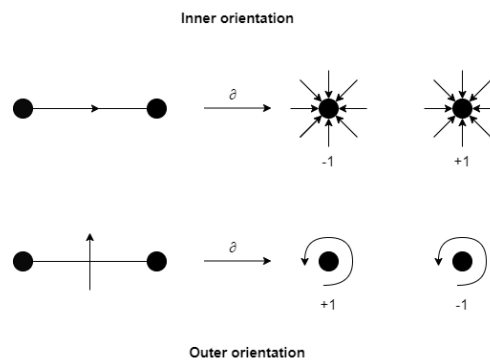
Figure 2.3: Boundary operator acting on 1-submanifold embedded in a 2-manifold.

Working with algebraic topology we can mimic the structure of differential forms with the integrated values of them. These forms are integrated over sub-manifolds in the domain and yield discrete real values related to these sub-manifolds. Algebraic topology identifies the k-sub-manifolds as objects known a k-cells c_k^i. In this research the k-cells are straight lines and points due to the choice of the one dimensional grid and. The different k-cells have a predefined bi-valued orientation and positiveness in that orientation. In Fig. 2.2 and Fig. 2.3 the orientations of squares and lines in a 2-manifold are visualized. The definition of an orientation allows for defining a discrete boundary operator, ∂, that relates enveloping $(k-1)$-cells to the k-cells. Series of k-cells that are a linear combinations of them are called k-chains $\mathbf{c}_{(k)}$. The boundary operator can act on a k-chain which gives a $(k-1)$-chain. This boundary operation is a topological operation which gives a zero/(minus) one matrix between chains and their boundaries respecting the positiveness of the directions.The action of the boundary is also visualized in Fig. 2.2 and Fig. 2.3. Applying the boundary operation twice gives a null space since the boundary itself has no boundary. This boundary operator is the discrete analogue of the continuous boundary operator acting on domains of integration. For a further brief discussion consult [8, 7]. An extensive treatment of orientations of k-cells and their boundaries and boundary operators can be found in [23].

A vector space of k-chains symbolized as C_k can be formed. Thus there is a collection $\{C_0, C_1, \ldots, C_k\}$ of k-chain spaces at a cell complex D. We can define a collection of linear functionals in $\mathbf{c}^{(k)}$ in dual space C^k acting on elements of C_k D-grid. This is a famous result from linear algebra that any vector space has a dual space. Elements of canonical basis of C_k and C^K will be symbolized respectively as $\tau_{(k),i}$ and $\tau^{(k),i}$.

The linear combinations of the dual space vectors (dual k-cells) are called k-co-chains. In conclusion chains and co-chains can be topologically paired to each other resulting in a real value. The mathematical definition of this duality pairing and of reduction is shown in (2.17) shows. This duality pairing of k-cell in the k-co-chain and a k-cell in the k-chain is the discrete analogue of integration. It is equal to integrating of the local k-forms on the k-manifold-cell. Thus k-co-chains are the global and discrete counter parts of the local k-forms. We can conclude from this that a k-chain stores the discrete geometry on which the integration happens and a k-co-chain stores the integral value of k-forms that live on that domain [27]. This information storing by integration of the k-form in the k-co-chain is called reduction by the reduction operator $\mathcal{R}$ with its mathematical definition shown in equation (2.17).

$$\mathbf{c}^{(k)}(\mathbf{c}_{(k)}) := \langle \mathcal{R}c^{(k)} \, , \, \mathbf{c}_{(k)} \rangle = \sum_i c^i \langle \mathcal{R}c^{(k)} \, , \, \tau_{(k),i} \rangle = \sum_i c^i \int_{\tau_{(k),i}} c^{(k)} = \int_{c_{(k)}} c^{(k)} \tag{2.17}$$

After defining discrete analogues of the geometry of differential k-sub-manifolds and k-forms and how integration works regarding them we can now define a discrete analogue of the exterior derivative. This is known as the co-boundary operator. It generates $(k+1)$-cells from a k-cell and thus when acting on k-co-chain a $(k+1)$-co-chain results. This co-boundary operator, δ, follows from defining a duality pairing of the chains and co-chains that is analogous to generalized Stokes theorem (2.7) but in a discrete setting. This relation is shown in equation (2.18) and shows that similarly to the exterior derivative it can be defined as the formal adjoint of the boundary operator such that there exists a discrete generalized theorem [8]. This makes it an exact topological operator from k-co-chains to $(k+1)$-co-chains.

$$\langle \delta\mathbf{c}^{(k)} \, , \, \mathbf{c}_{(k+1)} \rangle \equiv \langle \mathbf{c}^{(k)} \, , \, \partial\mathbf{c}_{(k+1)} \rangle, \quad \forall\mathbf{c}^{(k)} \in C^k(\mathcal{M}) \quad \forall\mathbf{c}_{(k+1)} \in C_{k+1}(\mathcal{M}) \tag{2.18}$$

Equation (2.18) together with generalized Stokes theorem (2.7) can be used to show that the co-boundary δ / exterior derivative d commute with the reduction operator $\mathcal{R}$. As an example that shows the definition of co-boundary operator a subset of a 0-co-chain and a 1-co-chain from a two dimensional grid is visualized in Fig. 2.4. The co-boundary of x^1 here would be $(-\dot{x}^2 + \dot{x}^1)$. What is observed is that the co-boundary of a k-cell in a co-chain are all the $(k+1)$-cells connected to it with a plus or minus sign depending on their direction relative to the k-cell direction. applying the co-boundary twice is exactly zero which is analogous to the double exterior derivative. This is the behaviour of the co-boundary operator when acting on a single cell in a co-chain.
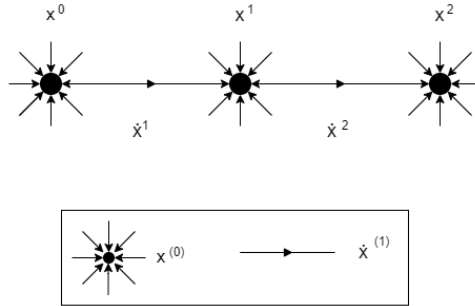
Figure 2.4: co-chains of 0-cells and 1-cells with their orientations

A k-co-chain can be represented using arrays of real values obtained from reduction on the k-cell-manifolds depending on the chosen ordering. For instance considered the sub-grid in Fig. 2.4 where the cells are ordered lexicographically. If N is the order of the mesh than there are $(N+1)$ 0-cells and N 1-cells in the co-chains. The 0-co-chain after reducing is the 0-form stored in the points as: $\mathbf{x}^{(0)} = (x^0 \ x^1 \ x^3)^T$. The co-boundary operator can than be described with a so-called incidence matrix that maps the 0-co-chain to the associated 1-co-chain: $\dot{\mathbf{x}} = (\dot{x}^1 \ \dot{x}^2)^T$. For the co-boundary operator this means that when a line is generated from a point and they are in the same direction the action of the point is positive and when they are opposite the action is negative. These actions generate the incidence matrix which is shown in (2.19) for the cell complex in Fig. 2.4.

$$\mathbb{E}^{(1,0)} = \begin{bmatrix} -1 & 1 & 0 \\ 0 & -1 & 1 \end{bmatrix} \tag{2.19}$$

The same can be done for two dimensional grids. Here 2-co-chains are introduced which are rectangles. When direction and topological order are defined, incidence matrices can also be constructed for this grid. There are exactly two incidence matrices where one takes the a 0-co-chain to 1-co-chains and 1-co-chains to 2-co-chains. This however not elaborated upon since this is a one dimensional case study. It can also be shown that two incidence matrices, $\mathbb{E}^{(k+2,k+1)}\mathbb{E}^{(k+1,k)}$, acting on each other give a zero matrix which is similar to the exterior derivative for a complete co-chain. For a thorough and more formal explanation of the co-boundary operator and how it works on k-cells [8, 7] can be consulted.

The approximation of the actual form will not be looked for in the complete space of differential k-forms but a subspace of it; namely $\Lambda_h^k(\mathcal{M}, C_k) \subseteq \Lambda^k\mathcal{M}$. This is the space associated with k-co-chains that can be obtained through integration of the k-form polynomial functions that approximate the actual k-forms. In our case the elements of a (primal) co-chain are coefficients of approximation polynomials. Approximate local k-forms can then be obtained through reconstruction, $\mathcal{I}$, using the approximation polynomials. The composition of both operators, π_h, is the projection from the exact solution in the complete exterior bundle to the subspace in which we look for for the solution; $\pi_h = \mathcal{I} \circ \mathcal{R}$ [8]. An overview of this projection from the solution space to the approximation space is shown in the diagram in Fig. 2.5.
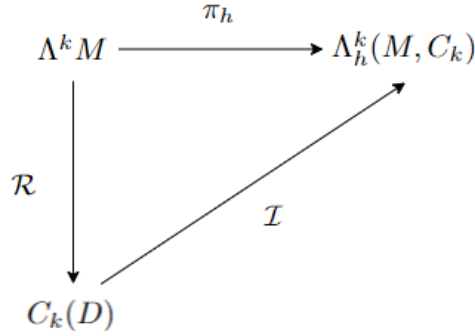
Figure 2.5: Diagram of the relation between elements of the spaces of exact k-forms, the co-chains and the approximation k-forms, adopted from [8]

In short reduction $\mathcal{R}$ is simply integrating the (expected function form of the) k-form over a k-cell in the k-chain which will give us the associated discrete k-form to that cell. Reduction to the complete k-co-chain is integrating over the complete k-chain as is shown in the set of equations (2.17). Reconstruction, $\mathcal{I}$, is the regeneration of the k-forms from k-co-chain to a section in a subspace of sections in the exterior k-bundle $\Lambda^k\mathcal{M}$ that are of a specific type, generally polynomials. The condition is set that the approximation model used must satisfy the property that reconstructing and than reducing give the same same co-chain back. This means that all the information about the co-chains must be stored in the approximations functions. However in the opposite order the model can induce an error since information loss on the local behaviour can happen during integrating to the global setting. In this work algebraic dual polynomials will be used for this task and they satisfy these properties. These polynomials are presented in Section 2.5. The exterior derivative provably commutating with both reduction and reconstruction and thus also with the projection [8]. This is summarized in equations (2.20).

$$\pi_h \circ d = \mathcal{I} \circ \mathcal{R} \circ d = \mathcal{I} \circ \delta \circ \mathcal{R} = d \circ \mathcal{I} \circ \mathcal{R} = d \circ \pi_h \tag{2.20}$$

Hodge operators transform inner oriented forms to outer oriented forms in the local sense. As mentioned before in Section 2.3.2 the Hodge operator for differential forms is induced through existence of an inner product and wedge product. This can be mimicked in the discrete setting with construction of mass matrices by using the L^2-inner product over a volume space. The construction of these Hodge matrices is presented in Section 2.5.2 and they relate primal co-chains on a primal grid to dual co-chains on a dual grid. This

mass matrix however is dependent on a metric since it stems from an inner product. Inner products are defined in normed spaces and a famous result in functional analysis is that every normed space is metric space. This means that our constructed Hodge matrix is dependent on the chosen grid. However due to the reference domain and interpolation polynomials properties this work uses, see Section 2.5.3, a reference mass matrix can be obtained that is transformed depending on a Jacobian with respect to how the domain is stretched (or deformed). Now again a discrete De Rham sequence can also be generated for the co-boundary operator where the modules are the k-co-chains. The same can be done for the dual k-co-chains and these can be connected to each other using the Hodge matrices.

Now in the same way as for the local forms we can introduce a De Rham complex for the (smoothed) projections of the forms as shown in [7, 31]. This enables also to have an exact De Rham like sequence for the co-chains where the local Hodge is replaced by a discrete Hodge $\mathbb{M}$ and the exterior derivative by the co-boundary operator.

2.4.3. Summary of the Introduced Discretization

The discretization of the forms happens through integration of the forms over a predefined cell complex. This is called reduction of the forms. The resulting values are ordered in a co-chain which are related to a chain of cells in the grid. Discrete analogues of the exterior calculus operators are constructed. The co-boundary is an exact topological operator in nature as it mimics the local exterior derivative. The Hodge matrix is a metric dependent operator that transforms a primal co-chain to a co-chains with a dual orientation. Eventually the differential equations are rewritten in a discrete scheme of co-chains and numerically solved. The resulting co-chains are used to reconstruct the forms using approximating functions. The approximating functions are introduced in the next section 2.5.

2.5. Reconstruction and Reduction using Algebraic Dual Polynomials

In this work algebraic polynomial associated with k-cells on a GLL-grid are used to approximate the exact solutions. These polynomials work as a reconstruction of the reduced co-chains. The projection from the exact form to an approximate form is done using linear combination of functions and co-chain coefficients. Such a linear combination is shown for a primal 0-form in (2.21) and a primal 1-form in (2.22). These two polynomials that are respectively related to points and lines are familiarized with in the next section. However there are to kinds of polynomials that can be used to interpolate on a point or line depending on the orientation of the forms. Both are discussed in separate sections that will follow. Also since the functions are defined on a reference domain, this is followed by transformation rules for the variables on a general stretched domain. This treatment is based on the work in [10]. For an exhaustive discussion consult this work.

$$\pi_h a^{(0)}(t) = \sum_{i=0}^{N} a^i h_i(t) \tag{2.21}$$

$$\pi_h \dot{a}^{(1)}(t) = \sum_{i=1}^{N} \dot{a}^i e_i(t) dt \tag{2.22}$$

2.5.1. The Primal Basis

For an N-th order one dimensional grid there can $(N+1)$ Lagrange N-polynomials be formulated as in equation (2.23). These polynomials are a basis that spans a polynomial vector space of degree N. The solutions for 0-forms, $\phi^h(0)$, will be looked for in this space were every member of this space can be written as a formal linear combination of them. This space of reconstructions is a subspace of the exterior bundle of 0-forms. So a solution in this space will have the form of (2.24). Here $h_i(t)$ are the Lagrange polynomials and $\mathcal{N}_i^0(x^h)$ are their coefficients.

$$h_i(t) = \prod_{m=0, m \neq i}^{N} \frac{t - t_m}{t_i - t_m}, \quad \forall i \in \{0, \ldots, N\} \tag{2.23}$$

$$x^h(t) = \sum_{i=0}^{N} \mathcal{N}_i^0(x^h) h_i(t) \tag{2.24}$$

To get the 0-co-chain associated with the cell complex a reduction $\mathcal{R}$ is required. Reduction as explained in Section 2.4.2 is integrating, i.e. duality pairing, of the 0-forms with the 0-chain of points. This is simply getting the values of the functions at the points. A well-known result is that the Lagrange polynomial has the property that it vanishes at all grid points except for the point associated with it where it is equal to one, see (2.25). Equation (2.26) shows that evaluating at the points, which is reduction $\mathcal{R}$, yields the coefficients of the approximation. This concludes that these coefficients $\mathcal{N}_i^0(x^h)$ constitute the 0-co-chain on the 0-chain of points and are obtained through applying the linear functionals $\mathcal{N}_i^0$.

$$h_i(t_j) = \delta_{ij}, \quad \forall i, j \in \{0, \ldots, N\} \tag{2.25}$$

$$\mathcal{N}_i^0(x^h(t)) := x^h(t_i), \quad \forall i \in \{0, \ldots, N\} \tag{2.26}$$

On a N-th order GLL-grid edge functions that are associated to 1-chains can be used to reconstruct 1-forms. These functions form a basis for the vector space of $(N-1)$-order polynomials. The definition of these edge function and their formal linear combinations are shown in (2.27) and (2.60). On an N-order GLL-grid there are N lines following one direction. To associate a 1-form to a line in the grid through
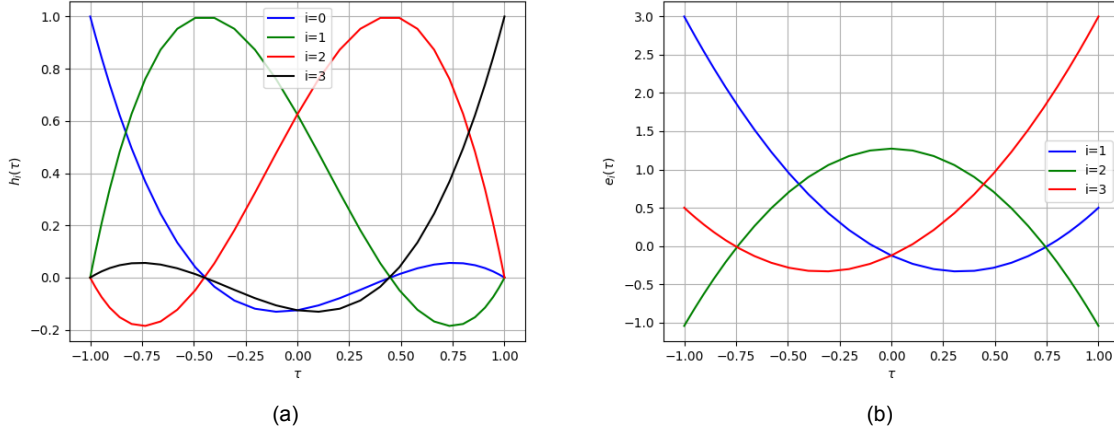
Figure 2.6: (a) All nodal (Lagrange) primal basis functions for $N = 3$ **(b)** All edge primal basis functions for $N = 3$

reduction, integration is performed over that line. The edge function has the property that its integrals vanish outside of the lines that are associated to it, as (2.61) shows. This means that the set of coefficients $\mathcal{N}_i^1(\dot{x}^h)$ of the polynomial of the 1-form is the 1-co-chain.

$$e_i(t) = -\sum_{j=0}^{i-1} \frac{dh_k}{dt}(t), \quad \forall j \in \{1, \ldots, N\} \tag{2.27}$$

$$\dot{x}^h(t) = \sum_{i=1}^{N} \mathcal{N}_i^1(\dot{x}^h) e_i(t) dt \tag{2.28}$$

$$\mathcal{N}_i^1(e_j(t)dt) = \int_{t_{i-1}}^{t_i} e_j(t)\, dt = \delta_{ij} \tag{2.29}$$

When a 0-form that is defined through Lagrange functions is differentiated a 1-from is the result as presented in (2.63). The incidence matrix than appears which relates the 0-form coefficients to the 1-form coefficients. This matrix is exactly the co-boundary matrix between the 0-co-chain and the 1-co-chain as is shown in (2.19) for the example of $N = 2$. These Lagrange and edge functions that form a basis for the space of approximate forms are plotted for third order grids in Fig. 2.6.

$$\dot{x}^h(t) = \frac{dx^h}{dt}(t)dt = \sum_{i=1}^{N}\sum_{j=0}^{N} \mathbb{E}_{i,j}^{1,0} \mathcal{N}_j^0(x^h) e_i(t)dt \tag{2.30}$$

2.5.2. The Dual Basis

The nodal Lagrange basis functions can be ordered in a row vector $\mathbf{h}(t) = (h_0(t) \quad h_1(t) \quad \cdots \quad h_N(t))$ and the degrees of freedom (0-co-chain) can be ordered in an column vector $\mathcal{N}^0(x^h) = (\mathcal{N}_0^0(x^h) \quad \mathcal{N}_1^0(x^h) \quad \cdots \quad \mathcal{N}_N^0(x^h))^T$. The product of these two yields the projected 0-form: $x^h(t) = \mathbf{h}(t)\mathcal{N}^0(x^h)$. We can use L_2-inner product of a 0-form with its dual oriented 1-form to define a discrete Hodge that gives the dual degrees of freedom. This matrix is shown below in (2.31) where T is the whole domain: $T = [t_{initial}, t_{final}]$.

$$\mathbb{M}^{(0)} = \int_T \mathbf{h}(t)^T \mathbf{h}(t)dt \tag{2.31}$$
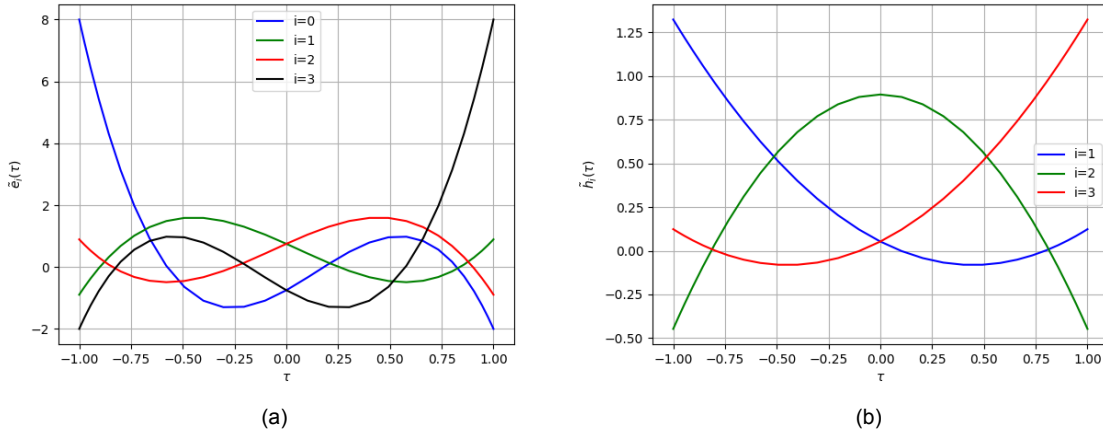
Figure 2.7: (a) All edge dual basis functions for $N = 3$ **(b)** All nodal dual basis functions for $N = 3$

The constructions of these dual degrees of freedom and dual polynomials are given in (2.68) and (2.69). As can be easily seen the discrete Hodge is chosen in such a manner that when it transforms the degrees of freedom its inverse transforms the polynomials. In this way multiplying the two vectors of the dual form with each other yields the same scalar value as the primal form expect with dual orientation.

$$\tilde{\mathcal{N}}^1(x^h) := \mathbb{M}^{(0)}\mathcal{N}^0(x^h) \tag{2.32}$$

$$\tilde{\mathbf{e}}(t) := \mathbf{h}(t)(\mathbb{M}^{(0)})^{-1} \tag{2.33}$$

These new dual polynomials of the nodal basis functions behave in such a way that their coefficients are associated with lines that are dual to the original nodes. We can then introduces a dual grid with cells were we can reduce the dual form to. The new coefficients are than associated with line segments instead of nodes. However the exact location of these line segments are not known. The way they are topologically ordered is known and can be seen in Fig. 2.8. The same process can be repeated for the edge polynomials with the same consequences. The resulting relations are shown between in the primal edge functions and their duals are shown in (2.34) and (2.35). Here the mass matrices of edge functions are obtained through the same integration but with vectors of edge functions: $\mathbf{e}(t) = (e_1(t) \quad e_2(t) \quad \cdots \quad e_N(t))$, as is shown in (2.36). Plots of the nodal dual polynomial and edge dual polynomial are shown in Fig. 2.7.

$$\tilde{\mathcal{N}}^0(x^h) := \mathbb{M}^{(1)}\mathcal{N}^1(x^h) \tag{2.34}$$

$$\tilde{\mathbf{h}}(t) := \mathbf{e}(t)(\mathbb{M}^{(1)})^{-1} \tag{2.35}$$

$$\mathbb{M}^{(1)} = \int_T \mathbf{e}(t)^T \mathbf{e}(t)dt \tag{2.36}$$

A vector of primal basis functions is bi-orthogonal to its dual vector. Furthermore the coefficients of the dual edge polynomials are associated with the nodes in the dual grid. However again the exact point locations are unknown. The topological order of the cells however can be stated and visualized as in Fig. 2.8. The co-boundary topological relation between dual forms also follows through an incidence matrix as done for primal forms in (2.19). A procedure for obtaining the incidence matrix between dual co-chains on a dual grid is done in Section 3.1. For further elaboration on algebraic dual polynomials consult [10].
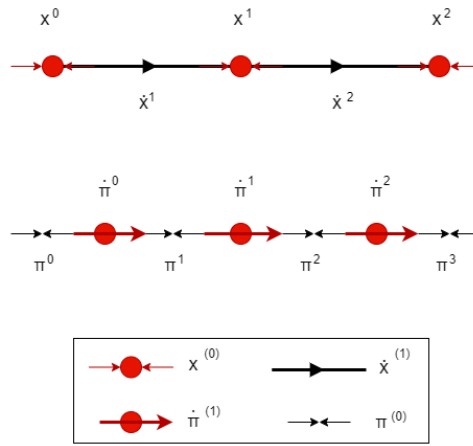
Figure 2.8: A primal (upper line) and dual (lower line) grid with primal and dual co-chains respectively and their orientations

2.5.3. Transformations of the Basis Polynomials

The standard nodal and edge polynomials are constructed on the reference domain [-1, 1]. However the time domain considered can be any general interval $[t_i, t_f]$. The transformation of the functions to this domain is done with the linear mapping $\phi(\tau)$ in the following way:

$$t = \phi(\tau) = \frac{t_i}{2}(1 - \tau) + \frac{t_f}{2}(1 + \tau), \quad \forall \tau \in [-1, 1]$$

The general primal nodal basis function array, h, and primal edge function array, e, are obrainted through a transformation of paramaters. Here the Jacobian determinant is $\mathbf{J} = \frac{(t_i - t_f)}{2}$. The arrays of the reference nodal and edge basis functions are respectively $\overline{\mathbf{h}}(t)$ and $\overline{\mathbf{e}}(t)$. The transformation are written out in the following lines:

$$h_i(t) = \overline{h}_i \circ \phi^{-1}(t), \quad \forall i \in \{0, \ldots, N\}$$

$$e_i(t) = \frac{1}{\mathbf{J}} \overline{e}_i \circ \phi^{-1}(t), \quad \forall i \in \{1, \ldots, N\}$$

The transformations of the general dual basis functions can similarly be formulated as follows:

$$\tilde{h}_i(t) = \frac{1}{\mathbf{J}} \overline{h}_i \circ \phi^{-1}(t), \quad \forall i \in \{1, \ldots, N\}$$

$$\tilde{e}_i(t) = \overline{e}_i \circ \phi^{-1}(t), \quad \forall i \in \{0, \ldots, N\}$$

The primal mass matrices of the nodal and edge basis functions are then, respectively, obtained through a transformation of parameters. The mass matrices with the bar are related to the reference basis functions on the reference domain. These matrices the discrete counter part of the Hodge star that map primal co-chains to dual co-chains. There defining relation becomes for edge functions and 1-co-cochains is:

$$\mathbb{M}^{(0)} = \int_{t_i}^{t_f} \mathbf{h}^T(t)\mathbf{h}(t) \, dt = \frac{(t_f - t_i)}{2} \overline{\mathbb{M}}^{(0)}$$

$$\mathbb{M}^{(1)} = \int_{t_i}^{t_f} \mathbf{e}^T(t)\mathbf{e}(t) \, dt = \frac{2}{(t_f - t_i)} \overline{\mathbb{M}}^{(1)}$$

These transformed basis polynomials satisfy the general properties of bi-orthogonality of primal and dual basis functions, the Kronecker delta property in co-chain creation and also the topological co-boundary operator relating them through the edge matrices.

2.6. Classical Theory of Lagrangian Mechanics

Newtonian mechanics is about looking at the equilibrium of forces that give the kinetics of the system. However here constraining forces appear in the equations of motion. Also the used coordinates are persistent on some axis system. The appearance of Lagrangian mechanics allowed for removing the constraints from the equations and introduced generalized coordinates that can be chosen usefully and minimalistic. More importantly all of the information about the system is contained at the level of the action which is the integral of the Lagrangian [32]. So knowing a proper formulation of the action allows for knowing every detail that can be known about the behaviour of the system depending on the boundary or initial conditions. Furthermore it has a natural way of formulating minimization and variational problems. Since reduction is integration of the forms, this action integral can be used to obtain a discrete system of equations that solves the problem numerically.

2.6.1. Non-Unique Lagranian Mechanics for Holonomic Systems

A Lagrangian can have different formulations depending on the physical system. When we start with the work in a general classical system, with particles labeled with i, there are constraint forces and reversed effective forces involved. D'Alembert's principle attains a useful shape by letting the virtual work -coming from constraining forces- vanish which results in the following balance equation:

$$\sum_i (\mathbf{F}_i^{(a)} - \mathbf{\dot{p}}_i) \cdot \delta \mathbf{r}_i = \mathbf{0}$$

This equation can be rewritten through the application of Newton's second law and and defining kinetic energy (starting from spatial coordinates) as $T = \sum_i \frac{1}{2}mv_i^2$. The coordinates of the particles are furthermore generalized to independent coordinates **q** with a transformation. A set of equations as in (2.37) is then obtained.

$$\frac{d}{dt}\left(\frac{\partial T}{\partial \dot{q}_j}\right) - \frac{\partial T}{\partial q_j} = Q_j \quad \forall j \in \{0, 1, \dots, N\} \tag{2.37}$$

However notice that the assumption here is that the constraints in the system are holonomic, that is the conditions of the constraints on the coordinates are expressed in terms of equations and they contain only coordinates and time as variables. Q_j in (2.37) is a generalized force whose form is yet to be specified. Further simplifications and formulations can be demonstrated. These are shown for instance in [33].

We can consequently specify the forms of kinetic energy T and generalized force Q. First the generalized form of kinetic energy can be expressed in terms of generalized independent coordinates as in (2.38) below. Here T_0 is an expression independent of generalized velocities, T_1 is linear in generalized velocities and T_2 is quadratic in generalized velocities. In the scleronomous setting, that is the constraints are not dependent on time and thus the transformation equations of the Cartesian coordinates to generalized coordinates do not explicitly depend on time, the kinetic energy equals $T = T_2$ and is thus always a quadratic homogeneous expression [33, 34].

$$T = T_0 + T_1 + T_2 \tag{2.38}$$

The system is monogenic if the generalized forces are functions of a velocity dependent scalar potential U that can be expressed as below in (2.39). This potential is not only academic but practical as can be seen for instance in [33, p. 22]) and later sections.

$$Q_j = -\frac{\partial U}{\partial q_j} + \frac{d}{dt}\left(\frac{\partial U}{\partial \dot{q}_j}\right) \quad \forall j \in \{0, 1, \dots, N\} \tag{2.39}$$

The Lagrangian can be defined as $L = T - U$. From combining (2.39) and (2.37) the famous Euler-Lagrange equations in (2.40) can be obtained.

$$\frac{d}{dt}\left(\frac{\partial L}{\partial \dot{q}_j}\right) - \frac{\partial L}{\partial q_j} = 0 \quad \forall j \in \{0, 1, \ldots, N\} \tag{2.40}$$

A conservative system has a force potential that is derivable from a scalar potential that is dependent on the generalized degrees of freedom but not on their derivatives or explicitly on time, i.e. $U = U(\mathbf{r}_0, \mathbf{r}_1, \ldots, \mathbf{r}_M)$. This potential generates $(N + 1)$ generalized forces $Q_j = -\frac{\partial U}{\partial q_j}$. This means that it is merely a specific case of monogenic systems. What makes the word choice of "conservative" well placed is that for every two states r and k of the system it holds that: $T_r + U_r = T_k + U_k = E_{mech}$ [33]. The property E_{mech}, mechanical energy, is always conserved in the particles of the conservative systems. This means that when we start in time at configuration r and arrive at configuration k we only need to know the initial conditions (configuration r) and the spatial position of the particle where we arrive at in k to determine the kinetic energy. Notice that by configuration here is meant the set of independent generalized coordinates. So we don't need the knowledge of what happens to the system in between. In non-conservative systems knowledge of what happened during the process of configuration evolution is required to determine how much of the work by forces acting on a particle is transformed in and out of kinetic energy. The idea of capturing this information will turn out to be useful in working with non-conservative systems. If we consider a non-monogenic (and thus non-conservative) system where some of the the forces can be written as a velocity dependent scalar potential and others not, then (2.40) can be written as (2.41) below [33]:

$$\frac{d}{dt}\left(\frac{\partial L}{\partial \dot{q}_j}\right) - \frac{\partial L}{\partial q_j} = Q_j \quad \forall j \in \{0, 1, \ldots, N\} \tag{2.41}$$

The action $\mathcal{S}$ between two time instants can be defined as the integral of the Lagrangian over a time domain as (2.42) shows.

$$\mathcal{S} = \int_{t_i}^{t_f} L \, dt \tag{2.42}$$

Hamilton's action principle states that the motion of a monogenic system (of particles) is along a path that is stationary. The physical path is thus the path that is followed when a first order variation happens and the action does not change. Mathematically this is summarized in (2.43) where δ is a variation of generalized coordinates over the whole time domain [33, 35]. Variations of the integral of the Lagrangian functional, functional (Gâteaux) derivatives, are done through the use of calculus of variations as is shown in Section 2.8. With reference to discretization, the principle of least or stationary action can be seen as a reduction of the Lagrangian. Notice that Hamilton's principle of stationary action (2.43), Lagrange's equation (2.40) and Newton's second law are equivalent for a monogenic system [36]. This than holds also for conservative systems since it is a subset of it.

$$\delta \mathcal{S} = \delta \int_{t_i}^{t_f} L(q_0, \ldots, q_N, \dot{q}_1, \ldots, \dot{q}_N) \, dt = 0 \tag{2.43}$$

When we apply the invariance of actions of monogenic systems with respect to time only, we get a quantity that is time symmetric [34, 37] which can be defined as the energy function [33, p. 61]. This expression is also justified by the theory of Legendre transforms [36]. This so called energy function is given in (2.44) below:

$$E = \left(\sum_{j=0}^{N} \dot{q}_j \frac{\partial L}{\partial \dot{q}_j}\right) - L \tag{2.44}$$

This energy function is exactly equal to the definition of the Hamiltonian [34, 33]. The difference is in treating the domain variables. In the case of the energy function it is treated as a function of the generalized coordinates, their time derivatives and time, while the Hamiltonian is a function of the generalized coordinates, generalized momenta, $\frac{\partial L}{\partial \dot{q}_j}$, and possibly time [33].

A subclass of generalized velocity potentials, linear generalized velocity potentials, can be written as below. Notice that this class is presented as it will appear as a coupling potential of non-conservative doubled degree of freedom systems which will be encountered later. It also gives a relation for the mechanical energy of the damped harmonic oscillator as seen in Section 2.9. In this section it is shown how the energy function and mechanical energy can be related.

$$U(q_0, q_1, \ldots, q_N, \dot{q}_0, \dot{q}_1, \ldots, \dot{q}_N, t) = \sum_{j=0}^{N} \overline{U}_1^j(q_0, q_1, \ldots, q_N, t)\dot{q}_j + U_0(q_0, q_1, \ldots, q_N, t)$$

This equation above, of the linear generalized velocity potential, can be summarized in the equation below:

$$U(q_0, q_1, \ldots, q_N, \dot{q}_0, \dot{q}_1, \ldots, \dot{q}_N, t) = U_1 + U_0$$

If we apply this special case together with the generalized kinetic energy in (2.38) to (2.44) we get the dependence of the energy function on different terms of kinetic energy and (linear generalized velocity) potential energy in (2.45) below.

$$E = T_2 - T_0 + U_0 \tag{2.45}$$

When a system is conservative, i.e. $U_1 = 0$ and $U_0 \neq f(t)$ explicitly, and scleronomous, i.e. $T_0 = T_1 = 0$, we get that: $E = T_0 + U_0 = T + U$. This in conclusion means that the energy function (2.44) of a scleronomous holonomic conservative system is exactly the mechanical energy; $E = E_{mech}$. Notice that this also holds in the case where the scalar potential U_0 is explicitly dependent on time.

Taking the (total) time derivative of the energy function of a holonomic and general, i.e. with respect to monogeneity and scleronomousness, system and using the chain rule where we let L be a function of the q's, and $\dot{q}$'s and t we get:

$$\frac{dE}{dt} = \sum_{j=0}^{N} \left(\left(\frac{d}{dt} \frac{\partial L}{\partial \dot{q}_j} \right) \dot{q}_j + \frac{\partial L}{\partial \dot{q}_j} \ddot{q}_j \right) - \left(\sum_{j=0}^{N} \left(\frac{\partial L}{\partial q_j} \dot{q}_j + \frac{\partial L}{\partial \dot{q}_j} \ddot{q}_j \right) + \frac{\partial L}{\partial t} \right)$$

The second and fourth term cancel each other while the first and third term give the generalized forces as (2.41) shows. The equation above than becomes (2.46) below:

$$\frac{dE}{dt} = \sum_{j=0}^{N} \dot{q}_j Q_j - \frac{\partial L}{\partial t} \tag{2.46}$$

A monogenic system, $Q_j = 0$, is called totally closed if the Lagrangian does not depend explicitly on time, i.e. $\frac{\partial L}{\partial t} = 0$. This means that the generalized velocity potential is time independent or say there are no external forces acting on the system which makes $\frac{dE}{dt} = 0$ [36]. This means that the value of the energy function is constant in time, i.e. a conserved property. A conservative system satisfies the property that its energy function is constant in time since its scalar potential does not explicitly depend on time.

Now combining the above concludes that for a holonomic scleronomous conservative system, the energy function is equal to the mechanical energy $E_{mech} = E$ and it is conserved in time: $\frac{dE}{dt} = \frac{dE_{mech}}{dt} = 0$.

Now when we consider (2.46) that holds for general holonomic systems and narrow it down to scleronomous pure monogenic/non-monogenic systems for which the generalized potential forces are derivable from a scalar potential only that it is independent of time, i.e. $U = U_0(q_0, q_1, \ldots, q_N)$. We get in the same procedure as before that the energy function is equal to the mechanical energy $E = E_{mech}$. Due to (2.46) the change in mechanical energy is given in (2.47) below. In this way we have obtained well defined formulations of energy treated in this work.

$$\frac{dE_{mech}}{dt} = \frac{dE}{dt} = \sum_{j=0}^{N} \dot{q}_j Q_j \tag{2.47}$$

Now returning to the principle of stationary action, when we apply techniques from variational calculus the Lagrange's equations in (2.40) follow from this principle of Hamilton for monogenic systems [33]. Furthermore, Newton's second law can be derived from Lagrange's equations. The reverse can also be proven which means that Hamilton's principle, Lagrange's equation and Newton's second law are equivalent [36]. Hamilton's action principle covers more than monogenic systems but requires knowing a total Langrangian that satisfies the Lagrangian equations in (2.40) which in turn satisfy Newton's second law. The standard Lagrangian, for instance, does not imply Hamilton's principle when generalized forces are proportional to the velocity because they cannot be derived from a generalized velocity potential [33]. So the total Lagrangian that satisfies Lagrange's equations is not necessarily the standard Lagrangian, i.e. kinetic energy minus the generalized potential $L = T - U$ as is shown in the example of [38]. A total non-monogenic (read non-conservative) Lagrangian, for which stationary action implies Lagrange's equation and Newton's second law, can be the standard (read monogenic) Lagrangian plus the work done by the non-conservative forces [39]. Since this study considers numerical solutions under energy dissipation, where the damping force is proportional to the velocity, this requires finding a formulation of the stationary action when the system is non-monogenic. An attempt to resolve this difficulty for general cases with a case study to damped harmonic oscillators is introduced in Section 2.7. This is further expanded on and used in a numerical computation in Chapter 3.

2.6.2. Gauge Transformations and Uniqueness

It is obvious that adding a constant term outside of the action integral will not have an effect on the variations of an action. This newly transformed action than satisfies the same stationary principle. In electromagnetism and quantum mechanics these transformation are used to obtain some deep lying information of the constituents of the system. The invariance of the action due to this constant transformation is called a gauge symmetry.

We can transform a Lagrangian L with a gauge term as in equation (2.48) and get the transformed Lagrangian L' that still satisfies Lagrange's (2.40) and the same (partial) differential equations of motions. Integration of the Lagrangian over the time of action yields (2.49) with the transformed action $\mathcal{S}'$ and original action $\mathcal{S}$ related through the integrated gauge term G. The variation of coordinates that is done to vary the action is zero at the initial and final moments in the Hamiltonian principle; $\delta\mathbf{q}(t_i) = \delta\mathbf{q}(t_f) = \mathbf{0}$. This makes the final term vanish when the variation is applied. Thus the configuration paths that stationarize action $\mathcal{S}'$ also do that for action $\mathcal{S}$ [40].

$$L'(\dot{\mathbf{q}}, \mathbf{q}, t) = L(\dot{\mathbf{q}}, \mathbf{q}, t) + \frac{d}{dt}G(\mathbf{q}, t) \tag{2.48}$$

$$\mathcal{S}'[\mathbf{q}] = \mathcal{S}[\mathbf{q}] + G(\mathbf{q}, t)\big|_{t_i}^{t_f} \tag{2.49}$$

This added gauge term $\frac{d}{dt}G(\mathbf{q}, t)$ can be any differentiable function and will lead to the same equations of motion as the original non-unique Lagrangian [33]. This clearly means that in the action formulation this gauge term is dependent on the remainder of the system which are the initial conditions since these are the only remaining unknowns.

2.7. A Theory for Lagrangians of Non-Conservative Systems

The Lagrangian theory discussed in Section 2.6 is applicable only to monogenic (and thus also conservative) systems. This is because when various effects in physical systems can not be obtained from a generalized potential, the system is non-conservative with respect to energy. Then the Lagrangian functional does not satisfy Lagrange's equation (2.40), which is a condition for Hamilton's classical principle to hold [33]. A main branch of systems that are non-conservative occur when there are irreversible processes. These processes are shaped, for instance, by damping [32]. Damping is also non-monogenic [33]. Creating Lagrangian functionals for these non-conservative systems that are usable in the action have been long done however only for specific cases and not with a generalized method [32]. This is, for instance, the case for the Lagrangian of a damped mass string system shown in Section 2.9 obtained by [38].

The quest for obtaining a generalized way of formulating a suitable non-conservative classical action is still in progress. A predecessor of the main method that is discussed in this thesis was ad hocly done as early as 1953 for specifically dissipative classical systems. The core of the idea is to create a description of the system such that it is closed (up to an explicit dependence of the Lagrangian on time) and the energy (function) is thus conserved (up to this explicit time dependence). This is done by introducing a "mirror-image" of the system that tracks the friction of the system and generates its negative image [41]. This can be done with the coupling of an imaginary particle in the system that has its own degrees of freedom. Notice that integrating out the degrees of freedom a dissipation term appears in the action integral [42], which implies equivalence. For a damped harmonic oscillator, the physical equation of motion and the mirror equation of motion are shown respectively in (2.50) and (2.51) as obtained by [41]. As can be seen an imaginary back running motion is introduced that absorbs the lost energy with a negative friction in equation (2.51). Here x^* is the mirror degree of freedom that generates the negative dissipation of the system. The total Lagrangian of the total system is than produced in (2.52). Applying Lagrange's equations (2.40) to the Lagrangian yields zero and the equations of motion (2.50) and (2.51) as should be expected. This makes the Lagrangian in equation (2.52) of a dissipative system usable in a stationary action description as if it was monogenic [41, p. 298].

$$m\ddot{x} + \lambda\dot{x} + kx = 0 \tag{2.50}$$

$$m\ddot{x^*} - \lambda\dot{x^*} + kx^* = 0 \tag{2.51}$$

$$L(x(t), \dot{x}(t), x^*(t), \dot{x}^*(t)) = m\dot{x}\dot{x}^* - \frac{1}{2}\lambda(x^*\dot{x} - x\dot{x}^*) - kx x^* \tag{2.52}$$

These results are specific results for a damped harmonic oscillator. However the doubling of degrees of freedom and time contour integral procedure appears in various non-equilibrium quantum mechanical descriptions. For instance in the Schwinger-Keldysh formalism and closed time path formalism [42] this is encountered. It can be said that forward and backward integration here in classical mechanics is analogous to the description of non-adiabatic (non-conservative) quantum systems in the Schwinger-Keldysh formalism. Also there a contour time integral is performed over the whole time domain back and forth. To achieve this contour time integral a doubling of the degrees of freedom is performed through a natural isomorphism found in measure theory. This Choi-Jamiokolski isomorphism allows for doubling the quantum state from a mixed state in one Hilbert space to a pure state in a doubled Hilbert space [43]. This gives us an intuition that it is a natural way in non-conservative systems to be described with an action performed under doubled degrees of freedom in a contour integral to accommodate for information and energy transformation.

This aforementioned idea can be applied to the classical mechanics of discrete systems and continuous fields. This theory will be presented in this chapter but further extended in the next chapter 3. An application to damped harmonic oscillators in the context of the mimetic method is done in Section 3.2. The remainder of this section will present Galley's work which introduced a structured methodology of it in [44, 32].

Looking purely at the action, it was figured out by [44] that the principle of stationarity describes only systems that are time symmetric. A time symmetric system, as shown by Noether, is an energy (function)

conserving system [37, 34]. Energy function conserving systems are monogenic totally closed systems [36]. To resolve this hurdle, [44] introduced a formal doubling of the variables to become $i \in \{1, 2\}$ where $\mathbf{q}_i = (q_{1,i}, q_{2,i}, \ldots, q_{n,i})$. Here the integration of the second degree of freedom runs backwards to accommodate for the loss of energy such that a new doubled system is created for which we can write down a total Lagrangian in the way it is done for conservative and monogenic systems. This new Lagrangian avoids the necessity of time symmetry since it accommodates its need of a conserved energy (function) by retrieving back the lost energy through backward integration. So Lagrange's degrees of freedom are mapped to a doubled space:

$$\mathbf{q}(t) \rightarrow (\mathbf{q}_1(t), \mathbf{q}_2(t))$$

The action, $\mathcal{S}$, can than be written as in (2.53). Here the total Lagrangian, Λ, can be broken down in three parts as is shown in (2.54). We see that both individual sets of degrees of freedom run a classical monogenic/conservative Lagrangian L. To the histories of both sets of degrees of freedom we can add a generalized potential since this is allowed by the properties of the Lagrangian when we derive it from Alembert's principle [33]. This means that the non-conservative part K of the total Lagrangian Λ is a function of all degrees of freedom as it contains the generalized potential of both the physical and created degree of freedom. In this thesis this is often referred to as the coupling potential since it is a potential that couples the physical and imaginary degrees of freedom.

$$\mathcal{S}[\mathbf{q}_1, \mathbf{q}_2] = \int_{t_i}^{t_f} \Lambda(\mathbf{q}_1, \dot{\mathbf{q}}_1, \mathbf{q}_2, \dot{\mathbf{q}}_2, t) \, dt \tag{2.53}$$

$$\Lambda(\mathbf{q}_1, \dot{\mathbf{q}}_1, \mathbf{q}_2, \dot{\mathbf{q}}_2, t) = L(\mathbf{q}_1, \dot{\mathbf{q}}_1, t) - L(\mathbf{q}_2, \dot{\mathbf{q}}_2, t) + K(\mathbf{q}_1, \dot{\mathbf{q}}_1, \mathbf{q}_2, \dot{\mathbf{q}}_2, t) \tag{2.54}$$

The minus sign in the second term appears due to the fact that in the original formulation it is integrated from the final to the initial time in contrast to the standard direction of integration in first term. This is visualised in Fig. 2.9
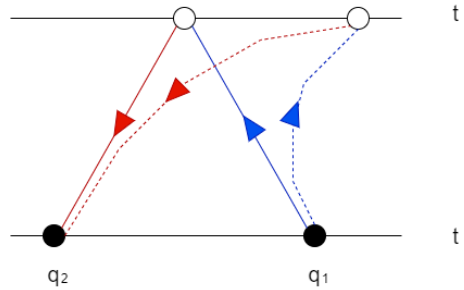
Figure 2.9: Paths of doubled degrees of freedom $\mathbf{q}_1$ and $\mathbf{q}_2$ from the initial time t_i to the final time t_f. Here filled dots allow no variation, because they are predetermined, in contrast to empty ones. The dashed lines are variation paths on the actual paths that are represented by filled lines. The blue and red lines represent the first and second of doubled degrees of freedom respectively.

Since this is an initial value problem the initial conditions of the degrees of freedom are fixed, $(\mathbf{q}_1(t_i), \mathbf{q}_2(t_i)) = (\mathbf{q}_{1,initial}, \mathbf{q}_{2,initial})$. This means that no variations will be introduced which results in: $(\delta\mathbf{q}_1(t_i), \delta\mathbf{q}_2(t_i)) = (\mathbf{0}, \mathbf{0})$. This dictates two of the four conditions that must be specified for the system to be uniquely determined. The second two conditions can be induced by the work of the action itself. Here the final values are kept variable since they are to be determined by the history of the degrees of freedom which is distinctive for a non-conservative irreversible motion. However the final values and generalized momenta are kept equal as Fig. 2.9 shows and can be written as: $\mathbf{q}_1(t_f) = \mathbf{q}_2(t_f)$ and $\pi_1(t_f) = \pi_2(t_f)$. This means that a variation $(\delta\mathbf{q}_1(t_f), \delta\mathbf{q}_2(t_f))$ can be non-zero [42].

The action integral then yields (2.56) after applying the variation (2.55) and implementing the conditions of the previous paragraph. Here ϵ is the variation parameter of the parameterized paths of the degrees of

freedom: $\mathbf{q}_i(t, \epsilon) = \mathbf{q}_i(t, 0) + \epsilon \delta \mathbf{q}_i(t)$. The individual integrands in equation (2.56) than become zero due to the fact that variations are arbitrary and thus Lagrange's equation (2.40) are satisfied as a consequence. Which is a necessary and required consequence of the action principle since complying with Euler-Lagrange is complying with Newton's laws of motion. Notice that the equivalence of the stationary action principle, Euler-Lagrange equations and Newton's equations of motions is applicable for energy (function) conservative systems and the doubled system is conserves the energy (function). Furthermore after performing manipulation to attain the physical relations, a physical limit needs to be introduced for the degrees of freedom. This physical limit is when the doubled degrees are equal to each other since the second history runs the same path inversely gaining back the lost energy (function) value.

$$\left[\frac{d\mathcal{S}}{d\epsilon} \right]_{\epsilon=0} = 0 \tag{2.55}$$

$$\sum_{i=1}^{n} \int_{t_i}^{t_f} dt \left(\delta q_{i,1} \left[\frac{\partial \Lambda}{\partial q_{i,1}} - \frac{d}{dt} \frac{\partial \Lambda}{\partial \dot{q}_{i,1}} \right]_{\epsilon=0} - \delta q_{i,2} \left[\frac{\partial \Lambda}{\partial q_{i,2}} - \frac{d}{dt} \frac{\partial \Lambda}{\partial \dot{q}_{i,2}} \right]_{\epsilon=0} \right) = 0 \tag{2.56}$$

Another way of doubling the degrees of freedom, which will be useful in the application to numerical analysis, is by defining the average and difference degrees of freedom of the two histories. The three equations below show the formal doubling, the definition of the average degree of freedom and the difference degree of freedom respectively. Here it can be clearly seen that the physical limit is when the average approaches the actual degree of freedom, $\mathbf{q}_+ \to \mathbf{q}$, and when the difference goes to zero: $\mathbf{q}_- \to \mathbf{0}$. It can also be easily noticed that they are independent degrees of freedom since one cant written as a function of the other only.

$$\mathbf{q}_i = (q_{1,i}, q_{2,i}, \ldots, q_{n,i}) \quad \forall i \in \{-, +\}$$

$$q_{i,+} \equiv \frac{q_{i,1} + q_{i,2}}{2}$$

$$q_{i,-} \equiv q_{i,1} - q_{i,2}$$

From this the total Lagrangian can be rewritten from equation (2.54) to become a function of the new degrees of freedom $\Lambda = \Lambda(\mathbf{q}_+, \mathbf{q}_-, \dot{\mathbf{q}}_+, \dot{\mathbf{q}}_-, t)$. Applying the same conditions but reformulated in terms of the new degrees of freedom we get the stationary action principle with the same consequence but as a function of the new degrees of freedom. Executing the physical limits leads to the same equations of motion for both degrees of freedom sets $\{1, 2\}$ and $\{+, -\}$. The equations of motion and Euler-Lagrange's equations can besides taking limits of (2.56), and its $\{+, -\}$-degrees of freedom counterpart, also be formulated through the functional derivatives shown in equation (2.57). Which is in essence the physical limit of a variational gradient with respect to a certain degree of freedom as is briefly introduced in Section 2.8. A formal treatment of functional derivatives in calculus of variations can be found in [45].

$$\left[\frac{\delta \mathcal{S}}{\delta q_{i,-}} \right]_{PL} = 0 \tag{2.57}$$

A step-by-step derivation of the non-conservative total Lagrangian Λ in equation (2.54) for a damped harmonic oscillator follows now. Here is the usual Lagrangian $L = T - U$ and how it fits with coupling potential K, i.e. source of the non-monogenic force, to give the total Lagrangian shown below:

$$L = \frac{1}{2} m \dot{x}^2 - \frac{1}{2} k x^2$$

$$\Lambda(\dot{x}_1, \dot{x}_2, x_1, x_2, t) = L(x_1, \dot{x}_1, t) - L(x_2, \dot{x}_2, t) + K(\dot{x}_1, \dot{x}_2, x_1, x_2, t)$$

The doubled (front and back going) conservative Lagrangian $L(\dot{x}_1, x_1) - L(\dot{x}_2, x_2)$ can be written as:

$$L(\dot{x}_1, x_1) - L(\dot{x}_2, x_2) = \frac{1}{2}m(\dot{x}_1^2 - \dot{x}_2^2) - \frac{1}{2}k(x_1^2 - x_2^2)$$

Rearranging the degrees of freedom makes this equation:

$$L(\dot{x}_1, x_1) - L(\dot{x}_2, x_2) = m\frac{(\dot{x}_1 + \dot{x}_2)}{2}(\dot{x}_1 - \dot{x}_2) - k\frac{(x_1 + x_2)}{2}(x_1 - x_2)$$

Since the average $\frac{(x_1 + x_2)}{2} \equiv x_+$ and difference $x_1 - x_2 \equiv x_-$ degrees of freedom are now identified we can write the sum of the back and forth standard Lagrangian, L_{dc}, as below:

$$L_{dc}(\dot{x}_+, \dot{x}_-, x_+, x_-) = L(\dot{x}_1, x_1) - L(\dot{x}_2, x_2) = m\dot{x}_+\dot{x}_- - kx_+x_-$$

The non-conservative term K of the total Lagrangian Λ, that makes the system satisfy monogenity and thus being closed (up to possible explicit time dependence), is shown below[32]. A method to obtain this term is shown in Section 3.2.4.

$$K(\dot{x}_+, \dot{x}_-, x_+, x_-, t) = -\lambda x_- \dot{x}_+ \tag{2.58}$$

The total Lagrangian Λ is than completed in the following equation (2.59) :

$$\Lambda(\dot{x}_+, \dot{x}_-, x_+, x_-, t) = m\dot{x}_+\dot{x}_- - kx_+x_- - \lambda x_- \dot{x}_+ \tag{2.59}$$

In Section 3.2.4 a general procedure is suggested with which we can obtain the non-conservative part K of the total Lagrangian Λ. Furthermore since the boundary conditions are 'too rigid' to work with in numerical analysis a new set of integration conditions is introduced. This leads to obtaining a new more suitable Lagrangian for the use in numerical computations.

2.8. A Variational Calculus Perspective of the Action

This section introduces the basics of calculus of variations to describe the formulation of the functional derivative and its integrarion. Furthermore, some relevant properties of the extremals and inflections are discussed. Also the solution space of the stationary problem is given such that it is well-defined and how to define numerical errors with respect to this exact solution. These extremals and inflections are the degrees of freedom functions (paths) that make the action stationary. The variables of the case study in this thesis, harmonic oscillators, are used.

2.8.1. Basics of First Variations

The action of an objective (one dimensional) functional L is the integral of (2.60). The variation $\delta\mathcal{S}(x, \delta x_-)$ of this functional integral - action $\mathcal{S}$ - at x in the direction of the variational function of x namely δx is defined in (2.61) where δx is some function in t. This is called the first variation of the calculus of variations which is the same as (2.43) in Section 2.6. The gradient $\delta\mathcal{S}$ (also called variation of it) can be defined through imposing an L^2-inner product between this gradient and the variational function δx as shown in the left side of (2.62) [46].

$$\mathcal{S}[x] = \int_{t_i}^{t_f} L(x, \dot{x}, t)dt \tag{2.60}$$

$$\delta\mathcal{S}(x, \delta x) := \frac{d}{d\epsilon}\mathcal{S}[x + \epsilon\delta x]|_{\epsilon=0} \tag{2.61}$$

$$\langle \delta\mathcal{S}[x] \; ; \; \delta x \rangle := \delta\mathcal{S}(x, \delta x) \tag{2.62}$$

Assuming that the functional L has continuous second derivatives, C^2, we arrive at (2.63) [47] after applying the chain rule. This gives the integral in terms of derivatives of the objective functional and the variational function.

$$\delta\mathcal{S}(x, \delta x) = \int_{t_i}^{t_f} \left(\delta x \frac{\partial L}{\partial x}(t, x, \dot{x}) + \delta\dot{x}\frac{\partial L}{\partial \dot{x}}(t, x, \dot{x}) \right) dt \tag{2.63}$$

Applying integration by parts to (2.63) gives (2.64) below:

$$\delta\mathcal{S}(x, \delta x) = \int_{t_i}^{t_f} \delta x \left(\frac{\partial L}{\partial x}(t, x, \dot{x}) - \frac{d}{dt}\frac{\partial L}{\partial \dot{x}}(t, x, \dot{x}) \right) dt + \left[\frac{\partial L}{\partial \dot{x}}(t, x, \dot{x})\delta x \right]_{t_i}^{t_f} \tag{2.64}$$

A stationary $\mathcal{S}$ means that the (2.61), and so (2.64) is zero for arbitrary variations with the specified initial and final states. If variation function is zero at the initial and final state, i.e. the states are specified, than the boundary term in (2.64) becomes zero. This leads to the fact that the action gradient $\delta\mathcal{S}[x]$ in (2.62) is actually an Euler-Lagrange equation of (2.40) that equals zero [46]. Which is a consequence of the action principle for monogenic systems as mentioned before in Section 2.6.

A zero value for (2.63) and (2.64) does not necessarily mean that extremals are necessarily minimizations of the action since they can be inflections (or saddle points). For it to be a minimization two conditions must be satisfied. The first one is the vanishing of Lagrange's equation in (2.40). Next the second derivative of the action with respect to the variation quantifier, $h(\epsilon) = \mathcal{S}[x + \epsilon\delta x]$, must be positive at the solution. The general Hamilton's principle however does not state that the action must be minimized but to be stationary [48]. So no such conditions need to be introduced on the second derivative of the action with respect to the quantifier. A formal treatment of calculus of variations can be found in [45].

2.8.2. Solution Spaces and A Priori Approximation Errors

The considered class of admissible functions (degrees of freedom) in the space of solutions only contains functions that are square integrable on the computation domain T [31]. These are the functions $x(t), \forall t \in T$, that are elements of the space below. We also say that the L^2-norm of the function $x(t)$, $||x(t)||^2_{L^2(T)} = \int_T |x(t)|^2 \, dt$, exists and is finite.

$$L^2(T) := \left\{ x(t) \Big| \int_T |x(t)|^2 \, dt < \infty \right\}$$

Besides this the exact functions $x(t)$ must satisfy the boundary conditions and be weakly differentiable since the stationarity is formulated in degrees of freedom and their derivatives. This means that the solutions are in the first Sobolev space $H^1 := W^{1,2}$ that is defined below. Here $D^\alpha x$ is the weak derivative of α order [49]. This ensures that the problem is well-defined. The H^1-norm in this space $H^1(T)$ is than $||y(t)||^2_{H^1(T)} = ||y(t)||^2_{L^2(T)} + ||D^1 y(t)||^2_{L^2(T)}$. For a review of the theory of Sobolev space see [49].

$$W^{1,2}(T) = \{x | D^\alpha x \in L^2(T), \forall |\alpha| \leq 1\}$$

This is a definition of Sobolev spaces for scalar functions, but Sobolev spaces for k-forms can also be defined in the same manner. The L^2-norms are then obtained through simply the duality pairing (integration) on the domain such that $||x^{(k)}||^2_{L^2 \Lambda^k(T)} = \int_T x^{(k)} \wedge \star x^{(k)}$. The exact solutions of primal 0-forms (positions) in this work are in $H^1 \Lambda^0(T)$, first Sobolev space of zero forms, such that at least their first weak derivatives in the exterior 1-bundle have a finite L^2-norm on the domain T of this bundle. The primal 1-forms (velocities) are in the $L^2 \Lambda^1(T)$ space of 1-forms. This means that the dual 0-forms (momenta) are in $L^2 \tilde{\Lambda}^0(T)$ since they are simply Hodges of them multiplied with mass. The approximate solution is in the projection space which is a N-th order polynomial vector space of k-differential forms $\mathcal{P}_N \Lambda^k(T) \subseteq \Lambda^k(T, C^k(D)) \subset \Lambda^k(T)$ [7]. As mentioned the primal forms treated in this thesis are either one or zero forms; $k = 0$ or $k = 1$.

Now the error with respect to the mimetic approximation ϵ_x of the primal 0-form (positions) can be computed in the H^1-norm as:

$$\epsilon_x^2 = ||x^{(0)} - x^h||^2_{H\Lambda^1(T)} = ||x^{(0)} - x^h||^2_{L^2 \Lambda^0(T)} + ||\dot{x}^{(1)} - \dot{x}^h||^2_{L^2 \Lambda^1(T)}$$

Furthermore errors with respect to the mimetic approximation ϵ_π of the dual 0-form (momenta) are than computed in the L^2-norm as below. Notice that due to the Hodge operator it is equal up to a constant to the same error of the primal 1-form (velocities) in this study.

$$\epsilon_\pi^2 = ||\pi^{(0)} - \pi^h||^2_{L^2 \tilde{\Lambda}^0(T)}$$

The error of the 1-form energy ϵ_E is calculated by:

$$\epsilon_E^2 = ||E^{(1)} - E^h||^2_{L^2 \Lambda^1(T)}$$

The approximations are reconstructed using the mimetic spectral element basis functions. They consist of Lagrange polynomials and edge functions introduced in Section 2.5. Application of the a priori error estimates proposed by [50], the error should converge as is shown in the equation. Where Δt is the element time length and N is the GLL Lagrange polynomial order while C_x and C_π are constants independent of them.

$$\epsilon_x \leq C_x \Delta t^N \quad \wedge \quad \epsilon_\pi \leq C_\pi \Delta t^N$$

The solution is thus convergent with a decreasing time length of elements in the mesh. We can deduce that with mesh Δt-refinement the logarithm of the number of elements has a descending linear relation with the logarithm of the errors. The rate of convergence is than $l \geq N$. This can be seen from taking the

natural logarithm of the error $ln(\epsilon) \leq ln(C\Delta^N)$. This implies that $ln(\epsilon) \leq D - N \cdot ln(K)$ where $K = \frac{T}{\Delta t}$ is the amount of elements and $D = ln(CT^N)$ is a constant independent of Δt. On Δt-refinement plots we can find the slope s to satisfy $l = -s \geq N$ where s is:

$$s = \frac{ln(\epsilon_{K_2}) - ln(\epsilon_{K_1})}{ln(K_2) - ln(K_1)}$$

Additionally when $x^{(0)} \in H^1\Lambda^0(T)$ and x^h is a polynomial of order N, a famous result in Galerkin methods is that the error in $L^2\Lambda^1(T)$ is proportional to the order of approximation polynomials N as is shown in the equation below [51]. This means that the relation can be visualised as a descending linear function when the scale of the y-axis is logarithmic as below where B and β are constants.

$$ln||x^{(0)} - x^h(t)||_{L^2\Lambda^0(T)} = B - \beta N$$

2.9. The Theory of Harmonic Oscillators

The harmonic oscillator model is not applicable only to spring mass systems or pendulums. These are just examples where physical phenomena can be modelled by this abstraction. Other examples are the mechanics of atoms in a lattice or behaviour in electric circuits. In this work the mass spring system shown in Fig. 2.10 is considered as the practical model to look at.
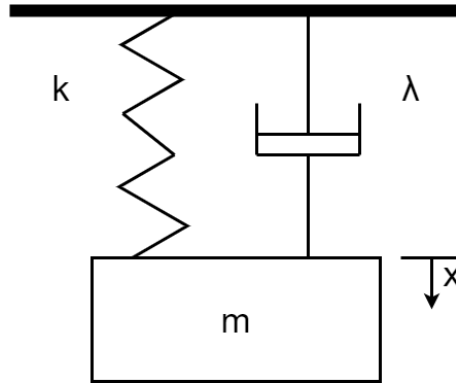
Figure 2.10: The set up of a damped mass spring system.

In the case of simple harmonic oscillator the force that describes the motion is obtained from Hooke's law $F_k = -kx$. Which means that it is derivable from a time independent scalar potential. Now Newton's second law is a second order linear differential equation (2.65) that can analytically be solved to result in (2.66). The simple frequency of the oscillations is given by $\omega_0 \equiv \sqrt{\frac{k}{m}}$.

$$m\ddot{x} + kx = 0 \tag{2.65}$$

$$x(t) = X_1 sin(\omega_0 t) + X_2 cos(\omega_0 t) \tag{2.66}$$

From a Lagrangian mechanics perspective this is a scleronomous, holonomic monogenic (conservative) system, so the force stems from a (generalized) potential. The standard Lagrangian can simply be formulated to be the difference between the kinetic energy and the potential energy as shown below:

$$L(t, x(t), \dot{x}(t)) = \frac{1}{2}m\dot{x}^2(t) - \frac{1}{2}kx^2(t)$$

In contrast to the previous system a damped harmonic oscillator has an additional force involved that damps the motion. This force is proportional to the velocity of the mass such that, $F_\lambda = -\lambda\dot{x}$, which can not be formulated thought a generalized velocity potential [33]. Notice that this makes it a non-monogenic, and by default a non-conservative system, as discussed in Section 2.7. The kinetics of the system due to Newton's second law yields a second order differential equation (2.67). This equation can be rewritten as (2.68). Here $\omega_0 \equiv \sqrt{\frac{k}{m}}$ the simple frequency and $\beta \equiv \frac{\lambda}{2m}$ is the damping parameter.

$$m\ddot{x} + \lambda\dot{x} + kx = 0 \tag{2.67}$$

$$\ddot{x} + 2\beta\dot{x} + \omega_0^2 x = 0 \tag{2.68}$$

Differential equation (2.68) yields three types of analytical solutions of the initial value problem depending on the relation of the simple frequency to the damping parameter. Underdamping is when $\omega_0^2 > \beta^2$, critical damping is when $\omega_0^2 = \beta^2$ and overdamping is when $\omega_0^2 < \beta^2$. The solutions for the positions x are given respectively in equations (2.69), (2.70) and (2.71).

$$x(t) = Xe^{-\beta t}cos(\omega_1 t - \delta) \tag{2.69}$$

$$x(t) = (X_1 + X_2 t)e^{-\beta t} \tag{2.70}$$

$$x(t) = e^{-\beta t}[X_1 e^{\omega_2 t} + X_2 e^{-\omega_2 t}] \tag{2.71}$$

The characteristic frequencies of the underdamped and overdamped motion are defined respectively as $\omega_1^2 = \omega_0^2 - \beta^2$ and $\omega_2^2 = \beta^2 - \omega_0^2$. The dependence of integration constants X, X_1, X_2, δ on the initial conditions in the solutions above is given in Appendix A. Note that these constants are different dependent on the damping situation. The velocity $\dot{x}(t)$, acceleration $\ddot{x}(t)$, momentum $\pi(t) = m\dot{x}(t)$ and total force $\dot{\pi}(t) = m\ddot{x}(t)$ are simply obtained through the familiar derivatives.

From a Lagrangian mechanics perspective this is a totally closed holonomic, scleronomous, non-monogenic system. The part of generalized force that can be obtained through a generalized (velocity) potential is a scalar potential that is time independent as shown in Hook's law in the beginning of this section. From Section 2.7 this implies that the energy function is equal to the mechanical energy, $E = E_{mech}$, of the damped harmonic system. Mechanical energy is in turn equal to the sum the kinetic energy of the mass added to the potential energy of the spring. This is shown below in equation (2.72).

$$E(t) = E_{mech}(t) = \frac{1}{2}m\dot{x}^2(t) + \frac{1}{2}kx^2(t) \tag{2.72}$$

The derivative of the mechanical energy is equal to the derivative of the energy function. How to obtain the derivative of the energy function of a totally closed non-monogenic is shown in Section 2.6. Applying this to the damped harmonic oscillator gives (2.73). The change of the mechanical energy of the system with time, i.e. dissipation, is than also given below in equation (2.73) below. Asserting the generalized force to be $-\lambda\dot{x}$ through doubling degrees of freedom is shown later in Section 3.2.3 in (3.17).

$$\frac{dE_{mech}}{dt}(t) = \frac{dE}{dt}(t) = \dot{x}F_\lambda = -\lambda\dot{x}^2(t) \tag{2.73}$$

These two properties, E and E_{mech}, can be interchanged in this work in the context of the damped harmonic oscillator whenever convenient since they are equal.

We can also obtain a Lagrangian functional that satisfies homogeneity of the Euler-Lagrange differential equation (2.40) and thus the equation of motion (2.68) through a transformation of the variables that make the differential equation of motion look like an undamped one [38]. This yields the formulation $L_{modified}$ shown in (2.74). The last term is a gauge fixing term that also satisfies Lagrange's equations (2.40) on itself. However we notice that the system becomes not totally closed due to this transformation due to the explicit dependence of $L_{modified}$ on time. This means that this system can be seen as either totally closed and non-monogenic or closed up to an explicit time dependence of Lagrangian on time and monogenic. We observe that this formulation is not useful for application in the mimetic spectral element used here due to the this explicit dependence. Namely, we prefer a Lagrangian that explicitly depends on configuration or source variables alone and not on (time) domain itself.

$$L_{modified}(t, x, \dot{x}) = e^{\frac{-\lambda}{m}t}\left(\frac{1}{2}m\dot{x}^2 - \frac{1}{2}kx^2\right) + \frac{d}{dt}\left[\frac{1}{4}\lambda x^2 e^{\frac{\lambda}{m}t}\right] \tag{2.74}$$

The analytical solution of the overdamped case is shown in Fig. 2.11. The position, momentum and energy as functions of time are shown in Fig. 2.11 (a), (b) and (c) respectively with initial conditions position $x_i = 1$ and momentum $\pi_i = 1$. After a slight increase in the deviation due to the initial velocity the position goes to the equilibrium state as is expected due the loss of potential spring energy. The momentum and energy go to zero in the limit which is expected due to the loss of kinetic energy for momentum and energy as a whole. The momentum position is shown in Fig. 2.11 where the degrees of freedom $(x, \dot{x})$ start from
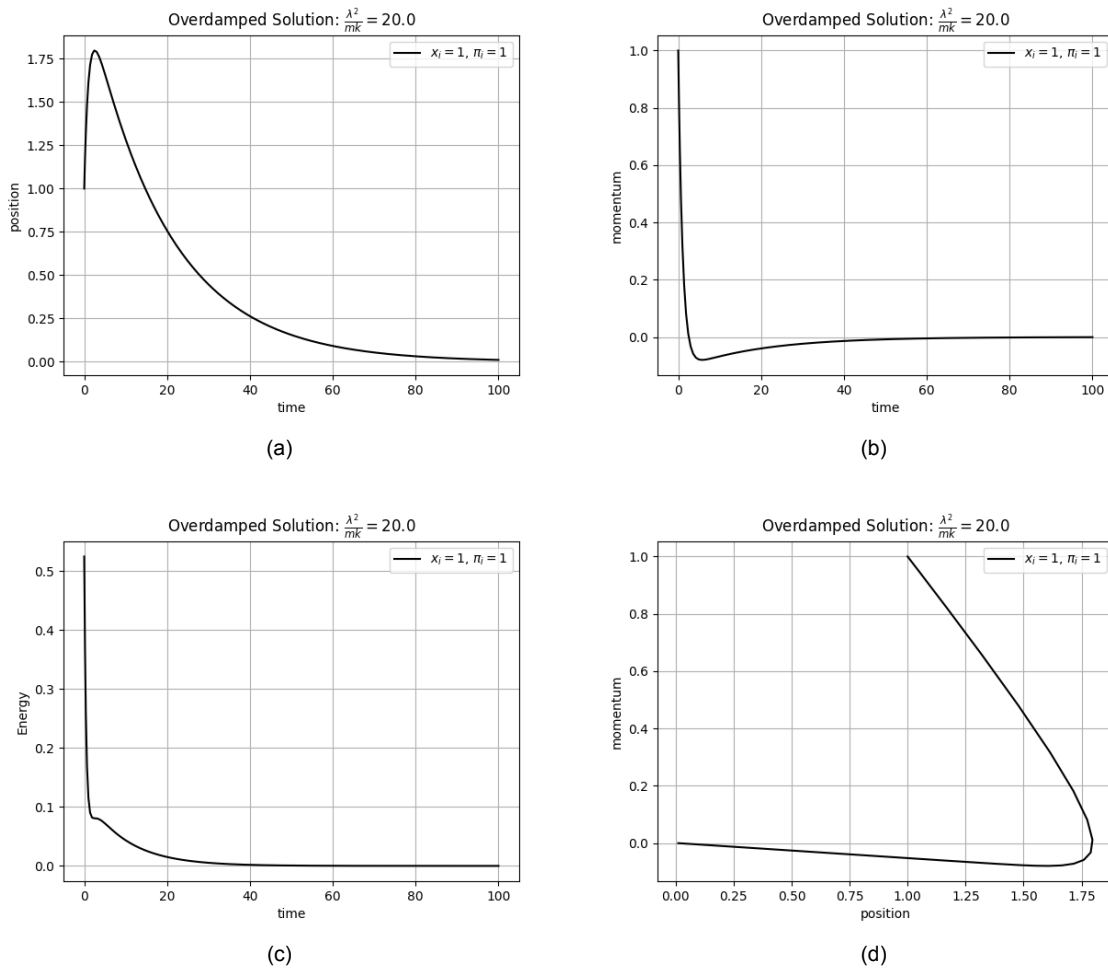
Figure 2.11: (a) Evolution of position of an overdamped oscillator with time **(b)** Evolution of momentum of an overdamped oscillator with time **(c)** Evolution of energy of an overdamped oscillator with time **(d)** Momentum in relation to position of an overdamped oscillator

the initial conditions and end at the equilibrium zero state. The same behaviour can be observed for the underdamped case as shown in Fig. 2.12 (a), (b), (c) and (d) in the same order under the same initial conditions. The difference that characterizes the underdamped case is that the mass is oscillating with a decreasing amplitude to zero.
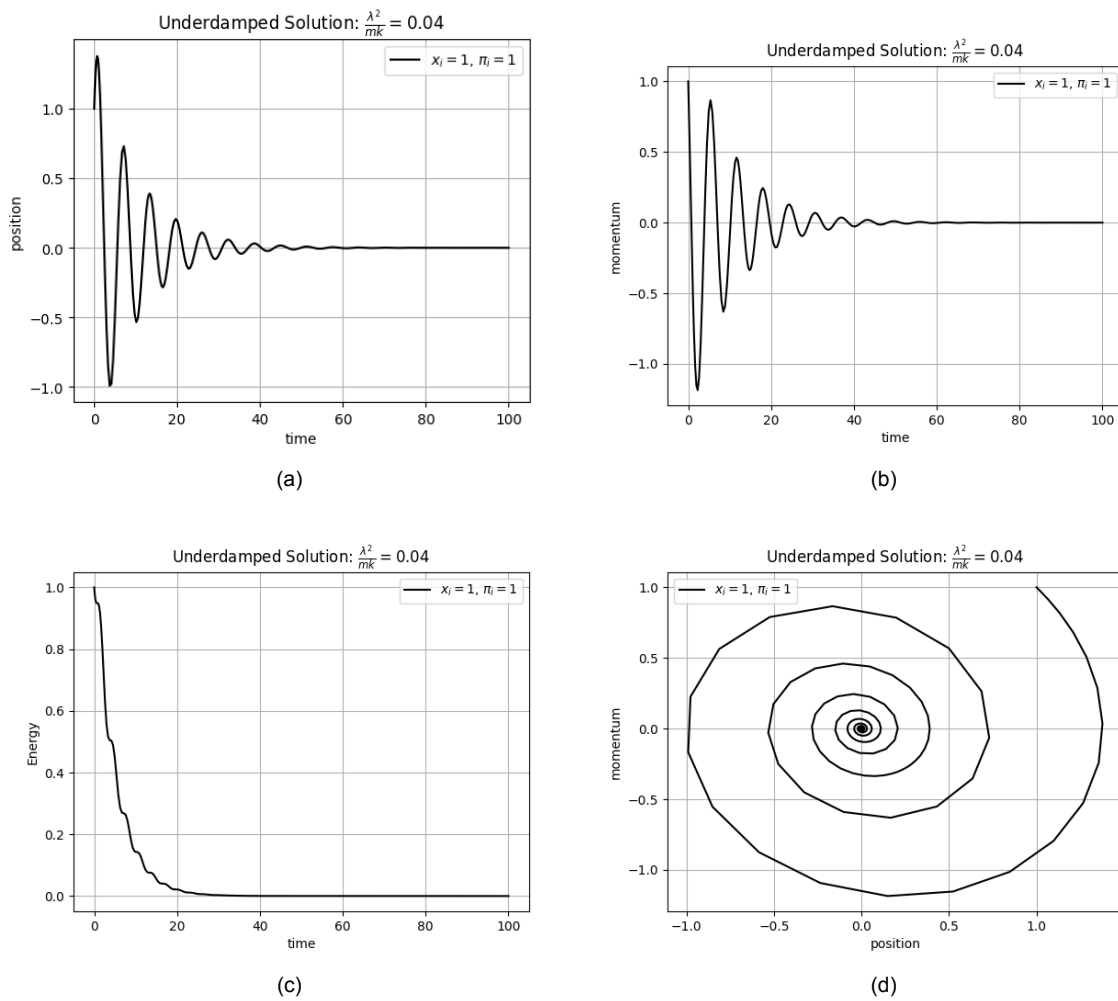
Figure 2.12: **(a)** Evolution of position of an underdamped oscillator with time **(b)** Evolution of momentum of an underdamped oscillator with time **(c)** Evolution of energy of an underdamped oscillator with time **(d)** Momentum in relation to position of an underdamped oscillator

3

Discrete Damped Harmonic Oscillator

This part presents an application of the mimetic method to a specific non-conservative system, namely the damped harmonic oscillator presented in Section 2.9. First a differential and discrete geometry of the system is identified and the variables are formulated in terms of differential forms and co-chains. Than the doubling method is modified to accommodate for the use of algebraic dual polynomials as variations and introduce initial conditions. From these a discrete is scheme is set up to obtain results of the different cases of solutions. Finally compliance with the conservation of energy is treated.

3.1. A Geometry of the Damped Harmonic Oscillator

We start by first defining the topological space in which the physics of the damped harmonic oscillator happens and by what kind of geometrical objects the physical variables are described. The manifold of time $\mathcal{M}$ is a 1-manifold on which the physical variables live. To determine what is chosen as inner orientation and what as outer orientation the guidelines of Tonti [23] are used. The configuration variables, which are the degrees of freedom of the Lagrangian, are position and velocity. The source variables are than the forces and momenta. Toni [23] states that through examination, the configuration variables are inner oriented and source variables are outer oriented. So the position $x^{(0)}(t)$ of the mass is defined as a primal 0-form. This means that position is associated with a point (0-sub-manifold) which is a time instant. Velocity $\dot{x}^{(1)}(t)$ can be defined as an inner 1-form that is the exterior derivative of the position: $\frac{d}{dt}x^{(0)}(t)dt = \dot{x}^{(1)}(t)$. Thus velocity is associated with lines (1-sub-manifolds) which are time increments. The Hodge of position can be seen as the spring force at unit stiffness outer oriented 1-form: $\star x^{(0)}(t) = \frac{1}{k}\sigma^{(1)}(t)$. Taking the Hodge of velocity $\star\dot{x}^{(1)}(t) = \frac{1}{m}\pi^{(0)}(t)$ gives the outer-oriented 0-form which is the velocity related to a point. This can be seen as the momentum per unit mass. The exterior derivative of the momentum $\frac{d}{dt}\pi^{(0)}(t)dt = \dot{\pi}^{(1)}(t)$ is the 1-form actual total force related to lines. The mechanical energy given in (2.72) can be defined on a time increment using the wedge product from section (2.3.2) as:

$$E^{(1)}(t) = \frac{m}{2}\dot{x}^{(1)}(t) \wedge \star\dot{x}^{(1)}(t) + \frac{k}{2}x^{(0)}(t) \wedge \star x^{(0)}(t)$$

When evaluating the Hodges this becomes a topological exact relation as below:

$$E^{(1)}(t) = \frac{1}{2}\dot{x}^{(1)}(t) \wedge \pi^{(0)}(t) + \frac{1}{2}x^{(0)}(t) \wedge \sigma^{(1)}(t)$$

The exterior derivative of the Hodge of energy is equal to dissipation as shown in Section 2.9. It is formed by multiplication of the dissipation force F_λ, which is a source variable, and derivative of the degree of freedom $\dot{x}$ which is a configuration variable. Thus due to Tonti [23] the force is chosen to have an outer orientation and the degree of freedom to have an inner orientation. This gives the outer dissipation force $\tilde{F}_\lambda^{(0)} = -\lambda \star \dot{x}^{(1)} = -\lambda\pi^{(0)}$. The dissipation of (mechanical) energy is than in (3.1) below:

$$d\tilde{E}^{(0)}(t) = \dot{x}^{(1)} \wedge \tilde{F}_\lambda^{(0)} = -\frac{\lambda}{m}\dot{x}^{(1)} \wedge \pi^{(0)} \tag{3.1}$$

The differential equation in Section 2.9 that discribes the kinetics of the damped harmonic oscillator can than be written in exterior calculus formulation as:

$$\dot{\pi}^{(1)}(t) - \star \tilde{F}_{\lambda}^{(0)}(t) + \sigma^{(1)}(t) = 0$$

All these (zero and one) forms are sections in the 1-exterior bundle on the time manifold $\mathcal{T}: \Lambda^k \mathcal{T}$. We want to obtain an approximation of these variables through a projection π_h to a polynomial subspace in $\Lambda^k(\mathcal{T}, C_k)$ of this exterior bundle as is shown in the diagram of Fig. 2.5 in Section 2.4.2 for $k = 1$. This is explained in the following paragraphs.

We follow the projection diagram shown in Fig. 2.5 to obtain reductions and reconstruction of the forms and thus their respective geometries. First we reduce (inner oriented) sections to co-chains related to cells in the cell complex of the of the N-th order GLL-grid of Fig. 3.1 with the reduction operator $\mathcal{R}$. The (one and zero) cells of the cell complex here are embedded in the time manifold as a chain of $(N + 1)$ points $\mathbf{t}_{(0)} = \{\tau_0, \tau_1, \ldots, \tau_N\}$ and a chain of N lines $\Delta \mathbf{t}_{(1)} = \{[\tau_0, \tau_1], [\tau_1, \tau_2], \ldots, [\tau_{N-1}, \tau_N]\}$. Their locations are determined by the GLL-grid construction in Section 2.4.1. The union of both is the cell complex shown on the right side in Fig. 3.1. With the reduction of $x^{(0)}(t)$ at 0-cells in the 0-chain $\mathbf{t}_{(0)}$, i.e. evaluating $x^{(0)}(t)$ at time instants t_j associated with the vector $\tau_j \in \mathbf{t}_{(0)}$, we can obtain the co-chain $\mathbf{x}^{(0)} = (x^0 \ x^1 \cdots x^N)^T$ in vector form. Here we have that $x^j = x^{(0)}(t_j)$. Reduction of $\dot{x}^{(1)}$ over the chain of lines in the GLL-grid is done by integration over each line. The co-chain obtained is written in vector form as $\dot{\mathbf{x}}^{(1)} = (\dot{x}^1 \ \dot{x}^2 \cdots \dot{x}^N)^T$ where $\dot{x}^j = \int_{t_{j-1}}^{t_j} \dot{x}^{(1)}(t)$.
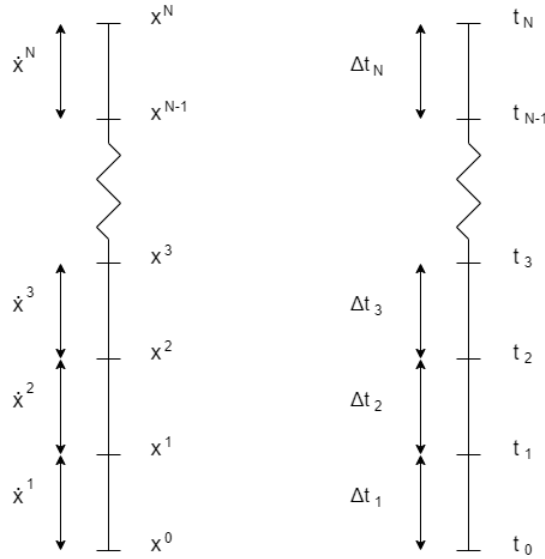
Figure 3.1: The topology of the primal co-chain is left and the associated primal grid (chain) on the right

We reconstruct the approximate primal forms from the co-chains using the algebraic dual polynomials in Section 2.5. As mentioned this is possible since these polynomials satisfy the properties of the reconstruction operator $\mathcal{I}$. The fundamental property of reconstruction, $\mathcal{I} \circ \mathcal{R} = Id$, is easily observed in (2.26) and (2.25) for the Lagrange polynomials and in (2.60) and (2.61) for the edge polynomials. The primal 0-forms, $x^{(0)}(t)$, are approximated by a linear combination of the Lagrange basis polynomials and 1-forms, $\dot{x}^{(0)}(t)$, by the edge basis polynomials. The co-chain elements, x^i and $\dot{x}^i$ respectively, are their coefficients and thus the approximations are in a polynomial subspace in space $\Lambda^k(\mathcal{T}, C_k) \subset \Lambda^k \mathcal{T}$. The composition $\mathcal{R} \circ \mathcal{I}$ which is the projection π_h operator from the exact to the approximate forms, as in Fig. 2.5, then works as in the equations below. Notice the polynomials $h_i(t)$ and $e_i(t)$ are the Lagrange and edge polynomials respectively over the $[t_i, t_f]$ domain.

$$\pi_h x^{(0)}(t) = x^h(t) = \sum_{i=0}^{N} x^i h_i(t)$$

$$\pi_h \dot{x}^{(1)}(t) = \dot{x}^h(t) = \sum_{i=1}^{N} \dot{x}^i e_i(t) dt$$

Since the position $x^{(0)}$ and velocity $\dot{x}^{(1)}$ are related through the exterior derivative we can relate their co-chains applying the exterior derivative relation to their projections:

$$\dot{x}^h(t) = \frac{d}{dt} x^h(t) dt = \sum_{i=1}^{N} (x^i - x^{i-1}) e_i(t) dt$$

Reducing this result gives the relation between the zero and one co-chain by the co-boundary operator $\mathbb{E}^{1,0}$ as (3.2) shows. The incidence matrix $\mathbb{E}_p^{1,0}$ with N rows and $(N+1)$ columns is expanded in (3.3). This relation could be obtained directly by applying the co-boundary on the already existing co-chains. This is because the exterior derivative / co-boundary commute by the definition of reduction [8]. This is true since we can first observe that $\delta \circ \mathcal{R} \circ x^{(0)}(t) = \delta \circ \mathbf{x}^{(0)}$ and $\mathcal{R} \circ d \circ x^{(0)}(t) = \mathcal{R} \circ \dot{x}^{(1)}(t) = \dot{\mathbf{x}}^{(1)}$ and that $\delta \circ \mathcal{R} = \mathcal{R} \circ d$ so we conclude that $\delta \circ \mathbf{x}^{(0)} = \dot{\mathbf{x}}^{(1)}$.

$$\dot{\mathbf{x}}^{(1)} = \mathbb{E}_p^{1,0} \mathbf{x}^{(0)} \tag{3.2}$$

$$\mathbb{E}_p^{1,0} = \begin{bmatrix} -1 & 1 & & & \\ & -1 & 1 & & \\ & & \ddots & \ddots & \\ & & & -1 & 1 \\ & & & & -1 & 1 \end{bmatrix}$$

The projections of the inner position and inner velocity can be written in array multiplication as below. Here polynomial horizontal vectors $\mathbf{h}(t)$ and $\mathbf{e}(t)$ are defined as $\mathbf{h}(t) = (h_0(t)\, h_1(t) \cdots h_N(t))$ and $\mathbf{e}(t) = (e_1(t)\, e_2(t) \cdots e_N(t))$.

$$x^h(t) = \mathbf{h}(t) \mathbf{x}^{(0)}$$

$$\dot{x}^h(t) = \mathbf{e}(t) dt \dot{\mathbf{x}}^{(1)}$$

To get from the inner to the outer oriented projected forms, constructed from dual to the primal co-chains, we need a discrete Hodge operator as analogue to the classical Hodge star. First we notice that the outer momentum $\pi^h(t)$, which is the projection of the Hodge of the velocity times the mass $m \star \dot{x}^h(t)$, can be defined with some linear combination of polynomials as is shown below:

$$\pi^h(t) = \tilde{\mathbf{h}}(t) \boldsymbol{\pi}^{(0)}$$

The Hodge of the inner velocity can be written as below where $\overline{\mathbb{M}}^{(0)}$ is the mass matrix of reference edge functions determined in Section 2.5. It stems from the integration of the inner product of the inner velocity with its Hodge over the whole domain [10]. This gives a co-chain associated with points on the dual grid that are dual to the lines of the velocity co-chain.

$$\star \dot{x}^h(t) = \mathbf{e}(t) \dot{\mathbf{x}}^{(1)} = \mathbf{e}(t) \left(\frac{2}{t_f - t_i} \overline{\mathbb{M}}^{(1)} \right)^{-1} \frac{2}{t_f - t_i} \overline{\mathbb{M}}^{(1)} \dot{\mathbf{x}}^{(1)}$$

So the polynomial array for the linear combination to construct $\pi^h(t)$ are $\tilde{\mathbf{h}}(t) = (\tilde{h}_1(t)\, \tilde{h}_2(t)\cdots \tilde{h}_N(t))$ which are the dual edge polynomials introduced in Section 2.5. As for $\boldsymbol{\pi}^{(0)} = (\pi^1\, \pi^2 \cdots \pi^N)^T$ it is the dual co-chain related to points on the dual grid in Fig. 3.2. Thus the discrete Hodge operator on the inner velocity co-chain that gives the outer velocity co-chain is $\frac{2}{t_i - t_f}\overline{\mathbb{M}}^{(1)}$. Which gives the relation between instantaneous momentum chain and velocity chain as in (3.3) below. It is easy to show that the reduction after reconstruction identity property again holds here for these reconstruction polynomials.

$$\boldsymbol{\pi}^{(0)} = \frac{2m}{t_f - t_i}\overline{\mathbb{M}}^{(1)}\dot{\mathbf{x}}^{(1)} \tag{3.3}$$
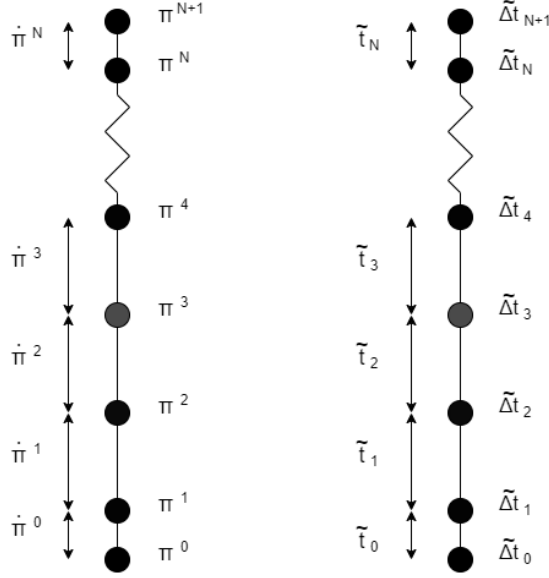
Figure 3.2: The topology of the dual co-chain is left and the associated dual grid (chain) on the right. Notice that the dual grid is not an actual grid of points and lines, but the dual co-cochain behaves as if it is reduced to a dual grid with this topology.

The same process can be repeated for the outer oriented spring force $\sigma^{(1)}(t)$. We obtain a discrete Hodge of the position 0-co-chain to spring force 1-co-chain as $\frac{t_f - t_i}{2}\overline{\mathbb{M}}^{(0)}$. The equations below are the approximation projection of the spring force and the relation between the two aforementioned co-chains. Here similarly row vector $\tilde{\mathbf{e}}(t)$ consists of the $(N+1)$ dual Lagrange polynomials and the column vector $\boldsymbol{\sigma}^{(1)}$ is the spring force co-chain associated to the lines in dual grid Fig. 3.2.

$$\sigma^h(t) = \tilde{\mathbf{e}}(t)dt\boldsymbol{\sigma}^{(1)}$$

$$\boldsymbol{\sigma}^{(1)} = \frac{k(t_f - t_i)}{2}\overline{\mathbb{M}}^{(0)}\mathbf{x}^{(0)}$$

We can reduce the 1-form force to the lines of the dual grid through integration between the momentum points. These are the time intervals between the instants t_{s+1} and t_s where $\pi^{s+1} - \pi^s = \pi^h(t_{s+1}) - \pi^h(t_s)$ $\forall s \in \{1, \ldots, N\}$. Even though we do not know where these points lie we can get a topological relation between them through this reduction. Reduction of $\dot{\boldsymbol{\pi}}^{(1)}$ leads to a co-chain $\dot{\boldsymbol{\pi}}^{(1)} = (\dot{\pi}^2\, \dot{\pi}^3 \cdots \dot{\pi}^N)^T$. This reduction on the dual grid lines between the points t_s, above, $\forall s \in \{1, 2, \ldots, N\}$ is than shown as below:

$$\int_{t_{s-1}}^{t_s} \dot{\pi}^h(t) = \dot{\pi}^s \quad \forall s \in 2, 3, \ldots, N$$

Where $\dot{\pi}^h$ can be rewritten as $\frac{d}{dt}\pi^h dt$ so that we have:

$$\int_{t_{s-1}}^{t_s} \frac{d}{dt}\pi^h(t)\, dt = \pi^s - \pi^{s-1} \quad \forall s \in \{2, 3, \ldots, N\}$$

We have now a relation between the 0-co-chain and 1-co-chain of the pseudo forms:

$$\begin{bmatrix} \pi^2 - \pi^1 \\ \pi^3 - \pi^2 \\ \vdots \\ \pi^N - \pi^{N-1} \end{bmatrix} = \begin{bmatrix} \dot{\pi}^2 \\ \dot{\pi}^3 \\ \vdots \\ \dot{\pi}^N \end{bmatrix}$$

As can be seen from the dual grid in Fig. 3.2 the two lines before t_1 and after t_N are not included. To reduce $\dot{\pi}^{(1)}$ to these line-cells, so that we can work with a complete cell complex that covers the whole time-manifold, we integrate from the initial time t_i to t_1 and from t_N to the final time t_f.

$$\int_{t_i}^{t_1} \dot{\pi}^h(t) = \dot{\pi}^0 = \pi^1 - \pi^{(0)}(t_i) = \pi^1 - \pi^0$$

$$\int_{t_N}^{t_f} \dot{\pi}^h(t) = \dot{\pi}^{N+1} = \pi^h(t_f) - \pi^N = \pi^{N+1} - \pi^N$$

Here t_i and t_f are boundary points of the first and final line-cells and $\pi0$ and π^{N+1} are the reductions related to them. Note that this gives us an initial condition at t_i. Now a complete dual cell complex is generated where the related forms are reduced on the respective cells. The reduced forms, co-chains, can now be related through an incidence matrix in the following equations:

$$\dot{\boldsymbol{\pi}}^{(1)} = \mathbb{E}_d^{1,0}\boldsymbol{\pi}_{ext}^{(0)} \tag{3.4}$$

Where $\dot{\boldsymbol{\pi}}^{(1)} = (\dot{\pi}^1\ \dot{\pi}^2 \cdots \dot{\pi}^{N+1})^T$ and $\boldsymbol{\pi}_{ext}^{(0)} = (\pi^0\ \pi^1 \cdots \pi^{N+1})^T$. The incidence matrix $\mathbb{E}_d^{1,0}$ with $(N+1)$ rows and $(N+2)$ columns is than:

$$\mathbb{E}_d^{1,0} = \begin{bmatrix} -1 & 1 & & & \\ & -1 & 1 & & \\ & & \ddots & \ddots & \\ & & & -1 & 1 \\ & & & & -1 & 1 \end{bmatrix}$$

This reduction of $\dot{\pi}^{(1)}$ and its relation to the reduction of $\pi^{(0)}$ is obtained with rigour in [10]. The approximation outer 1-form that satisfies the above presented reduction is shown below as a linear combination of the dual 1-co-chain elements. Here the array of dual Lagrange polynomials is $\tilde{\mathbf{e}}(t) = \mathbf{h}(t)(\mathbb{M}^{(0)})^{-1}$.

$$\dot{\pi}^h(t) = \tilde{\mathbf{e}}(t)dt\dot{\boldsymbol{\pi}}^{(1)}$$

To present a brief confirmation of this from [10] we give the reduction of a dual Lagrange polynomial representation of a pseudo 1-form, that is (a weak) exterior derivative of a pseudo 0-form. The source [10] proves that this reduction can be written as:

$$\tilde{\mathcal{N}}^1\left(\widetilde{\frac{d}{dt}}(\pi^h(t), \hat{\pi}^h)dt\right) = -(\mathbb{E}_p^{1,0})^T\tilde{\mathcal{N}}^0(\pi^h(t)) + \mathbb{N}\tilde{\mathcal{B}}^0(\hat{\pi}^h)$$

Here $\widetilde{\frac{d}{dt}}(\pi^h(t), \hat{\pi}^h)dt$ is the pseudo force 1-form $\pi_h \dot{\pi}^1(t) = \dot{\pi}^h(t)$ which is expanded as $\tilde{\mathbf{e}}(t)dt\widetilde{\mathcal{N}}^1\left(\widetilde{\frac{d}{dt}}(\pi^h(t), \hat{\pi}^h)dt\right)$. The polynomial vector $\tilde{\mathbf{e}}(t)$ consists of the dual Lagrange polynomials and their coefficients $\widetilde{\mathcal{N}}^1\left(\widetilde{\frac{d}{dt}}(\pi^h(t), \hat{\pi}^h)dt\right)$ can be labeled as $\dot{\boldsymbol{\pi}}^{(1)}$. Matrix $\mathbb{E}_p^{1,0}$ is the primal Incidence matrix shown earlier and $\mathbb{N}$ is the inclusion matrix with $(N+1)$ rows:

$$\mathbb{N} = \begin{bmatrix} -1 & 0 \\ 0 & 0 \\ \vdots & \vdots \\ 0 & 0 \\ 0 & 1 \end{bmatrix}$$

The reduction of momentum at the two boundary points $\widetilde{\mathcal{B}}^0(\hat{\pi}^h)$ creates two additional co-chain cells $\pi^{(0)}(t_i)$ and $\pi^{(0)}(t_f)$. The (dual) reduction of momentum is worked out below where the integration of the edge function vector $\mathbf{e}(t)^T$ and its dual $\widetilde{\mathbf{h}}(t)$ have the property that they than yield an identity matrix:

$$\widetilde{\mathcal{N}}^0(\pi^h(t)) = \int_{t_i}^{t_f} \mathbf{e}(t)^T \widetilde{\mathbf{h}}(t) \boldsymbol{\pi}^{(0)} \, dt = \boldsymbol{\pi}^{(0)}$$

Evaluating the reduction of the weak derivative of momentum with the results found above gives the same relation between $\dot{\boldsymbol{\pi}}^{(1)}$ and $\boldsymbol{\pi}^{(0)}$ in (3.4) that was deduced from the dual cell complex in Fig. 3.2. Here again in the same manner as for the primal forms it is easy to show that this process satisfies the commutative property of Reduction $\mathcal{I}$ and of the exterior derivation d / co-boundary operator δ. For a more detailed discussion on obtaining the dual co-chains of the (virtual) dual cell complex consult [10].

Using the various obtained approximate forms the approximation of energy $E^h(t)$ can now be written as:

$$E^h(t) = \frac{1}{2}\left(\dot{x}^h(t) \wedge \pi^h(t) + x^h(t) \wedge \sigma^h(t)\right)$$

Expanding the projected forms in terms of the dual polynomials and their coefficients in terms of co-chains gives:

$$E^h(t) = \frac{dt}{2}\left(\mathbf{e}(t)\dot{\mathbf{x}}^{(1)}\tilde{\mathbf{h}}(t)\boldsymbol{\pi}^{(0)} + \mathbf{h}(t)\mathbf{x}^{(0)}\tilde{\mathbf{e}}(t)\boldsymbol{\sigma}^{(1)}\right)$$

In this section we have constructed the geometry of the local physical variables (forms) that appear in the partial differential equation that describes the damped harmonic oscillator. Furthermore we have created two cell complexes on which the forms are reduced to co-chains. These co-chains are related to each other with the co-boundary operator in case they are on the same cell complex or with a discrete Hodge operator when they are on different ones. The co-chains are used as coefficients of the basis polynomials with which we approximate the exact forms.

3.2. Mimicking by Doubling the Degrees of Freedom

This chapter shows a possible method for obtaining the non-conservative Lagrangian. Afterwards the initial and final conditions of the action are reformulated to become usable for the numerical scheme. Thirdly a gauge transformation is introduced to get a Lagrangian for the action that directly satisfies the initial conditions of the differential equation problem. This is followed by a theoretical analysis of the Lagrangian mechanics of systems of doubled degrees of freedom. The geometry is then introduced in the action formulation and the first variation is applied to it. Reduction through integration than gives the system of equations which are solved through numerical computation with a Python program. The results of the variables and error convergence are than presented and discussed. Finally to test the energy conservation the problem is approached from both a theoretical and numerical perspective.

3.2.1. A Method for Obtaining the Non-Conservative Lagrangian Term

In Section 2.7 following results and guidelines from the theory by [32] a (non-unique) complete Lagrangian is obtained of the damped harmonic oscillator. Galley [32] gives some guidelines but no standardized method has been shown for obtaining the non-conservative term. This section tries to show a self obtained method that can be used to obtain non-conservative part of the Lagrangians for a class of some systems. This method works if K is a coupling source that contributes to the total potential with a form that looks like linear generalized velocity potentials in classical Lagrangian mechanics, see Appendix B. First we notice that the total Lagrangian has the form as in (3.5) as argued for in Section 2.7.

$$\Lambda(\dot{x}_+, \dot{x}_-, x_+, x_-, t) = m\dot{x}_+\dot{x}_- - kx_+x_- + K(\dot{x}_+, \dot{x}_-, x_+, x_-, t) \tag{3.5}$$

From [32, 44] and as explained in Section 2.7 the total Lagrangian Λ must satisfy (3.6). Where the physical limit PL is when the doubled degrees of freedom approach each other such that $PL : x_- \to 0 \quad \wedge \quad x_+ \to x$.

$$\left[\frac{d}{dt}\frac{\partial\Lambda}{\partial\dot{x}_-} - \frac{\partial\Lambda}{\partial x_-}\right]_{PL} = 0 \tag{3.6}$$

Evaluating (3.5) for Λ in the previous equation (3.6) gives (3.7):

$$\left[m\ddot{x}_- - kx_+ + \frac{d}{dt}\frac{\partial K}{\partial\dot{x}_-} - \frac{\partial K}{\partial x}\right]_{PL} = 0 \tag{3.7}$$

The kinetics of a damped harmonic oscillator presented in (2.67) can be written as:

$$[m\ddot{x}_+ + kx_+]_{PL} = m\ddot{x} + kx = -\lambda\dot{x} = [-\lambda\dot{x}_+]_{PL} = 0$$

Inserting this in equation (3.7) yields the following equation (3.8):

$$\left[-\lambda\dot{x}_+ + \frac{d}{dt}\frac{\partial K}{\partial\dot{x}_-} - \frac{\partial K}{\partial x_-}\right]_{PL} = 0 \tag{3.8}$$

We proceed for the case of working with a closed system. As argued in Section 2.6 this means that K is not an explicit function of time. Now the non-conservative source term K will be looked for in the class of functions called multilinear polynomials with $\alpha_i \in \mathbb{R}$ and $a_j^i \in \mathbb{N}$ such that:

$$K(\dot{x}_+, \dot{x}_-, x_+, x_-, t) = \sum_{i=1}^{k} \alpha_i \dot{x}_+^{a_1^i} \dot{x}_-^{a_2^i} x_+^{a_3^i} x_-^{a_4^i}$$

The unknown terms in equation (3.8) can then be written as shown below:

$$\frac{\partial K}{\partial x_-} = \sum_{i=1}^{k} \alpha_i a_4^i \dot{x}_+^{a_1^i} \dot{x}_-^{a_2^i} x_+^{a_3^i} x_-^{(a_4^i-1)}$$

$$\frac{d}{dt}\frac{\partial K}{\partial \dot{x}_-} = \sum_{i=1}^{k} \alpha_i a_1^i \Bigg[(a_1^i-1)\ddot{x}_+ \dot{x}_+^{(a_1^i-2)} \dot{x}_-^{a_2^i} x_+^{a_3^i} x_-^{a_4^i} + \dots$$

$$\dots + a_2^i \dot{x}_+^{(a_1^i-1)} \ddot{x}_- \dot{x}_-^{(a_2^i-1)} x_+^{a_3^i} x_-^{a_4^i} + \dots$$

$$\dots + a_3^i \dot{x}_+^{a_1^i} \dot{x}_-^{a_2^i} x_+^{(a_3^i-1)} x_-^{a_4^i} + \dot{x}_+^{a_1^i} \dot{x}_-^{a_2^i} x_+^{a_3^i} x_-^{a_4^i} + \dots$$

$$\dots + a_4^i \dot{x}_+^{(a_1^i-1)} \dot{x}_-^{(a_2^i+1)} x_+^{a_3^i} x_-^{(a_4^i-1)} \Bigg]$$

Choosing $\alpha_1 = \lambda$, $a_1^1 = 1$, $a_4^1 = 1$ and zero for all other exponents and coefficients allows (3.8) to vanish in the physical limit. This yields the non-conservative source K below. We can observe that this has the form of a linear generalized velocity potential.

$$K(\dot{x}_+, \dot{x}_-, x_+, x_-, t) = -\lambda x_-(\dot{x}_+ + \dot{x}_-)$$

The total conservative Lagrangian in this formulation now satisfies Lagrange's (2.40) and gives the actual and virtual equations of motion presented by Morse and Feshbach [41] that each either describe the absorption or the realising of the damping energy. Furthermore when a variation is applied to the negative degree of freedom and then the physical limit is taken we get exactly the same expression as the one that follows from (2.58) in Section 2.7. This is because in the physical limit x_- and $\dot{x}_-$ go to zero by definition even if their variations are arbitrary. This latter means we can drop the term:$-\lambda x_- \dot{x}_-$ and keep: $-\lambda x_- \dot{x}_+$ as the non-conservative part of the total Lagrangian. The total non-conservative Lagrangian is than given below in (3.9):

$$\Lambda(\dot{x}_+, \dot{x}_-, x_+, x_-, t) = m\dot{x}_+ \dot{x}_- - kx_+ x_- - \lambda x_- \dot{x}_+ \qquad (3.9)$$

3.2.2. Reformulating the Initial and Final Conditions

In the context of mimetic spectral element methods there is a slight issue with Galley's [44, 32] formulation of the total Lagrangian of non-conservative mechanics. The formalism of Galley builds on specific conditions that don't work for the mimetic method when the the algebraic dual polynomials of chapter (2.5) are used as variations. This is because they are not necessarily zero at the initial time instant. The test functions in the numerical system to be implemented are the variations δx_- as is shown in Section 3.2.4. However these $\delta x_-(t_i)$ must vanish according to the derivation of [44]. Besides this theoretical conclusion a numerical scheme using these algebraic dual polynomials as variations has been applied with to Galley's method and no correct results have been obtained. Furthermore the initial conditions of the system do not (implicitly or explicitly) appear in the formulation of the action.

The inconsistency between the dual polynomials and the integrating conditions in [44, 32] is circumvented by changing the conditions in such a way that variations will be allowed in the initial state and the conditions of the stationary principle are still satisfied. This will on itself induce a natural gauge transformation of the total Lagrangian.

Instead of specifying the individual initial degrees of freedom we specify the average value of the degrees of freedom but let them individually vary:$\frac{1}{2}(x_1(t_i) + x_2(t_i)) = x_{initial} = x_+(t_i)$. We can write the equation of varying the average $x_+(t)$ as:

$$x_+(t, \epsilon) = x_+(t, 0) + \epsilon \delta x_+(t)$$

By evaluating at the initial condition $t = t_i$ we get $\delta x_+(t_i) = 0$. Writing out the variation of the average in terms of the separate degrees of freedom 1 and 2 we get that $\delta x_1(t_i) = -\delta x_2(t_i)$. Note that values of varied

individual degrees of freedom x_1 or x_2 are not specified at the initial state and so they can vary as long as their average is as specified. This makes one of the variations δx_1 and δx_2 arbitrary but dependent on the other. Now also writing out the variation of the difference variable x_- at the initial condition shows that it is varying as the equation below. So a variation of the difference is a multiple of just one of them which makes it completely arbitrary. This can seen in the equation below. The same procedure can be repeated for the final states where we again do not specify the final states individually but only predetermine the average: $\frac{1}{2}(x_1(t_f) + x_2(t_f)) = x_{final} = x_+(t_f)$. A visualization of these new path histories is shown in Fig. 3.3.
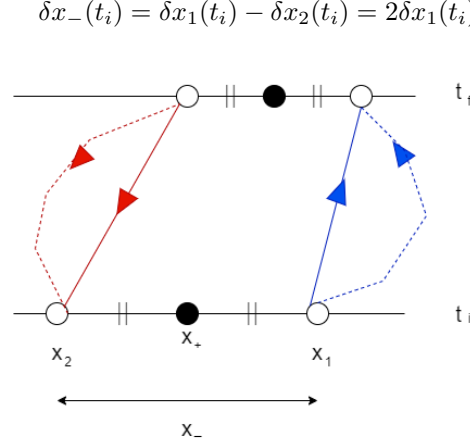
$$\delta x_-(t_i) = \delta x_1(t_i) - \delta x_2(t_i) = 2\delta x_1(t_i)$$

Figure 3.3: Paths of doubled degrees of freedom x_1 and x_2 from the initial time t_i to the final time t_f. All degrees of freedom at both instances allow variation and are symbolised as empty circles. The filled point is the initial physical state $x_+(t_i) = x_i$ and at the final state it is $x_+(t_f) = x_f$. The dashed lines are variation paths on the actual paths that are represented by filled lines. The blue and red lines represent the first and second of doubled degrees of freedom respectively.

3.2.3. Introducing a Gauge Transformation

After modifying (2.56) introduced by [32], due to the new conditions specified in the former section, the equation gets a non-vanishing boundary term. The new formulation of the first variation of the action is at first obtained by applying the chain rule and then performing integration by parts which gives (3.10). Before applying the initial and final conditions the result is similar to equation (2.56) but with the additional boundary terms $-[\delta x_1 \pi_1 - \delta x_2 \pi_2]_{t=t_i}^{t=t_f}$.

$$\left[\frac{d\mathcal{S}}{d\epsilon}\right]_{\epsilon=0} = \int_{t_i}^{t_f} \left(\delta x_1 \left[\frac{\partial \Lambda}{\partial x_1} - \frac{d}{dt}\frac{\partial \Lambda}{\partial \dot{x}_1}\right]_{\epsilon=0} - \delta x_2 \left[\frac{\partial \Lambda}{\partial x_2} - \frac{d}{dt}\frac{\partial \Lambda}{\partial \dot{x}_2}\right]_{\epsilon=0}\right) - \left[\delta x_1 \pi_1 - \delta x_2 \pi_2\right]_{t=t_i}^{t=t_f} \quad (3.10)$$

Notice that here the first and second momenta are defined in terms of the generalized momenta in analytical mechanics [36] such that:

$$\pi_1 := \frac{\partial \Lambda}{\partial \dot{x}_1} \quad \wedge \quad \pi_2 := -\frac{\partial \Lambda}{\partial \dot{x}_2}$$

Furthermore we define the average and difference generalized momenta as:

$$\pi_+ := \frac{(\pi_1 + \pi_2)}{2} \quad \wedge \quad \pi_- := \pi_1 - \pi_2$$

This means that the average and difference generalized momenta can be written as below [32]:

$$\pi_+ = \frac{\partial \Lambda}{\partial \dot{x}_-} \quad \wedge \quad \pi_- = \frac{\partial \Lambda}{\partial \dot{x}_+}$$

Applying the condition of invariance of the average degree of freedom at the initial and final state the additional term becomes $-[\delta x_1 \pi_1 - \delta x_2 \pi_2]_{t=t_i}^{t=t_f} = -[2\delta x_1 \pi_+]_{t=t_i}^{t=t_f} = -[\delta x_- \pi_+]_{t=t_i}^{t=t_f}$. This is a first variation of $\int_{t_i}^{t_f} \frac{d}{dt} G(\pi_+, x_-)\, dt$ when x_- is varied where $G = -x_- \pi_+$. This $\frac{d}{dt}G(\pi_+, x_-)$ will be used as a transformation of the Lagrangian to get exactly the same form as (2.56). The remainder of this section will show this together with some of its consequences.

Classical Mechanics [33, 35, 36] shows that a stationary action of conservative systems necessarily leads to Euler-Lagrange's equations (2.40) and these Euler-Lagrange equations are themselves derived from Newtons laws through Alembert's principle. The same can be shown in the opposite order which means all three perspectives are equivalent [36]. As argued in Section 2.7 from [32], the aforementioned equivalence of the stationary action principle with Euler-Lagrange and Newton is satisfied whith time symmetry or conservation of the energy (equation). If we define a doubled monogenic system from the single non-monogenic (non-conservative) system, the stationary action then satisfies Euler-Lagrange's equations, and also satisfies newton's equation of motion for that system.

As shown in Section 2.7 Galley [32, 44] does this by treating the doubled system as an energy conserving system and then by manipulating the conditions such that the individual integrands are zero and Euler-Lagrange equations (2.40) hold for the introduced total Lagrangian Λ. This latter is however not obvious from (3.10) when there is an additional boundary term. We will add a gauge term to the Lagrangian but first we write the (same) action variation in terms of the average and difference degree of freedom. From [44] the functional variation of the action with the total Lagrangian before implementing the initial and final conditions can be rewritten as in (3.11) below in terms of the average and difference degrees of freedom. Where a parametrization of the variation paths is given by: $x_\pm(t, \epsilon) = x_\pm(t, 0) + \epsilon \delta x_\pm(t)$ and the generalized momenta are defined earlier.

$$\left[\frac{dS}{d\epsilon}\right]_{\epsilon=0} = \int_{t_i}^{t_f} dt \left(\delta x_+ \left[\frac{\partial \Lambda}{\partial x_+} - \frac{d}{dt}\frac{\partial \Lambda}{\partial \dot{x}_+}\right]_{\epsilon=0} + \delta x_- \left[\frac{\partial \Lambda}{\partial x_-} - \frac{d}{dt}\frac{\partial \Lambda}{\partial \dot{x}_-}\right]_{\epsilon=0}\right) + \left[\delta x_+ \pi_- + \delta x_- \pi_+\right]_{t=t_i}^{t=t_f} \tag{3.11}$$

If we apply $\frac{d}{dt}G(\pi_+, x_-)$ as transformation to Λ. This gives the transformation Λ':

$$\Lambda'(\dot{x}_+, \dot{x}_-, x_+, x_-, t) = \Lambda(\dot{x}_+, \dot{x}_-, x_+, x_-, t) + \frac{d}{dt}G(\pi_+, x_-, t) \tag{3.12}$$

The new total (transformed) action S' then becomes:

$$S' = \int_{t_i}^{t_f} \Lambda'\, dt = \int_{t_i}^{t_f} \left(\Lambda + \frac{d}{dt}G\right) dt$$

The first variation of this total action can then be written in two parts, an untransformed and a transformation part:

$$\left[\frac{dS'}{d\epsilon}\right]_{\epsilon=0} = \left[\frac{dS}{d\epsilon}\right]_{\epsilon=0} + \left[\frac{dS_G}{d\epsilon}\right]_{\epsilon=0}$$

The first - untransformed action - term is written out in (3.11). The first variation of the transformation term can be written out as (3.13) below. Here we use (2.64) in Section 2.8.1 to write out the variation.

$$\left[\frac{dS_G}{d\epsilon}\right]_{\epsilon=0} = \int_{t_i}^{t_f} dt \left(\delta x_+ \left[\frac{\partial \frac{d}{dt}G}{\partial x_+} - \frac{d}{dt}\frac{\partial \frac{d}{dt}G}{\partial \dot{x}_+}\right]_{\epsilon=0} + \delta x_- \left[\frac{\partial \frac{d}{dt}G}{\partial x_-} - \frac{d}{dt}\frac{\partial \frac{d}{dt}G}{\partial \dot{x}_-}\right]_{\epsilon=0}\right) - \left[\delta x_+ \pi_- + \delta x_- \pi_+\right]_{t=t_i}^{t=t_f} \tag{3.13}$$

Adding (3.13) to (3.11) gives the total (transformed) action. As can be seen the boundary terms annihilate each other and the integrands can be joined together which gives (2.56) as below:

$$\left[\frac{dS'}{d\epsilon}\right]_{\epsilon=0} = \int_{t_i}^{t_f} dt \left(\delta x_+ \left[\frac{\partial \Lambda'}{\partial x_+} - \frac{d}{dt}\frac{\partial \Lambda'}{\partial \dot{x}_+}\right]_{\epsilon=0} + \delta x_- \left[\frac{\partial \Lambda'}{\partial x_-} - \frac{d}{dt}\frac{\partial \Lambda'}{\partial \dot{x}_-}\right]_{\epsilon=0}\right) \tag{3.14}$$

When stationary action is satisfied, i.e. $\left[\frac{dS'}{d\epsilon}\right]_{\epsilon=0} = 0$, Euler-Lagrange equations are satisfied for the total transformed Lagrangian. This means that the equations of motion are also satisfied for the total doubled system. This shows that $\frac{d}{dt}G(\pi_+, x_-)$ is a proper gauge transformation of the Lagrangian of an action with the new initial and final conditions imposed on the variations in section (3.2.2). That is the new Lagrangian describes the equations of motion of the system. Specifically we want to work at the level of the action for this numerical method. Due to these newly introduced conditions in the doubling principle, we are now allowed to use the algebraic dual polynomial as variations of the action in Section 3.2.4 to obtain the numerical scheme.

Notice that this is proven for doubled one degree of freedom non-conservative systems but trivially through a summation the same holds for a doubled multiple degree of freedom non-conservative systems as shown below:

$$\sum_{j=1}^{n} \int_{t_i}^{t_f} dt \left(\delta x_{j,+} \left[\frac{\partial \Lambda'}{\partial x_{j,+}} - \frac{d}{dt}\frac{\partial \Lambda'}{\partial \dot{x}_{j,+}}\right]_{\epsilon=0} + \delta x_{j,-} \left[\frac{\partial \Lambda'}{\partial x_{j,-}} - \frac{d}{dt}\frac{\partial \Lambda'}{\partial \dot{x}_{j,-}}\right]_{\epsilon=0}\right) = 0$$

As for the gauge term we note first that the double degrees of freedom contain underlying original degrees of freedom; i.e. $\mathbf{q}_\pm = (q_{1,\pm}, q_{2,\pm}, \ldots, q_{n,\pm})$. As for the generalized momenta they are simply the standard vector derivatives of the Lagrangian scalar function; i.e. $\pi_\pm = \frac{\partial \Lambda}{\partial \mathbf{q}_\pm}$. Since the Lagrangian is now a function of vector degrees of freedom if we apply the chain rule and partial derivative to get the functional derivative we end up with vector multiplication in the boundary term. Applying the newly introduced initial and final conditions for the vectors yields a remaining gauge term as: $\frac{dG}{dt} = \frac{d}{dt}(-\pi_+ \cdot \mathbf{x}_-)$. We will proceed with one variable that is doubled for convenience since this fits the case study of this work, however this can be generalized as mentioned.

The introduced gauge term is somewhat different than the classical gauge transformation as for instance in electromagnetism from [40] that is shown in Section 2.6.2. The classical (electromagnetic) gauge term, $\frac{d}{dt}G(x,t)$, could be added to the Lagrangian because it is constant after integrating the action, which yields the Euler-Lagrange equations and thus the same equations of motion and same extremal variation paths. In this new method the gauge term is a proper gauge transformation that gives a Lagrangian that satisfies Euler-Lagrange transformations because when added to the original Lagrangian under the new conditions they together satisfy Euler-Lagrange equations. The gauge term of the damped harmonic oscillator is a special case where the gauge vanishes under the application of Euler-Lagrange's equations (2.40). This is shown later in this section.

Now we can introduce a general formulation for the gauge transformation by applying first the chain rule to the gauge term and rewriting the generalized momenta in terms of the total original Lagrangian. This gives:

$$\frac{d}{dt}G = \frac{d}{dt}(-\pi_+ x_-) = -\dot{\pi}_+ x_- - \dot{x}_- \pi_+ = -\frac{d}{dt}\frac{\partial \Lambda}{\partial \dot{x}_-}x_- - \frac{dx_-}{dt}\frac{\partial \Lambda}{\partial \dot{x}_-}$$

The total transformed Lagrangian Λ' can than be written as in (3.15) below:

$$\Lambda' = \Lambda - \frac{d}{dt}\left(\frac{\partial \Lambda}{\partial \dot{x}_-}x_-\right) = \Lambda - \frac{d}{dt}\frac{\partial \Lambda}{\partial \dot{x}_-}x_- - \frac{dx_-}{dt}\frac{\partial \Lambda}{\partial \dot{x}_-} \tag{3.15}$$

As clearly visible, by the lemma of DuBois-Reymond, integrands of (3.14) should be zero. This should than also be the case in the physical limit as seen below for the difference degree of freedom:

$$\left[\frac{\partial \Lambda'}{\partial x_-} - \frac{d}{dt} \frac{\partial \Lambda'}{\partial \dot{x}_-} \right]_{PL} = 0$$

Breaking Λ' down to its constituents and applying the physical limit to: $x_- \to 0$ and $x_+ \to x$ to the doubled conservative Lagrangian part gives (3.16) below as shown in [32] but now with an additional gauge related generalized force. As a reminder here $L = T - U$, the kinetic energy minus the potential energy, which is the standard Lagrangian formulation of the single system. Furthermore here K is the non-conservative coupling source of the doubled system and $\frac{d}{dt} G$ is the gauge term of the doubled system.

$$\frac{d}{dt} \frac{\partial L}{\partial \dot{x}} - \frac{\partial L}{\partial x} = \left[\frac{\partial K}{\partial x_-} - \frac{d}{dt} \frac{\partial K}{\partial \dot{x}_-} + \frac{\partial \frac{d}{dt} G}{\partial x_-} - \frac{d}{dt} \frac{\partial \frac{d}{dt} G}{\partial \dot{x}_-} \right]_{PL} = Q(x, \dot{x}, t) \qquad (3.16)$$

Before we proceed to work out the generalized force dependent on the gauge term, there is a note on the average generalized momentum. For the damped harmonic oscillator it can be worked out as below:

$$\pi_+ = \frac{\partial \Lambda}{\partial \dot{x}_-} = \frac{\partial}{\partial \dot{x}_-} (m\dot{x}_+ \dot{x}_- - kx_+ x_- - \lambda x_- \dot{x}_+) = m\dot{x}_+$$

Which means that for the damped harmonic oscillator it holds that this generalized average momentum is actually the average linear momentum as shown above. This relation was needed during the set up of the local and global geometry of the system, in Section 3.1, where we related the velocity and generalized momentum with the Hodge operator.

$$\pi_+ = m\dot{x}_+ \to \pi^{(0)} = m \star \dot{x}^{(1)}$$

From the previous results on momentum the following shows that for $\frac{d}{dt} G(\pi_+, x_-, t) = \frac{d}{dt}(-x_- \pi_+) = -\dot{x}_- \pi_+ - x_- \dot{\pi}_+$, the Euler-Lagrange (2.40) is satisfied with respect to the difference degree of freedom x_- in the physical limit. This however is restricted only to the case where π_+ and $\dot{\pi}_+$ are not explicit functions of x_- and $\dot{x}_-$. This does not need to be case if K has other forms as is shown in Appendix B. However for the damped harmonic oscillator this is satisfied as shown earlier.

$$\left[\frac{d}{dt} \left(\frac{\partial \frac{d}{dt} G}{\partial \dot{x}_-} \right) - \frac{\partial \frac{d}{dt} G}{\partial x_-} \right]_{PL} = [\dot{\pi}_+ - \dot{\pi}_+]_{PL} = 0$$

Now we can get rid of the term dependent on the gauge and (3.16) becomes as (3.17) below:

$$\frac{d}{dt} \frac{\partial L}{\partial \dot{x}} - \frac{\partial L}{\partial x} = \left[\frac{\partial K}{\partial x_-} - \frac{d}{dt} \frac{\partial K}{\partial \dot{x}_-} \right]_{PL} := Q(x, \dot{x}, t) \qquad (3.17)$$

With reference to (2.41) this is a formulation of a single degree of freedom where Q is the generalized non-conservative force which can not be written in terms of a generalized velocity potential as presented in Section 2.6.

The remainder of this section will be specific to verify that a stationary action of the total non-conservative Lagrangian implies that the configuration variables in the physical limit satisfy the equations of motion of the damped harmonic oscillator. To do this we work out (3.17) which is a consequence of this stationary action. This gives the generalized force due to the non-conservative part $K = -\lambda x_- \dot{x}_+$:

$$\left[\frac{\partial K}{\partial x_-} - \frac{d}{dt} \frac{\partial K}{\partial \dot{x}_-} \right]_{PL} = [-\lambda \dot{x}_+ - 0]_{PL} = -\lambda \dot{x}$$

The left side of the equation is applied to the standard Lagrangian of a single degree of freedom oscillator where $L = T - U = \frac{1}{2}m\dot{x}^2 - \frac{1}{2}kx^2$:

$$\frac{d}{dt}\frac{\partial L}{\partial \dot{x}} - \frac{\partial L}{\partial x} = m\ddot{x} + kx$$

This yields the equation below which is exactly the Newtonian equation of motion for the damped harmonic oscillator:

$$m\ddot{x} + kx = -\lambda\dot{x}$$

This means that stationary action of the doubled system of a damped harmonic oscillator implies that the degrees of freedom involved in the action obey Newton's equation of motion for the damped harmonic oscillator in the physical limit. So the information contained in this (doubled) stationary action about the degrees of freedom describes the motion of the system.

Finally, for the average degree of freedom x_+ we can resolve the Euler-Lagrange equation as below. We note first that the physical degree of freedom x_+ satisfies the standard Newtonian equation of motion with a positive damping $+\lambda$: $m\ddot{x}_+ + \lambda\dot{x}_+ + kx_+ = 0$. As shown in the introductory part of Section 2.7, Morse and Feshbach [41] presents that the second degree of freedom satisfies the same equation but with a negative dissipation constant $-\lambda$ that reintroduces the energy in the system: $m\ddot{x}_- - \lambda\dot{x}_- + kx_- = 0$. So, Euler-Lagrange equation for $\frac{d}{dt}G$ with respect to the average degree of freedom x_+ is satisfied as the equations below show. Together with the satisfaction of the gauge term with Euler-Lagrange with respect to x_-, this means that both generalized forces, in the doubled damped harmonic oscillator, that are induced by the gauge term are zero. This means that the system is monogenic since the untrasformed Lagrangian Λ is also monogenic. Because it is also closed it is an energy (function) conserving system.

$$\frac{d}{dt}G = -m\ddot{x}_+ x_- - m\dot{x}_+\dot{x}_- = (\lambda\dot{x}_+ + kx_+)x_- - m\dot{x}_+\dot{x}_-$$

$$\left[\frac{d}{dt}\left(\frac{\partial \frac{d}{dt}G}{\partial \dot{x}_+}\right) - \frac{\partial \frac{d}{dt}G}{\partial x_+}\right]_{\text{e.o.m. of } x_-} = -(m\ddot{x}_- - \lambda\dot{x}_- + kx_-) = 0$$

In conclusion this is general new approach to Galley's method [32, 44] where the non-conservative Lagrangian and its action allow for working with arbitrary variations at the initial and final conditions. These arbitrary difference variations will be useful since the algebraic dual polynomials which will be used as variations can have non-zero values at the initial and final state. Furthermore the induced gauge term contains information on the initial condition and final state which are neither explicitly nor implicitly visible in the formulation of Galley [32].

3.2.4. A Mimetic Numerical Scheme from Doubled Degrees of Freedom

The total Lagrangian obtained Λ' from doubling the degrees of freedom consists of the double conservative terms, the non-conservative term and the gauge transformation as in equation (3.19)

$$\Lambda'(\dot{x}_+, \dot{x}_-, x_+, x_-, t) = m\dot{x}_+(t)\dot{x}_-(t) - kx_+(t)x_-(t) - \lambda\dot{x}_+(t)x_-(t) - \frac{d}{dt}(\pi_+(t)x_-(t)) \tag{3.18}$$

To take the geometry into account we write the Lagrangian out in exterior calculus form:

$$\Lambda'(\dot{x}_+, \dot{x}_-, \pi_+, \sigma_+, x_-, t) = \tilde{\pi}_+^{(0)}(t) \wedge \dot{x}_-^{(1)}(t) - \tilde{\sigma}_+^{(1)}(t) \wedge x_-^{(0)}(t) - \lambda\dot{x}_+^{(1)}(t) \wedge x_-^{(0)}(t) - d(\tilde{\pi}_+^{(0)}(t) \wedge x_-^{(0)}(t)) \tag{3.19}$$

The action $\mathcal{S}$ must satisfy the fact that the functional derivative, $\delta\mathcal{S}[x_-]$, of it with respect to δx_- is zero at the physical limit [32]. Galley [32] states that this is the more general form when higher order derivatives might appear in the formulation of the action. So we have to take this possibility into account while formulating the variation principle. This equation is shown below:

$$[\delta\mathcal{S}[x_-]]_{PL} = \left[\frac{\delta\mathcal{S}}{\delta x_-(t)}\right]_{PL} = 0$$

The L^2-inner product of this gradient with the variation function δx_- is than also zero - see Section 2.8 - as shown below:

$$[\langle\delta\mathcal{S}[x_-]\ ;\ \delta x_-\rangle]_{PL} = 0$$

This inner product is the first variation - see Section 2.8 - with respect to x_- which on its turn is thus also zero:

$$[\delta\mathcal{S}(x_-, \delta x_-)]_{PL} = 0$$

The action is the integral of the of the Lagrangian Λ' obtained in equation (3.19). Applying the integral to it and performing the first variation of it for a functional with multiple degrees of freedom by using (2.63) in Section 2.8 gives the equation below. Notice that the dimension of the forms is dropped in the notation however for reference one can return to (3.19).

$$[\delta\mathcal{S}(x_-, \delta x_-)]_{PL} = \left[\int_{t_i}^{t_f} (\pi_+\delta\dot{x}_- - \lambda\dot{x}_+\delta x_- - \tilde{\sigma}_+\delta x_- - d(\pi_+\delta x_-))\right]_{PL} = 0$$

Projecting Λ' from the exact space $\Lambda^k\mathcal{M}$ to the approximation space $\Lambda^k(\mathcal{M}, C^k(D))$ gives (3.20). Here $\delta\mathcal{S}(x_-, \delta x_-)]_{PL}$ is abbreviated as $\delta_{x_-}\mathcal{S}$. Furthermore $\delta x_-^{(0)}(t)$ and its exterior derivative $\delta\dot{x}_-^{(1)}(t)$ are arbitrary functions as long as $\delta x_-(t) \in C^1(\mathcal{M})$. This means that $\delta x_-(t)$ can be any algebraic dual polynomial from Section 2.5.

$$\pi_h\delta_{x_-}\mathcal{S} = \int_{t_i}^{t_f}\left[\tilde{\mathbf{h}}(t)\boldsymbol{\pi}_+^{(0)}\delta\dot{x}_-(t) - \lambda\mathbf{e}(t)dt\dot{\mathbf{x}}_+^{(1)}\delta x_-(t) - \tilde{\mathbf{e}}(t)dt\boldsymbol{\sigma}_+^{(1)}\delta x_-(t)\right] - \left[\pi_+^h(t)\delta x_-(t)\right]_{t_i}^{t_f} \tag{3.20}$$

Using the obtained facts that $\boldsymbol{\pi}^{(0)} = m\mathbb{M}^{(1)}\dot{\mathbf{x}}^{(1)}$ and $\tilde{\mathbf{h}}(t) = \mathbf{e}(t)(\mathbb{M}^{(1)})^{-1}$ for the first term and $\boldsymbol{\sigma}^{(1)} = k\mathbb{M}^{(0)}\mathbf{x}^{(0)}$ and $\tilde{\mathbf{e}}(t) = \mathbf{h}(t)(\mathbb{M}^{(0)})^{-1}$ for the third term we can write the former (3.20) as in equation (3.21) below.

$$\pi_h\delta_{x_-}\mathcal{S} = \int_{t_i}^{t_f}\left[m\mathbf{e}(t)\dot{\mathbf{x}}_+^{(1)}\delta\dot{x}_-(t) - \lambda\mathbf{e}(t)dt\dot{\mathbf{x}}_+^{(1)}\delta x_-(t) - k\mathbf{h}(t)dt\mathbf{x}_+^{(0)}\delta x_-(t)\right] - \left[\pi_+^h(t)\delta x_-(t)\right]_{t_i}^{t_f} \tag{3.21}$$

We choose a column array $\delta\mathbf{x}_-(t)$ of variation functions containing the $N + 1$ Lagrange polynomials:

$$\delta\mathbf{x}_-(t) = \begin{bmatrix} h_0(t) \\ h_1(t) \\ \vdots \\ h_N(t) \end{bmatrix}$$

First notice that $\delta\dot{x}_-^{(1)} = d\delta x_-^{(0)} = \frac{d}{dt}\delta x_-^{(0)}dt$. The derivative of Lagrange polynomials from [10] is $\frac{d}{dt}h_j(t) = e_j(t)dt - e_{j+1}(t)dt$ with the special cases $e_0(t) = e_{N+1}(t) = 0$. From this we get the derivative of the variation vector below. Here the extended edge polynomial vector is $\mathbf{e}_{ext}(t) = (e_0(t)\ e_1(t)\cdots e_{N+1}(t))$.

$$\delta\dot{\mathbf{x}}_-(t) = \begin{bmatrix} e_0(t) - e_1(t) \\ e_1(t) - e_2(t) \\ \vdots \\ e_N(t) - e_{N+1}(t) \end{bmatrix} dt = -\mathbb{E}_d^{1,0}\mathbf{e}_{ext}^T(t)dt$$

Applying $N+1$ variations using the variations in these arrays yields the following system of equations:

$$\overrightarrow{\pi_h\delta_{x_-}\hat{\mathcal{S}}} = \int_{t_i}^{t_f} \left[m\delta\dot{\mathbf{x}}_-(t)\mathbf{e}(t)\dot{\mathbf{x}}_+^{(1)} - \lambda\delta\mathbf{x}_-\mathbf{e}(t)dt\dot{\mathbf{x}}_+^{(1)} - k\delta\mathbf{x}_-(t)\mathbf{h}(t)dt\mathbf{x}_+^{(0)} \right] - \left[\pi_+^h(t)\delta\mathbf{x}_-(t) \right]_{t_i}^{t_f}$$

We proceed by working out all of the four terms in the system of equation. The terms contain vectors that can be reformulated from the earlier obtained definition of the Lagrange array and of the boundary of :

$$\delta\mathbf{x}_-(t) = \mathbf{h}^T(t)$$

$$\dot{\mathbf{x}}_+^{(1)} = \mathbb{E}_p^{1,0}\mathbf{x}_+^{(0)}$$

Integrating the two vectors of the edge polynomial vector in the first term give the mass matrix which can be related to the the reference mass matrix through a transformation given in section (2.5). However here the matrix $\begin{bmatrix} \mathbf{0}^T \\ \overline{\mathbb{M}}^{(1)} \\ \mathbf{0}^T \end{bmatrix}$ consists of two zero row arrays in the first above and under the edge mass matrix due to the extended edge polynomial vector. The first term becomes then as below after reduction:

$$\int_{t_i}^{t_f} -m\mathbb{E}_d^{1,0}\mathbf{e}_{ext}^T(t)dt\mathbf{e}(t)\dot{\mathbf{x}}_+^{(1)} = \frac{-2m}{(t_f-t_i)}\mathbb{E}_d^{1,0}\begin{bmatrix} \mathbf{0}^T \\ \overline{\mathbb{M}}^{(1)} \\ \mathbf{0}^T \end{bmatrix}\dot{\mathbf{x}}_+^{(1)}$$

The second term contains a mixed mass matrix $\mathbb{M}^{(1)(0)}$ that can be written like below after applying transformation rules of the polynomial functions:

$$\int_{t_i}^{t_f} \mathbf{h}^T(t)\mathbf{e}(t)\,dt = \int_{-1}^1 \bar{\mathbf{h}}(t)^T\bar{\mathbf{e}}(t)^1\,dt = \mathbb{M}^{(1)(0)} = \overline{\mathbb{M}}^{(1)(0)}$$

This second term may thus be rewritten as:

$$\int_{t_i}^{t_f} -\lambda\mathbf{h}^T(t)\mathbf{e}(t)\dot{\mathbf{x}}_+^{(1)}\,dt = -\lambda\overline{\mathbb{M}}^{(1)(0)}\mathbb{E}_p^{1,0}\mathbf{x}_+^{(0)}$$

The third contains a standard Lagrange mass matrix which is transformed to its reference variant with the rules shown in section (2.5). Thus the integration of this term yields:

$$\int_{t_i}^{t_f} -k\mathbf{h}^T(t)\mathbf{h}(t)\mathbf{x}_+^{(0)}\,dt = -\frac{k(t_f-t_i)}{2}\overline{\mathbb{M}}^{(0)}\mathbf{x}_+^{(0)}$$

The fourth is the gauge transformation term which included information about the initial condition.

$$-\left[\delta\mathbf{x}_-(t)\pi_+^h(t)\right]_{t_i}^{t_f} = -\left[\mathbf{h}^T(t)\pi_+^h(t)\right]_{t_i}^{t_f}$$

When implementing the boundary values the Lagrange equations vanishes if expect for reduction at $h_0(t_i) = 1$ and $h_N(t_f) = 1$. Also as shown in Section 3.1 on the geometry of the harmonic oscillator we can evaluate the boundaries as $\pi_+^h(t_i) = \pi_+^0$ and $\pi_+^h(t_f) = \pi_+^{N+1}$. Working the fourth term out gives the contribution of the gauge term as:

$$- \left[\delta\mathbf{x}_-(t)\pi_+^h(t) \right]_{t_i}^{t_f} = \pi_+^0 - \pi_+^{N+1} = -\mathbb{E}_d^{1,0}(\pi_+^0 \; 0 \cdots 0 \; \pi_+^{N+1})^T$$

The final vector can be added to the reduction vector of outer momentum $\pi^{(0)}(t)$ to get:

$$-\mathbb{E}_d^{1,0} \begin{bmatrix} \pi_+^0 \\ 0 \\ \vdots \\ 0 \\ \pi_+^{N+1} \end{bmatrix} - \frac{2m}{(t_f - t_i)}\mathbb{E}_d^{1,0} \begin{bmatrix} \mathbf{0}^T \\ \overline{\mathbb{M}}^{(1)} \\ \mathbf{0}^T \end{bmatrix} \dot{\mathbf{x}}_+^{(1)} = -\mathbb{E}_d^{1,0} \begin{bmatrix} \pi_+^0 \\ 0 \\ \vdots \\ 0 \\ \pi_+^{N+1} \end{bmatrix} - \mathbb{E}_d^{1,0} \begin{bmatrix} 0 \\ \boldsymbol{\pi}^{(0)} \\ 0 \end{bmatrix} = -\mathbb{E}_d^{1,0}\boldsymbol{\pi}_{+ext}^{(0)}$$

Implementing the above results in the equation of variation of stationary action (3.21) and letting this equation go to the physical limit where: $PL : (x_+, \dot{x}_+) \to (x, \dot{x})$ gives the following system of equation (3.22):

$$\mathbb{E}_d^{1,0}\boldsymbol{\pi}_{ext}^{(0)} + \left(\lambda\overline{\mathbb{M}}^{(1)(0)}\mathbb{E}_p^{1,0} + \frac{k(t_f - t_i)}{2}\overline{\mathbb{M}}^{(0)} \right)\mathbf{x}^{(0)} = \mathbf{0} \qquad (3.22)$$

With the discrete Hodge obtained in Section 3.1 we have another system of equations (3.23) below:

$$\frac{(t_f - t_i)}{2m}(\overline{\mathbb{M}}^{(1)})^{-1}\boldsymbol{\pi}^{(0)} - \mathbb{E}_p^{1,0}\mathbf{x}^{(0)} = \mathbf{0} \qquad (3.23)$$

In matrix notation equation (3.23) can be written as:

$$\begin{bmatrix} \frac{(t_f - t_i)}{2m}\left(\overline{\mathbb{M}}^{(1)}\right)^{-1} & -\mathbb{E}_p^{1,0} & \begin{matrix} 0 & 0 \\ \vdots & \vdots \\ 0 & 0 \end{matrix} \end{bmatrix} \begin{bmatrix} \boldsymbol{\pi}^{(0)} \\ \mathbf{x}^{(0)} \\ \pi^0 \\ \pi^{N+1} \end{bmatrix} = \mathbf{0}$$

Also (3.22) in matrix representation is:

$$\begin{bmatrix} -\left(\mathbb{E}_p^{1,0}\right)^T & \lambda\overline{\mathbb{M}}^{(1)(0)}\mathbb{E}_p^{1,0} + \frac{k(t_f - t_i)}{2}\overline{\mathbb{M}}^{(0)} & \mathbb{N} \end{bmatrix} \begin{bmatrix} \boldsymbol{\pi}^{(0)} \\ \mathbf{x}^{(0)} \\ \pi^0 \\ \pi^{N+1} \end{bmatrix} = \mathbf{0}$$

Combining the both systems above leads to a complete system of equations (3.24) below. The Matrix has $(2N + 3)$ column and $(2N + 1)$ rows so it is not a square because because it has two additional rows. However since the solution vector contains two known values, namely the initial conditions π^0 and x^0, we can multiply these with their corresponding column vectors out of the matrix to the residual vector. This yields a linear system of equations that can be solved. As shown in the discretization of the forms in Section 3.2.4 the solution vector of the system of equations contains all the co-chains from which these forms can be reconstructed.

$$
\begin{bmatrix}
& & 0 & 0 \\
\frac{(t_f - t_i)}{2m} \left(\overline{\mathbb{M}}^{(1)} \right)^{-1} & -\mathbb{E}_p^{1,0} & \vdots & \vdots \\
& & 0 & 0 \\
\\
-\left(\mathbb{E}_p^{1,0} \right)^T & \lambda \overline{\mathbb{M}}^{(1)(0)} \mathbb{E}_p^{1,0} + \frac{k(t_f - t_i)}{2} \overline{\mathbb{M}}^{(0)} & \mathbb{N}
\end{bmatrix}
\begin{bmatrix}
\boldsymbol{\pi}^{(0)} \\
\mathbf{x}^{(0)} \\
\pi^0 \\
\pi^{N+1}
\end{bmatrix}
= \mathbf{0}
$$

3.2.5. The Solution of the System without Damping

An intermediate discussion of the solution when there is no damping is presented in this section. When the damped mass spring system has no damping it means that $\lambda = 0$. The discrete system of equations in the previous section 3.2.4 than reduces to the system of equations below:

$$
\begin{bmatrix}
& & 0 & 0 \\
\frac{(t_f - t_i)}{2m} \left(\overline{\mathbb{M}}^{(1)} \right)^{-1} & -\mathbb{E}_p^{1,0} & \vdots & \vdots \\
& & 0 & 0 \\
\\
-\left(\mathbb{E}_p^{1,0} \right)^T & \frac{k(t_f - t_i)}{2} \overline{\mathbb{M}}^{(0)} & \mathbb{N}
\end{bmatrix}
\begin{bmatrix}
\boldsymbol{\pi}^{(0)} \\
\mathbf{x}^{(0)} \\
\pi^0 \\
\pi^{N+1}
\end{bmatrix}
= \mathbf{0}
$$

This system of equations is exactly the same as obtained by [52] except for a minus sign due to the opposite definition of the boundary matrix $\mathbb{N}$. The system of equations obtained for simple harmonic oscillators in [52] is based on the mimetic spectral element method with the standard Lagrangian of conservative systems with a one way integration. This means that when $\lambda = 0$ for the system of equations obtained for a damped harmonic oscillator by the mimetic spectral element method with the total non-conservative Lagrangian with doubled degrees of freedom (as in this thesis), the system reduces to the standard aforementioned case.

The results presented by [52] show that, aside from energy, the different physical variables are accurately simulated. Some results obtained here are plotted in Fig. 3.4 for 160 elements with a third order GLL-grid for a time interval of 16. This can be seen for the position as function of time in Fig. 3.4 (a) and for momentum to position in Fig. 3.4 (b). The exact (blue colored: ●) coincides with high accuracy with the approximate solution (red colored: ●). The initial velocity is zero and position is one where we can see that the momentum-position returns to after performing full cycles during the aforementioned time period. So no damping is visible in momentum position since the circle closes perfectly. Furthermore, the material constants are $k = 1$, $m = 1$ and obviously $\lambda = 0$. Convergence of the errors in general will be shown in Sections 3.2.6 and 3.3.

The expectation is that the method conserves energy locally as well as globally. However the numerical solution shows that energy oscillates close to the conservation value. With the same numerical scheme mentioned before, and third order GLL-grids, this can be seen in Fig. 3.5. The deviation from conservation is very small and in the order of 10^{-5}. When the order of polynomials is increased to the seventh order the deviation becomes way smaller, in the order 10^{-13}, as seen in Fig. 3.6. This behaviour of the numerical solution of being close to conservation is also observable in the damped case and still remains unexplained. A more elaborate treatment on the theoretical and experimental results of the conservation of energy in this method is presented in Section 3.4.

In the case of very low damping the approximations follow the exact solutions accurately. Fig. 3.7 shows this for the solutions of position and momentum in a period of 16 with 160 elements and third order GLL-grids approximation. Here the initial velocity and position are zero and one respectively while the damped mass spring system's material constants are $k = 1$, $m = 1$ and $\lambda = 10^{-5}$.

Energy for the same scheme, conditions and material constants, with third order GLL-grids, is presented in Fig. 3.8. The approximated energy (red colored: ●) shows oscillating behaviour that decreases as the actual energy (blue colored: ●) also decreases.
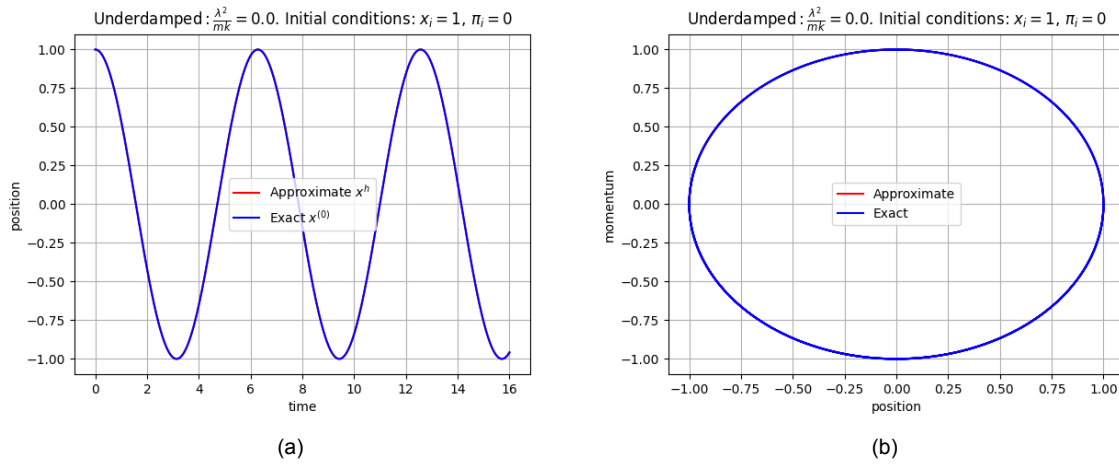
Figure 3.4: Mimetic numerical solution without damping for a discretization with 160 elements with a third order GLL-grid for: **(a)** the position to time with zero velocity and $x_i = 1$ initial conditions **(b)** momentum to position with zero velocity and $x_i = 1$ initial conditions.
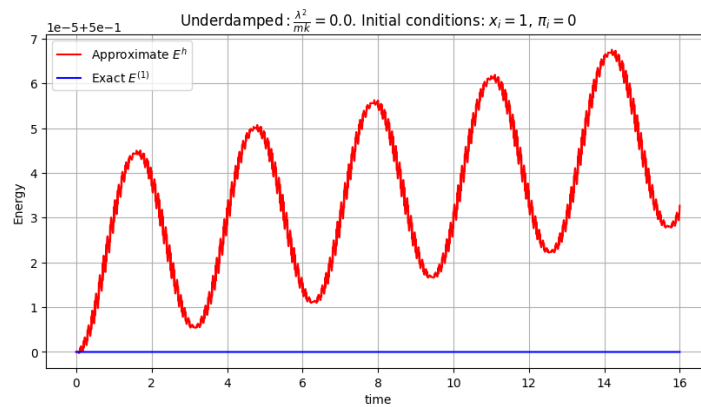

Figure 3.5: Mimetic numerical solution of energy without damping for a discretization with 160 elements with a third order GLL-grids with zero velocity and $x_i = 1$ initial conditions.
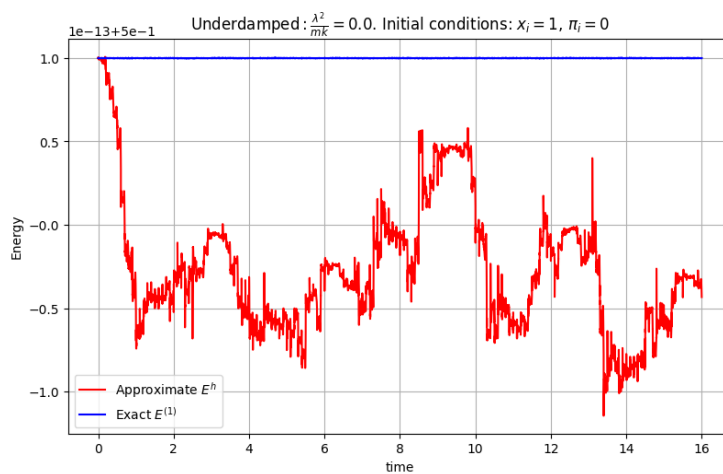

Figure 3.6: Mimetic numerical solution of energy without damping for a discretization with 160 elements with seventh order GLL-grids and velocity and $x_i = 1$ initial conditions.
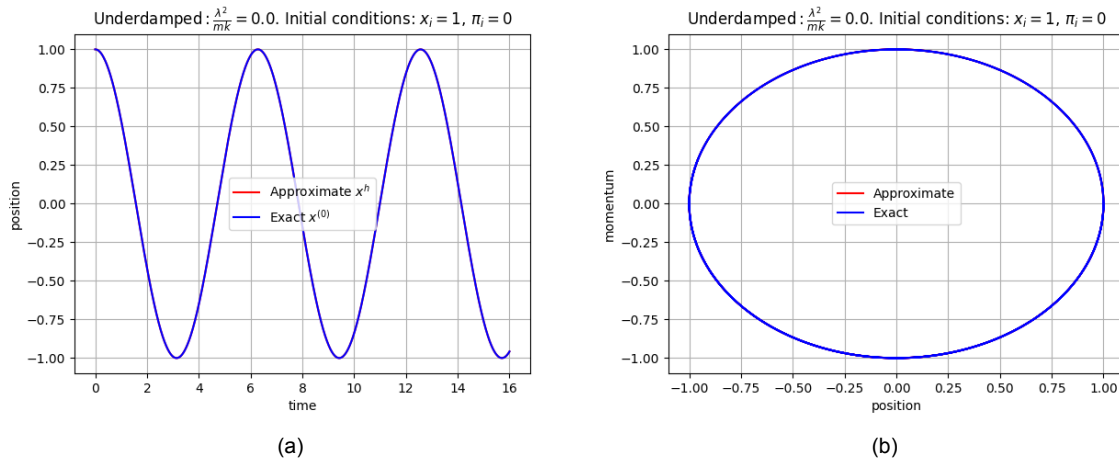
Figure 3.7: Mimetic numerical solution with extremely low damping ($\frac{\lambda^2}{mk} = 10^{-10}$) for a discretization with 160 elements with a third order GLL-grid for: **(a)** the position to time with zero velocity and $x_i = 1$ initial conditions **(b)** momentum to position with zero velocity and $x_i = 1$ initial conditions.
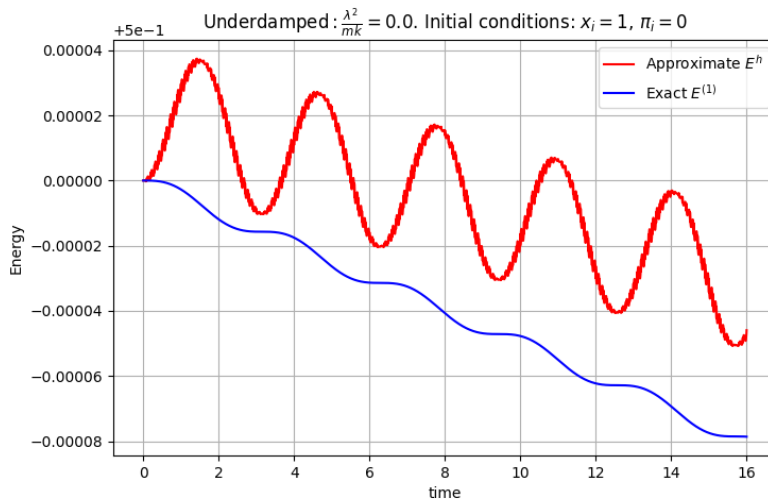

Figure 3.8: Mimetic numerical solution of energy with low damping ($\frac{\lambda^2}{mk} = 10^{-10}$) for a discretization with 160 elements on a third order GLL-grid with zero velocity and $x_i = 1$ initial conditions.
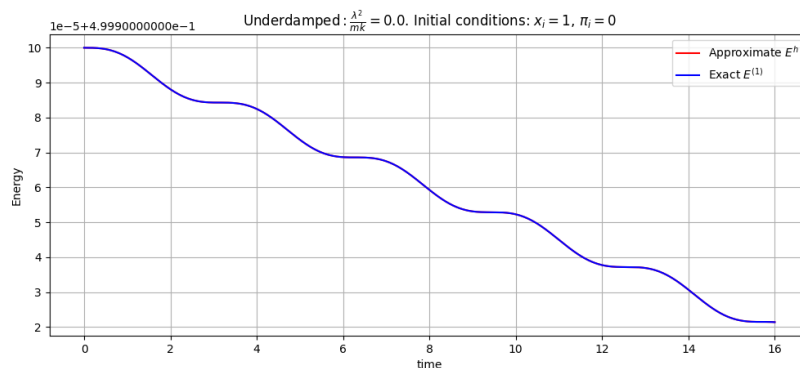

Figure 3.9: Mimetic numerical solution of energy with low damping ($\frac{\lambda^2}{mk} = 10^{-10}$) for a discretization with 160 elements on a seventh order GLL-grid with zero velocity and $x_i = 1$ initial conditions.

When the order of GLL-grids is increased to 7, which is an increase in the accuracy of the approximate solution due to increase of the order of approximation polynomials, the approximate energy than follows the exact energy more closely as can be seen in Fig. 3.9 for an elongated time period of 30. However this does not mean that the approximate energy is not oscillating with a very small amplitude around the exact solution. So again this does not imply that conservation is exact but it is approximated better. As will be seen in Section 3.4 the numerical solution of approximate energy exhibits a very low local non-conserved behaviour, even though the numerical scheme seems to show in theory that the conservation is exact.

In this section it was presented that when damping is zero the discretized system of equations for the damped harmonic oscillator reduces with the new doubling procedure to the discrete simple harmonic oscillator obtained from an undoubled method. The approximate physical variables follow the exact ones accurately. However energy seems not to be exactly conserved but closely oscillates near conservation. Approximate energy gets more accurate when the order of the grids in the elements is increased. This conclusion holds also for very low damping scenarios. The next section will present the solutions of the discrete damped harmonic oscillator.

3.2.6. Discussion of the Results for the Underdamped and Overdamped Solution

Section 3.2.6 shows different types of solutions depending on the physical constants. Different under-damped and overdamped solutions have been inspected for different time domains, initial conditions, physical constants, polynomial orders and amount of elements in the domain. Since they show similar behaviour a representative case will be discussed that shows the behaviour of the different solutions of the approximate forms. Afterwards the convergence of these solutions over an increasing element density and higher polynomial degree - i.e. larger solution space - is researched.

The solutions of the underdamped setting are shown in Fig. 3.10. The initial and final time between which the solution is shown are $t_i = 0$ and $t_f = 30$. The initial conditions are chosen as $x^0 = x^{(0)}(0) = 1$ and $\pi^0 = \pi^{(0)}(0) = 1$. Furthermore the stiffness constant of the spring is selected as $k = 1$, the damping coefficient is $\lambda = 0.2$ and the oscillating mass is $m = 1$. This makes the situation underdamped since: $\frac{\lambda^2}{mk} = 0.04 < 4$. The grid is divided in $K_{el} = 15$ uniform elements such that a 1-cell $\Delta t = 2$. The solution space, in each element, is chosen in the first exterior bundle and span a $4 - th$ order polynomial vector space. Both the exact (red colored: ●) and approximated (blue colored: ●) solutions are displayed in Fig. 3.10 and due to close overlay a small portion is zoomed in to distinguish between them.

It is directly visible, in Fig. 3.10 that the approximate solution closely follows the exact solution. As expected due to dissipation the mass approaches its equilibrium position, $x = 0$, and zero velocity, $\dot{x} = 0$, as time progresses in Fig. 3.10 (a) and (b). The oscillating behaviour is characterizing for the underdamped solution because the spring keeps its oscillating motion because of the low damping compared to the spring stiffness. The same holds for the pseudo-forms, momentum and force, which go gradually to zero as seen in Fig. 3.10 (c) and (d). This is explained by the decrease in energy of the system that in the limit goes to zero as the solution in Fig. 3.10 (e) shows. The ripples visible in the energy plot in Fig. 3.10 (e) are not due to instability or errors in the analytical or numerical solution but are expected as is shown in experiments in [53]. In contrast to a harmonic oscillator without damping where position to momentum is a perfect circle, the underdamping causes the circle to spiral smoothly to the origin where momentum is zero and the position moves to the spring equilibrium point as can be seen in Fig. 3.10 (f).

The L^2-norm errors of position, momentum and energy are shown in Fig. 3.11. As explained in Section 2.8 the theory of convergence of this error states that with an increasing order of the approximation polynomials, in the linear log plot this gives a straight line. This behaviour is visible in Fig. 3.11 (a), (b) and (c). Furthermore the logarithm of the error by theory also decrease linearly when the logarithm of the amount of elements, in which the domain is divided, increases. This can be somewhat but not perfectly observed in the results in Fig. 3.11 (d), (e) and (f). It must be noted that the higher the order of the approximation polynomials is, the closer this behaviour is followed. This can be explained by the fact that underdamped solutions are highly oscillating and require higher order polynomials or more elements to follow this convergence behaviour. When higher order polynomials are used within each element, this trend is more closely followed. Also at the higher end of the elements the linearity becomes visible. We say that the asymptotic limit is reached earlier for higher order grids and higher mesh refinement . As will be presented later this issue "unclean" linearity does fade way earlier in the overdamped case.
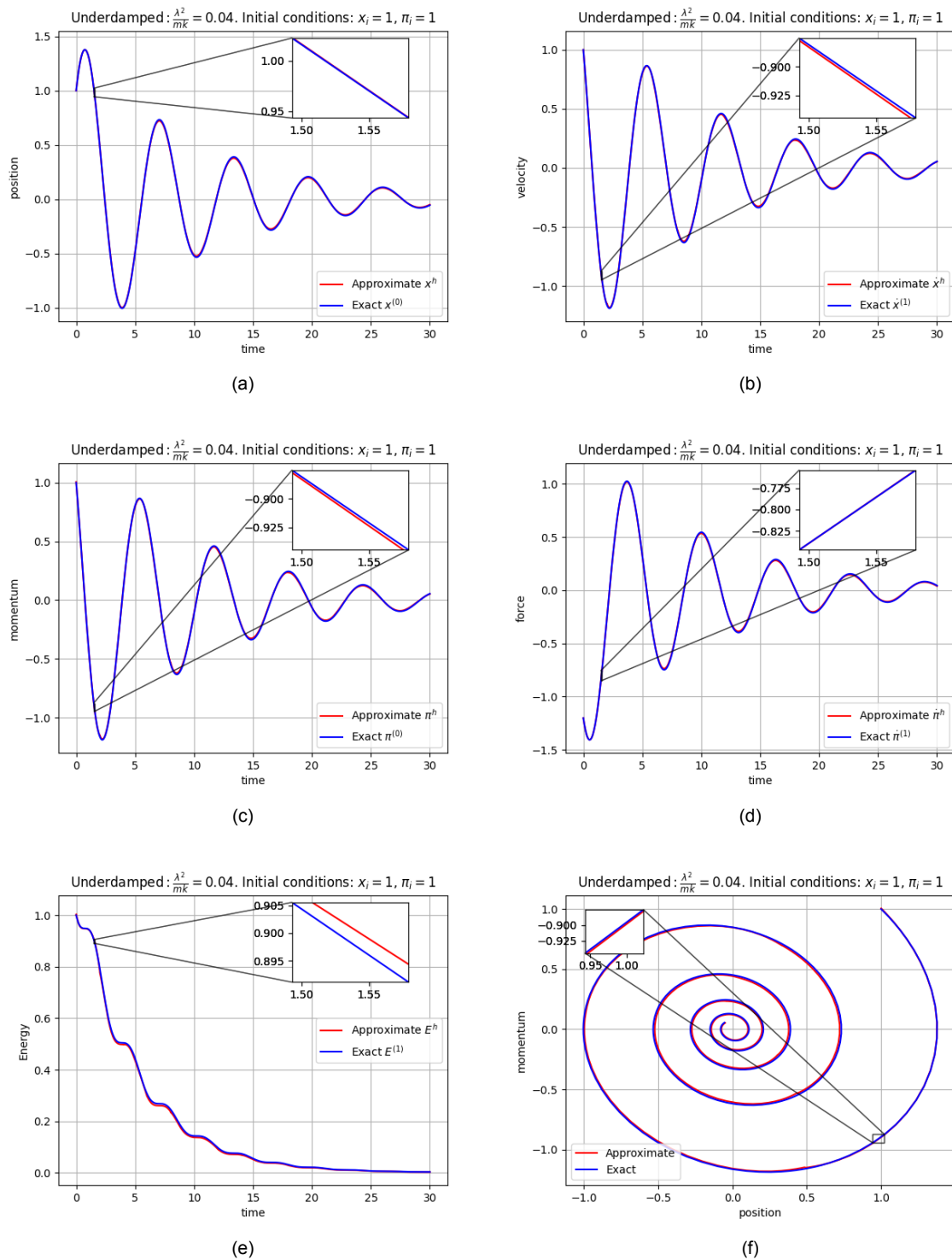
Figure 3.10: Comparison between the exact and double degrees of freedom mimetic solution of the: **(a)** Evolution of position of an underdamped oscillator with time **(b)** velocity of momentum of an underdamped oscillator with time **(c)** Evolution of momentum of an underdamped oscillator with time **(d)** Evolution of force of an underdamped oscillator with time **(e)** Evolution of energy of an underdamped oscillator with time **(f)** Relation of momentum to position of an underdamped oscillator.
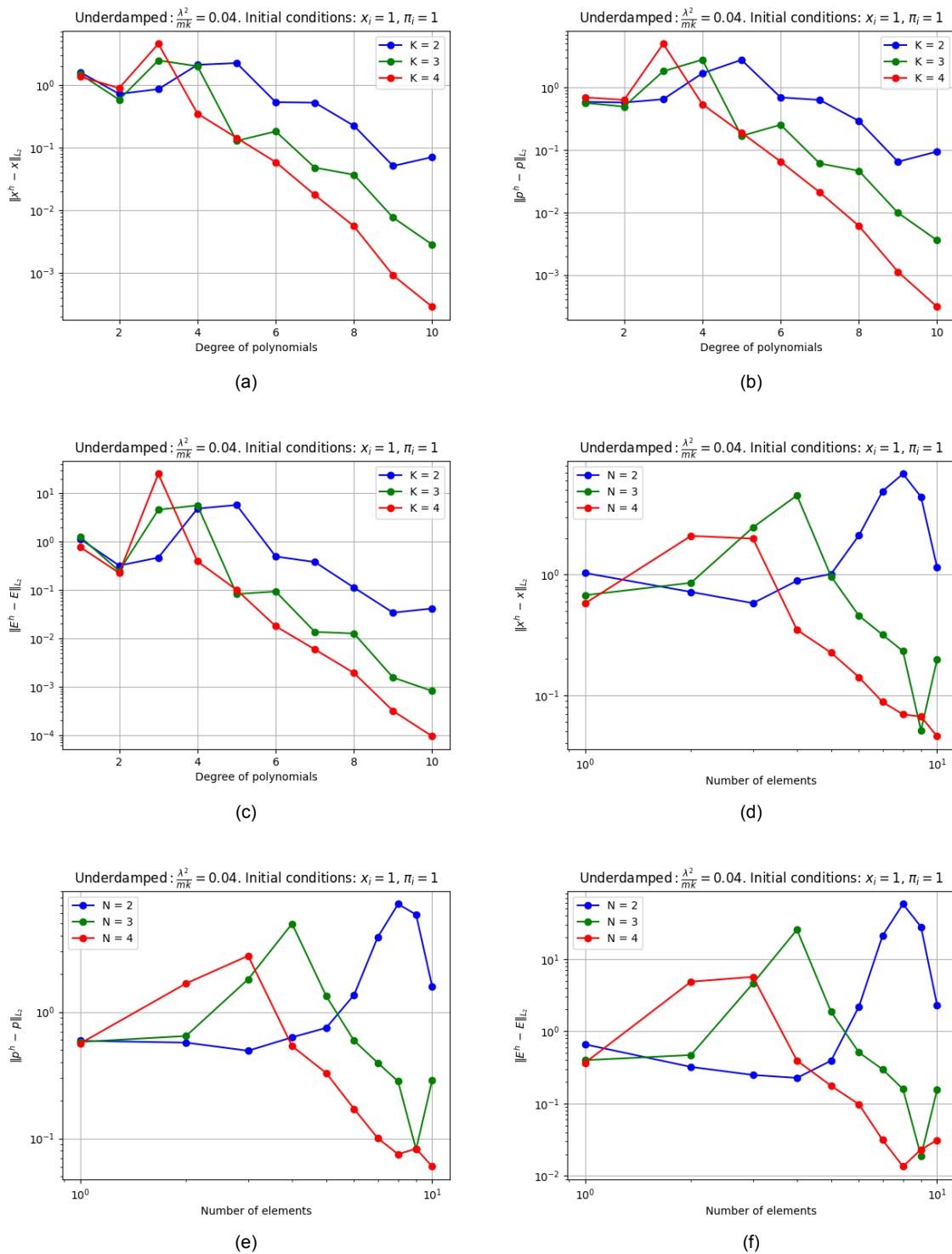
Figure 3.11: Convergence of the error of an underdamped oscillator: **(a)** with respect to position with increasing polynomial order **(b)** with respect to momentum with increasing polynomial order **(c)** with respect to energy with increasing polynomial order **(d)** with respect to position with increasing polynomial order **(e)** with respect to momentum with increasing polynomial order **(f)** with respect to energy with increasing polynomial order.

Figure 3.12: Comparison between the exact and double degrees of freedom mimetic solution of the: **(a)** Evolution of position of an overdamped oscillator with time **(b)** velocity of momentum of an overdamped oscillator with time **(c)** Evolution of momentum of an overdamped oscillator with time **(d)** Evolution of force of an overdamped oscillator with time **(e)** Evolution of energy of an overdamped oscillator with time **(f)** Relation of momentum to position of an overdamped oscillator.
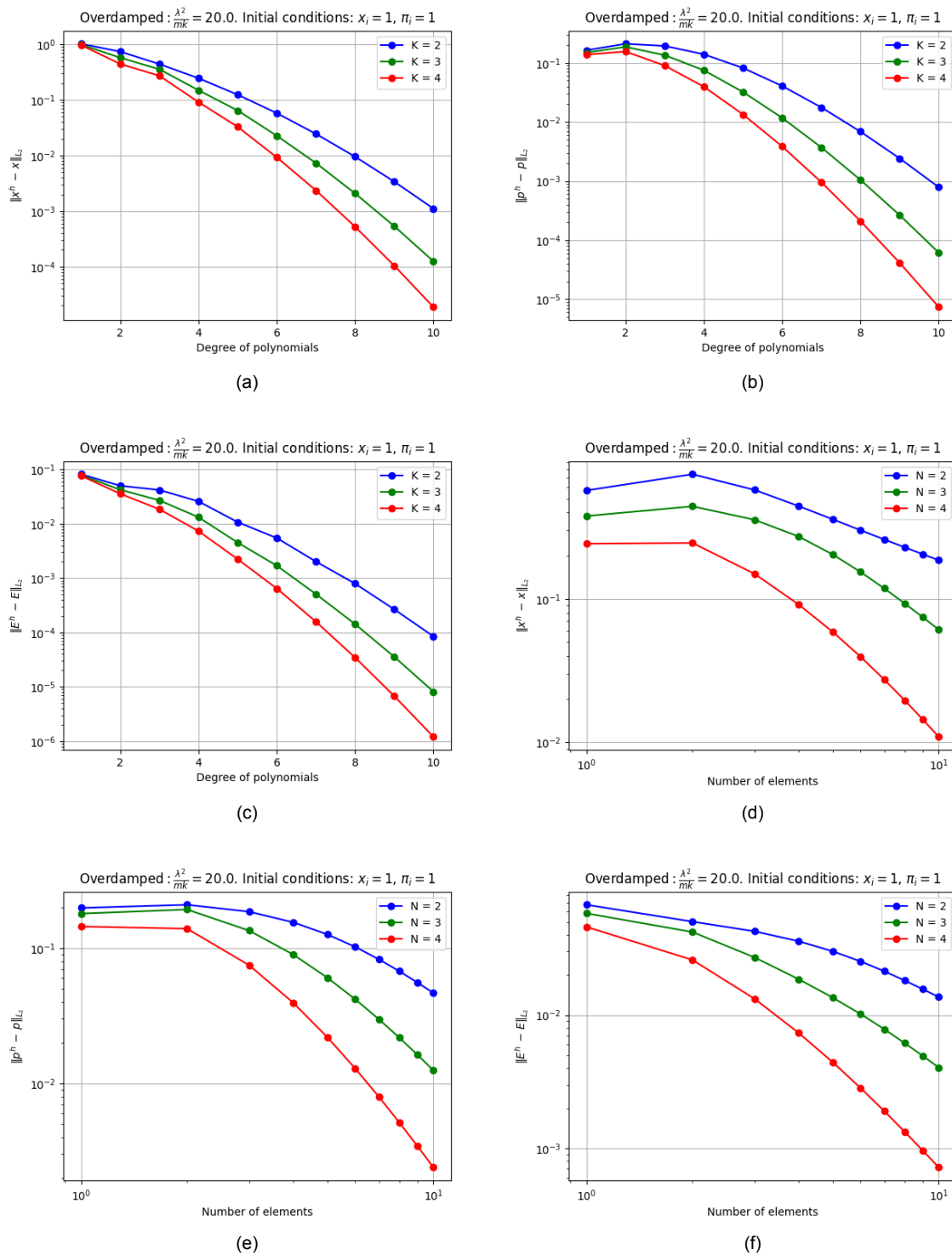
Figure 3.13: Convergence of the error of an overdamped oscillator: **(a)** with respect to position with increasing polynomial order **(b)** with respect to momentum with increasing polynomial ord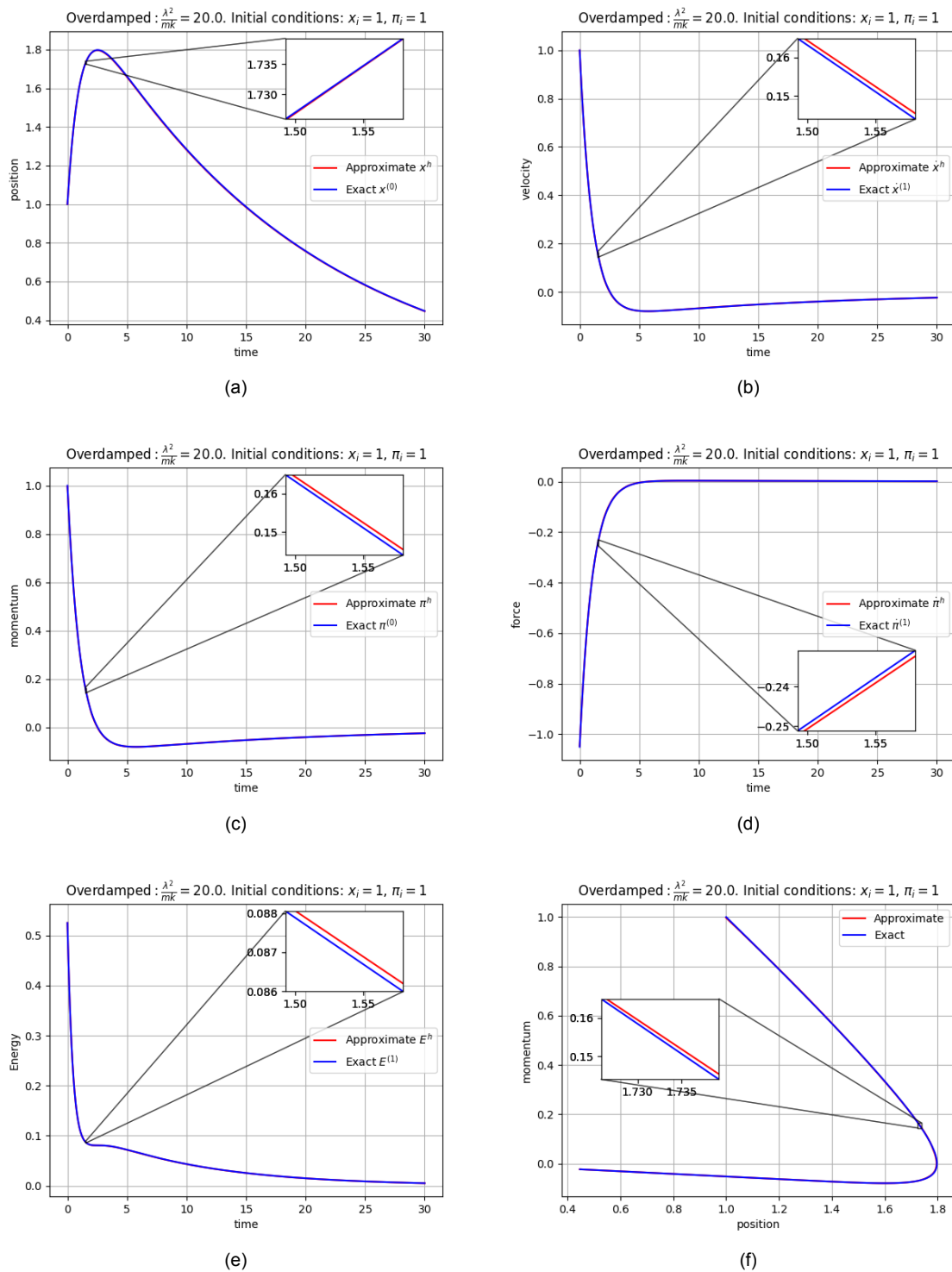er **(c)** with respect to energy with increasing polynomial order **(d)** with respect to position with increasing elements **(e)** with respect to momentum with increasing polynomial elements **(f)** with respect to energy with increasing polynomial elements.

Again but for an overdamped setting Fig. 3.12 shows that the approximate solution closely follows the exact solution. As expected due to dissipation the mass approaches its equilibrium position, $x = 0$, and zero velocity, $\dot{x} = 0$, as time progresses in Fig. 3.12 (a) and (b). However no oscillating behaviour occurs due to the high damping such the spring does not exert enough force to oscillate the mass. The same holds for the pseudo-forms, momentum and force, which approach zero as is shown in Fig. 3.12 (c) and (d). This approach of the equilibrium position is similarly explained by the decrease in energy of the system as the solution in Fig. 3.12 (e) shows. No ripples appear in the energy plot in Fig. 3.12 (e) since there are no oscillations. The position to momentum plot in Fig. 3.12 (f) is again no perfect circle but evolves to the equilibrium position with zero momentum.

The L^2-norm errors of position, momentum and energy are shown in Fig. 3.13. Here the theory of error convergence in section (2.8) is clearly visible. The logarithm of error is linearly decreasing when the the order of approximating polynomials increases as Fig. 3.11 (a), (b) and (c) shows. The logarithm of the error follows theory by decreasing linearly when the logarithm of amount of elements, in which the domain is divided, increases. In contrast to the underdamped case this is now clearly visible in Fig. 3.11 (d), (e) and (f) way earlier. This might be explained by the fact the overdamping solution have no oscillating behaviour.

3.3. Analysis of the Error Convergence with Δt Mesh Refinement

The L^2-norm error of both the overdamped and underdamped cases, in Fig. 3.13 (a), (b), (c) and Fig. 3.11 (a), (b), (c) respectively, clearly shows convergence with increasing the GLL-grid order. This is expected from theory. This error convergence holds also for Δt-refinement, i.e. increasing the number of elements in the time period, in the approximate overdamped solution as seen in Fig. 3.13 (d), (e) and (f). This is however not totally clear from the the error plots of the underdamped solution in Fig. 3.11 (d), (e) and (f). There we can observe fluttering which can be explained by the fact the the asymptotic limit is not reached yet for the underdamped solution.

In Fig. 3.14 the asymptotic limit of the error convergence plots with increasing elements is shown for the underdamped and overdamped solutions. The plots show the H^1-norm error of the position ϵ_x, the L^2-norm error of momentum, ϵ_π, and the L^2-norm error of energy ϵ_E. The definition of these errors is given in Section 2.8.2. The integration is performed on a fine GLL-grid using a 21 abscissas of a Gauss-Lobatto quadrature as described in Section 2.4.1. The plots in the figure are under initial position $x_i = 1$ and initial velocity $\pi_i = 1$. The material constants are mass $m = 1$, spring stiffness $k = 1$ and damping constant $\lambda = 0.2$ for the underdamped solution while $k = 0.2$ and $\lambda = 1$ for the overdamped solution. The convergence due to Δt-refinement is shown for second, third and fourth order GLL-gird. It becomes directly clear now that besides the overdemaped case, Fig. 3.14 (d), (e), (f), the underdamped case, Fig. 3.14 (a), (b), (c), is also convergent. The asymptotic limit is established at a higher element resolution where the the straight and decreasing line can be seen. There is however an unusual occurrence in the convergence of energy of only the underdamped oscillator. For second and fourth order GLL-grids the solution shows the expected behaviour. The third order however where a wiggle is observed where asymptotic limit is expected to be. This happens also for fifth order GLL-grids which raises the idea that this might be a behaviour of underdamped solutions when approximated with Lagrange basis polynomials of uneven order. Increasing the amount of integration abscesses to for instance 31 or doubling the amount of elements does not change this behaviour.

The slopes of the plots in the asymptotic limits in Fig. 3.14 should have some relation to the order of Lagrange polynomials in the GLL-points. The corresponding theory is presented in Section 2.8.2. Its application to the errors here means that convergence rate $l = -s \geq N$, where s is the slope of the convergence plots in logarithmic scale and N is the order of the GLL-grids used. The convergence rates in the asymptotic regime are calculated and shown in Table 3.1 for the underdamped solution and in Table 3.2 for the overdamped solution. We can observe that in general the convergence for underdamping and overdamping is almost exactly equal to $(N - 1)$ with the exeption of a two cases where it is a little larger. A convergence rate this is a little larger than $(N - 1)$ is observerd in second order GLL grids and for underdamped solution only. Secondly, the momentum convergence rate of the overdamped solution is also a little larger than $(N - 1)$. This determines that the rate of convergence is here $l \geq (N - 1)$ which deviates from the theory in Section 2.8.2 that states $l \geq N$. At the moment there is no clear explanation for this behaviour.
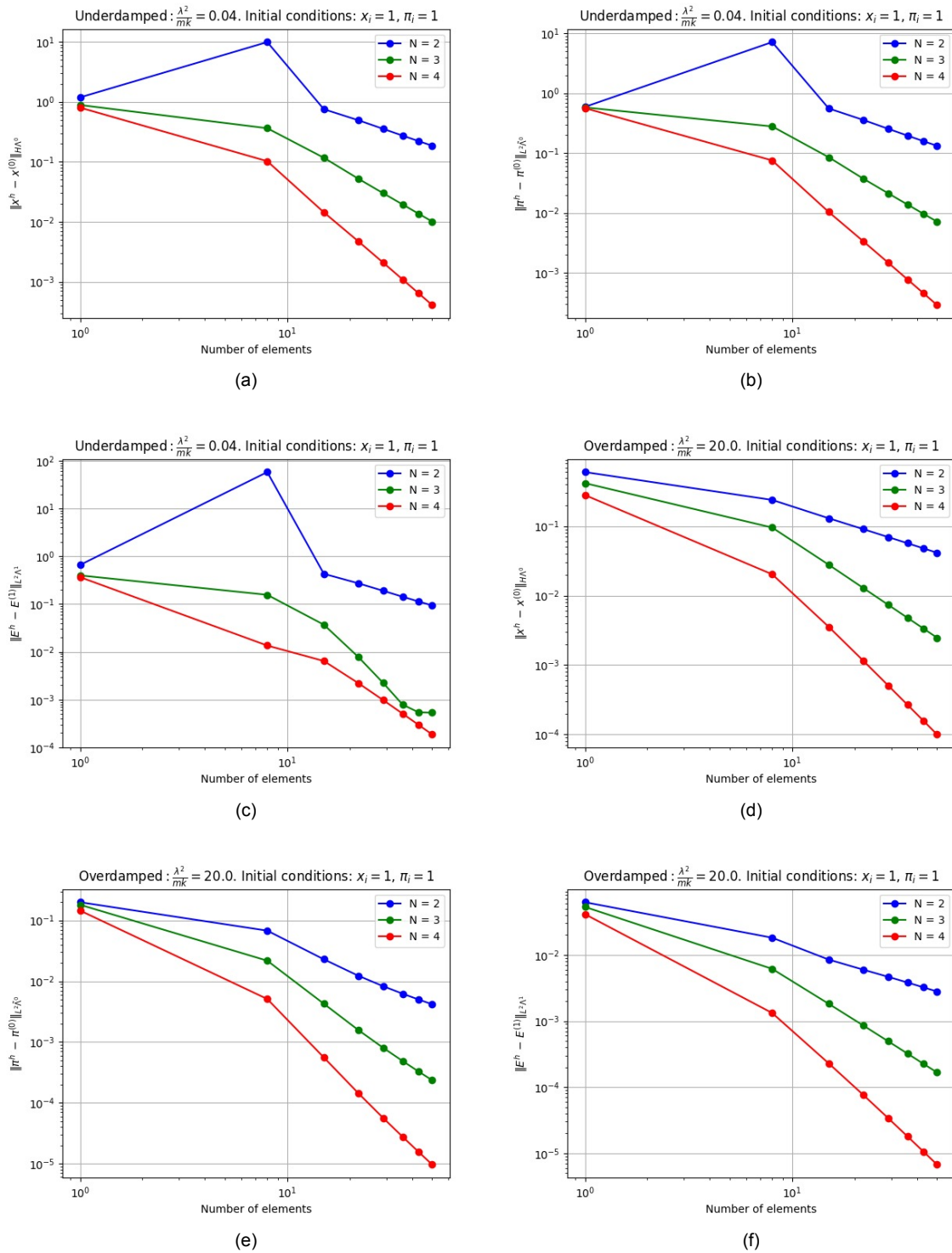
Figure 3.14: Convergence of the mimicking error of the damped harmonic oscillator with increasing elements (Δt-refinement): **(a)** for the underdamped position **(b)** for the underdamped momentum **(c)** for the underdamped energy **(d)** for the overdamped position **(e)** for the overdamped momentum **(f)** for the overdamped energy.

Underdamped Oscillator		
Variable	GLL-order	Rate of Convergence
	4	2.995
Position x^h	3	1.997
	2	1.179
	4	3.003
Momentum π^h	3	2.005
	2	1.196
	4	3.057
Energy E^h	3	undetermined
	2	1.282

Table 3.1: Δt-refinement error convergence of the approximate underdamped solutions of position, momentum and energy compared to the order of the GLL-grids in the elements.

Overdamped Oscillator		
Variable	GLL-order	Rate of Convergence
	4	2.994
Position x^h	3	2.01
	2	0.962
	4	3.208
Momentum π^h	3	2.216
	2	1.217
	4	2.985
Energy E^h	3	2.004
	2	0.952

Table 3.2: Δt-refinement error convergence of the approximate overdamped solutions of position, momentum and energy compared to the order of the GLL-grids in the elements.

3.4. Dissipation of the Energy

To test whether the law of energy conservation is satisfied in the mimetic solution we can check whether the energy change of the system is equal to the dissipated energy given in Section 2.9.

First we take the Hodge of energy which is:

$$\star E^{(1)}(t) = \tilde{E}^{(0)} = \frac{1}{2m}\pi^{(0)}(t) \wedge \pi^{(0)}(t) + \frac{k}{2}x^{(0)}(t) \wedge x^{(0)}(t)$$

Taking the exterior derivative of this gives the one form:

$$d\tilde{E}^{(0)}(t) = \frac{1}{m}\dot{\pi}^{(1)}(t) \wedge \pi^{(0)}(t) + k\dot{x}^{(1)} \wedge x^{(0)}(t)$$

As shown in (2.20) the projection and exterior derivative commute which gives the equation bellow that allows later for expressing the projection of the exterior of the outer energy.

$$d \circ \tilde{E}^h(t) = d \circ \pi_h \circ \tilde{E}^{(0)}(t) = \pi_h \circ d \circ \tilde{E}^{(0)}(t)$$

Expanding this expression in its constituent in polynomial and coefficient arrays and relating some co-chains with their co-boundaries using the incidence matrix gives:

$$d\tilde{E}^h(t) = \frac{1}{m}\boldsymbol{\pi}^{(0)T}\tilde{\mathbf{h}}^T(t)\tilde{\mathbf{e}}(t)\mathbb{E}_d^{1,0}\boldsymbol{\pi}_{ext}^{(0)}dt + k\mathbf{x}^{(0)T}\mathbf{h}^T(t)\mathbf{e}(t)\mathbb{E}_p^{1,0}\mathbf{x}^{(0)}dt$$

Integration of the outer energy over the domain gives the change in energy of the system over the period T below:

$$\Delta_T\tilde{E}_{sys}^h = \int_T d\tilde{E}^h(t) = \frac{1}{m}\boldsymbol{\pi}^{(0)T}\mathbb{M}^{(\tilde{0})(\tilde{1})}\mathbb{E}_d^{1,0}\boldsymbol{\pi}_{ext}^{(0)} + k\mathbf{x}^{(0)T}\mathbb{M}^{(0)(1)}\mathbb{E}_p^{1,0}\mathbf{x}^{(0)}$$

The equation of energy dissipation in (2.73) can be rewritten in exterior calculus as is obtained in (3.1):

$$d\tilde{E}^{(0)}(t) = -\frac{\lambda}{m}\dot{x}^{(1)}(t) \wedge \pi^{(0)}(t)$$

Applying the same procedure as before with respect to commutation of the exterior derivative and the projection gives:

$$d\tilde{E}^h(t) = -\frac{\lambda}{m}\dot{\mathbf{x}}^{(1)T}\mathbf{e}^T(t)\tilde{\mathbf{h}}(t)\boldsymbol{\pi}^{(0)}dt$$

Now integrating the previous equation and applying the fact that dual polynomial vectors are bi-orthogonal, as introduced in chapter (2.5) gives the dissipated energy over the period T. Notice there is some rearrangement and the 0-co-chain of location is related to 1-co-chain of velocity through the incidence matrix.

$$\Delta_T\tilde{E}_{dis}^h = -\frac{\lambda}{m}\boldsymbol{\pi}^{(0)T}\mathbb{E}_p^{1,0}\mathbf{x}^{(0)}$$

As mentioned for the law of energy conservation to hold the energy change of the system and the dissipated energy must be equal to each other. This gives the energy test equation below that is ideally zero when we have energy conservation:

$$\tilde{E}_{test}^h = \Delta_T\tilde{E}_{sys}^h - \Delta_T\tilde{E}_{dis}^h \xrightarrow{\text{Energy Conservation}} 0$$

Writing $\tilde{E}^h_{test}$ out gives:

$$\tilde{E}^h_{test} = \frac{1}{m}\boldsymbol{\pi}^{(0)T}\mathbb{M}^{(\tilde{0})(\tilde{1})}\mathbb{E}^{1,0}_d\boldsymbol{\pi}^{(0)}_{ext} + \left(k\mathbf{x}^{(0)T}\mathbb{M}^{(0)(1)} + \frac{\lambda}{m}\boldsymbol{\pi}^{(0)T}\right)\mathbb{E}^{1,0}_p\mathbf{x}^{(0)}$$

Using this with (3.22) and (3.3) obtained earlier this can be rewritten after some rearrangement as:

$$\tilde{E}^h_{test} = \mathbf{x}^{(0)T}\left(k\mathbb{M}^{(0)(1)}\mathbb{E}^{1,0}_p - k(\mathbb{E}^{1,0}_p)^T\mathbb{M}^{(1)}\mathbb{M}^{(\tilde{0})(\tilde{1})}\mathbb{M}^{(0)} + \lambda(\mathbb{E}^{1,0}_p)^T\mathbb{M}^{(1)}\mathbb{E}^{1,0}_p - \lambda(\mathbb{E}^{1,0}_p)^T\mathbb{M}^{(1)}\mathbb{M}^{(\tilde{0})(\tilde{1})}\mathbb{M}^{(0)(1)}\mathbb{E}^{1,0}_p\right)\mathbf{x}^{(0)}$$

We can use the primal to dual polynomial transformation rules in Section 2.5 to get that $\mathbb{M}^{(\tilde{0})(\tilde{1})} = (\mathbb{M}^{(1)})^{-1}\mathbb{M}^{(0)(1)}(\mathbb{M}^{(0)})^{-1}$ and implement this in the second term to get rid of the Lagrange and edge mass matrices. Afterwards we use the obtained fact that $\mathbb{M}^{(0)(1)}\mathbb{E}^{1,0}_p$ is symmetric which makes the first two terms eliminate each other. Now this equation can be written as:

$$\tilde{E}^h_{test} = \mathbf{x}^{(0)T}\left(\lambda(\mathbb{E}^{1,0}_p)^T\mathbb{M}^{(1)}\left(\mathbb{I} - \mathbb{M}^{(\tilde{0})(\tilde{1})}\mathbb{M}^{(0)(1)}\right)\mathbb{E}^{1,0}_p\right)\mathbf{x}^{(0)}$$

This means that the physical law of energy conservation is only fulfilled in the discrete setting when (3.24) below holds. Notice here that the transformation rules inn chapter (2.5.3) are used again.

$$\overline{\mathbb{M}}^{(\tilde{0})(\tilde{1})}\overline{\mathbb{M}}^{(0)(1)} \xrightarrow{\text{Energy Conservation}} \mathbb{I} \tag{3.24}$$

Computing the value of this matrix numerically shows that it is equal to the identity matrix (with an error of 1e-10) up at least the 5th order as is shown in Table 3.3 below. Which means that we can conjecture that the law of energy conservation is exact in the mimetic method.

GLL-grid order	$\mathbb{M}^{(\tilde{0})(\tilde{1})}\mathbb{M}^{(0)(1)}=\mathbb{I}$
1	True
2	True
3	True
4	True
5	True

Table 3.3: Results of a numerical test which confirm that the dual mixed mass, $\mathbb{M}^{(\tilde{0})(\tilde{1})}$ matrix is the inverse of a primal mixed mass matrix, $\mathbb{M}^{(0)(1)}$, for different polynomial orders.

Besides the investigating the behaviour of energy conservation from a theoretical perspective numerical computations are performed to verify the result. First energy discrepancy, $\tilde{E}^h_{d,k}$, at an element k as the energy that is not conserved over the element normalized by the average energy of the system in the element. This can be written as below where K_{el} is the total amount of elements $\tilde{E}^h_{k-1}$ is the energy at the beginning of element k and $\tilde{E}^h_k$ at the end of it. Δt_k is the time length of element k which are chosen to be equitemporal.

$$\tilde{E}^h_{d,k} = \frac{1}{2}(\Delta_{\Delta t_k}\tilde{E}^h_{sys} - \Delta_{\Delta t_k}\tilde{E}^h_{dis})/(\tilde{E}^h_{k-1} + \tilde{E}^h_k) = \frac{1}{2}\tilde{E}^h_{test,k}/(\tilde{E}^h_{k-1} + \tilde{E}^h_k) \quad \forall k \in \{1, \ldots, K_{el}\}$$

The value of energy discrepancy over an element, which corresponds to a time increment over which this occurs, is plotted for the underdamped and overdamped case. This is done over a period of 50 for a 3-rd order GLL-grid with 300 elements, i.e. $\Delta t = 0.1\underline{6}$ per element. The physical constants are kept the same as in the previous section 3.2.6. The mimetic approximate (red colored: ●) and exact (blue colored: ●) energy discrepancy are displayed in Fig. 3.15 (a) for the underdamped case and (b) for the
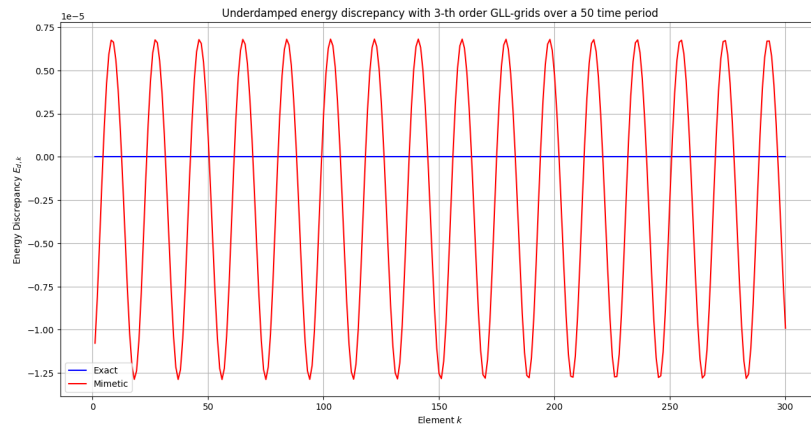
(a)
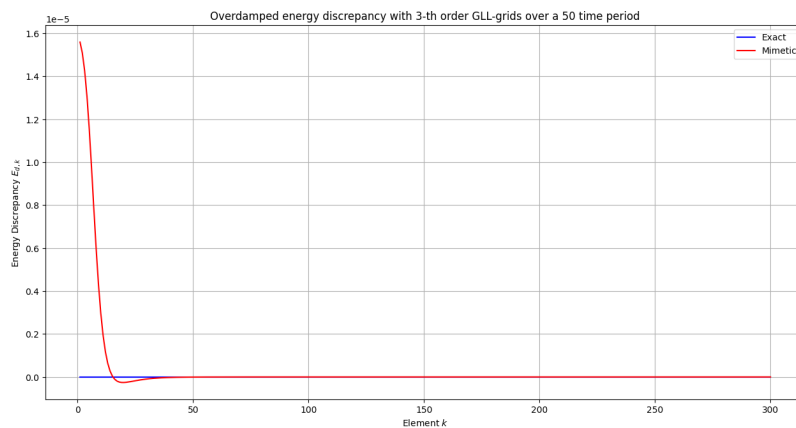
(b)

Figure 3.15: The energy conservation test in the case of the: **(a)** underdamped solution **(b)** overdamped solution.

overdamped case. As expected for the exact case there is no discrepenacy at any element for both the underdamped and overdamped case. The underdamped normalized energy discrepancy oscillates around a midline close to zero with an amplitude of about 0.001% of the system energy in an element. This means that a small amount of energy is lost and gained over the range elements. As for the overdamped case at the start there is some small energy discrepancy but this quickly goes to zero. From this it can be appreciated that the even though the numerical mimetic solution is is not exactly zero as the theoretical mimetic suggests but it still is close to zero and be treated a such within this tiny error.

To explain this smallish inexact behaviour of energy deviation we can look at the behaviour of energy of the system in Fig. 3.10 (e) and Fig. 3.12 (e). For the underdamped case of energy discrepancy in Fig. 3.15 (a) it can be observed that there are just under $15, 5$ cycles in a period of 50. So the time length of a cycle is about $3, 23$. As for the underdamped energy in the mimetic computation in Fig. 3.10 (e) we can observe 9 ripples in a period of 30 which again yields a close time period of about $3, 33$ per ripple. The deviation of the computation from theory might thus be attributed to the rippling behaviour of energy of the underdamped solution that somehow can not be accounted for in this computational solution. This observation is strengthened by that the fact that the deviation in the overdamped solution occurs just before the $15th$ element, i.e. around $t = 2, 5$. which is the time at which a small, and only, ripple occurs in the energy as can be seen in Fig. 3.12 (e).

4

Conclusions and Recommendations

The theory of mimetic spectral element methods (MSEMs) was presented in a pseudo-formal way that has an explanatory and practical style. This is followed by required insights from the formalism of Lagrangian mechanics, calculus of variations, and a priori error theory. The presented class of systems in the discussion is the holonomic (scleronomous) class which is widely applicable. When a system in this class is non-monogenic, the standard Lagrangian can not be used as the objective functional of the action. The action is useful since it contains all the information about the continuous system and is a natural reduction to the discrete analogue of the system. Investigation into the available literature showed that non-conservative phenomena in different branches of physics could be modeled by doubling their configuration states. Galley presents a systematized method for classical mechanics of non-monogenic systems by doubling their degrees of freedom. Stationary actions turn out to be compatible with the physics because of time symmetry. This time symmetric property is translated to monogeneity of the system, i.e. there is energy conservation up to an explicit time dependence of the Lagrangian on time. From this idea, one can construct a doubled system that is monogenic, even though the original physical system is open and non-monogenic. Two hurdles were observed in this method that made it incompatible with MSEM. Namely, the Lagrangian did not contain information on the initial conditions when reduction was applied through the action. Furthermore, the variations that are allowed by Galley's method are not completely arbitrary. The latter is problematic when the variations are chosen to be the algebraic dual polynomials of Gerritsma. To resolve this, the initial and final states of the doubled system were modified in this thesis such that the variations required for MSEM, were completely arbitrary even at the initial conditions. This induced a gauge transformation of the Lagrangian that produced the initial and final states when the action was carried out. The damped harmonic oscillator was used as a test case. A geometry for the damped harmonic oscillator compatible with Tonti's observations on physical systems was specified. Doubling this system and applying the variation to the modified action gave a solvable discrete system that is partially symmetric. When damping is removed, i.e. the conservative case, the numerical scheme reduces to the same one that can be obtained from the standard undoubled system. Two types of solutions that depend on the material constants of the damped harmonic oscillator that can be obtained analytically are the underdamped and overdamped solutions. The numerical solutions of the configuration and source variables for both cases obtained through the doubled MSEM are accurate and converging. The asymptotic limit of convergence is reached earlier for the overdamped solution than for the highly oscillating underdamped solution. For both cases, however, the convergence does not behave according to the expected theoretical rate but is one order less. One other anomaly is that even though the underdamped solution of energy converges, uneven order approximating polynomial grids give a wiggle in the convergence plot. Theoretical analysis of the approximation equations of energy obtained from doubling shows that it is exactly conserved over every time step. Computationally however, the energy oscillates very closely near the exact value, but it is still not exact. This behaviour of energy of not being exact where it theoretically seems to should be was observed in other research. There is no satisfactory explanation presented for these three computational deviations from theory. After this short summary of the results and observations of the research the main question is posed again and answered in:

Question: **"Can we find a systematic procedure to apply the mimetic spectral element method using algebraic dual polynomials to non-conservative systems such that energy conservation is exactly satisfied?"**

Answer: **"The modified doubling degree of freedom method can be used in MSEM and gives accurate and converging numerical results. Theoretically it should exactly conserve energy but the computational results show a minimal oscillation near the conservation value."**

Below is a list of recommendations and observations that require further investigation:

- The gauge term which is proven to be dependent on the non-conservative coupling source can thus become time dependent if there is a forcing term that is explicitly dependent on time. How does this translate in the modified method?

- The method is presented for a one dimensional case but can be extended to multiple dimensions. A next step is to apply it in two dimensions to test its compatibility with the tensor formulation of multidimensional algebraic dual polynomials.

- The mixed mass matrix identity shown in Section 3.4 is not theoretically proven but made plausible computationally. A theoretical proof needs to be presented.

- Even though theoretically it was shown that energy is exactly conserved, the computational results show a tiny discrepancy between the dissipation and lost mechanical energy. The reason behind this needs to be investigated.

- The reason behind deviation of the rate of error convergence with one order from the theoretical expectation needs to be looked into.

- The modified method was worked out for discrete Lagrangian systems. The next step is to work it out for the Lagrangian field theory. This can than be applied to simplified Navier-Stokes non-conservative viscous fluid flows.

References

[1] Gabriel Weinreich. "The Coupled Motions of Piano Strings". In: *Scientific American* 240.1 (1979), pp. 118–127.

[2] Enzo Tonti. "On the mathematical structure of a large class of physical theories". In: *Accademia Nazionale Dei Lincei, Estratto dai Rendiconti della Classe di Scienze fisische, matematische e naturali* 52.1 (1972), pp. 48–56.

[3] Josef Dodziuk. "Finite-Difference Approach to the Hodge Theory of Harmonic Forms". In: *American Journal of Mathematics* 98.1 (1973), pp. 79–104.

[4] James C. Scovel James M. Hyman. "Deriving Mimetic Difference Approximations to Differential Operators Using Algebraic Topology (Unpublished article)". In: *Los Alamos National Laboratoy, Center for Nonlinear Studies, Los Alamos, New Mexico, USA.* (1988).

[5] Alain Bossavit. "Computational electromagnetism and geometry: Building a finite-dimensional "Maxwell's house"(1): Network equations". In: *Journal of the Japan Society of Applied Electromagnetics* 7.2 (1999), pp. 150–159.

[6] Alain Bossavit Tim0 Tarhasaari Lauri Kettunen. "Some realizations of a discrete Hodge operator: A reinterpretation of finite element techniques". In: *IEEE TRANSACTIONS ON MAGNETICS* 35.3 (1999), pp. 1494–1497.

[7] Ragnar Winther Douglas N. Arnold Richard S. Falk. "Finite element exterior calculus, homological techniques, and applications". In: *Acta Numerica* 15 (2006), pp. 1–155.

[8] Marc Gerritsma Jasper Kreeft. "Mixed mimetic spectral element method for Stokes flow: A pointwise divergence-free solution". In: *Journal of Computational Physics* 240 (2013), pp. 284–309.

[9] Stanly Steinberg Nicolas Robidoux. "A Discrete Vector Calculus in Tensor Grids". In: *Computational Methods in Applied Mathematics* 1.1 (2001), pp. 1–44.

[10] Palha A. Gerritsma M. Jain V. Zhang Y. "Construction and application of algebraic dual polynomial representations for finite element methods on quadrilateral and hexahedral meshes". In: *Computers and Mathematics with Applications* 95 (2021), pp. 101–142.

[11] MI. Gerritsma D. Toshniwal RHM. Huijsmans. "A geometric approach towards momentum conservation. In M. Azaiez, H. El Fekih, JS. Hesthaven (Eds.), Spectral and High Order Methods for Partial Differential Equations". In: *Springer* 2 (2012), pp. 393–402.

[12] Varun Jain Marc Gerritsma Artur Palhaa et al. "Mimetic Spectral Element Method for Anisotropic Diffusion". In: *arXiv:1802.04597* (2018).

[13] Marc Gerritsma Artur Palhaa. "Mimetic spectral element method for Hamiltonian systems". In: *arXiv:1505.03422* (2015).

[14] Enzo Tonti. "Why starting from differential equations for computational physics?" In: *Journal of Computational Physics* 257 (2014), pp. 1260–1290.

[15] Theodore Frankel. *The geometry of physics : an introduction*. 3rd ed. Cambridge University Press, 2012.

[16] Steven H. Weintraub. *Differential Forms A Complement to Vector Calculus*. Academic Press, Inc., 1997.

[17] John M. Lee. *Introduction to Smooth Manifolds*. 2nd ed. Springer, 2013.

[18] James Raymond Munkres. *Topology*. 2nd ed. Prentice Hall, Inc., 2000.

[19] Dietmar A. Salamon Joel W. Robbin. *Introduction to Differential Geometry*. 1st ed. Springer Spektrum, 2022.

[20] David Bachman. *A Geometric Approach to Differential Forms*. 2nd ed. Birkhäuser, 2012.

[21] Serge Lang. *Real and Functional Analysis (Graduate Texts in Mathematics, 142)*. 3rd ed. Springer, 1993.

[22] D.A. Burton. "A primer on exterior differential calculus". In: *Journal of Theoretical and Applied Mechanics* 30.2 (2003), pp. 85–162.

[23] Enzo Tonti. *The Mathematical Structure of Classical and Relativistic Physics A General Classification Diagram*. Birkhäuser, 2013.

[24] Benjamin Szczesny. "De Rham's Theorem". In: *Australian Mathematical Sciences Institue, National Collaboration in the Mathematical Sciences* (2013).

[25] Patrick Greene. *De Rham Cohomology, Connections, and Characteristic Classes*. Aug. 2009.

[26] *Contractions, Yale University, Department of Mathematics*. Mar. 2012.

[27] James M. Hyman Pavel B. Bochev. "Principles of Mimetic Discretizations of Differential Operators". In: *Springer* 142.Compatible Spatial Discretizations (2006), pp. 89–119.

[28] Wolfgang Dahmen Kolja Brix Claudio Canuto. "Legendre-Gauss-Lobatto grids and associated nested dyadic grids". In: *Aachen Institute for Advanced Study in Computational Engineering Science* (2013).

[29] E. Babolian M.R. Eslahchi M. Masjed-Jamei. "On numerical improvement of Gauss–Lobatto quadrature rules". In: *Applied Mathematics and Computation* 164.3 (2005), pp. 707–717.

[30] I Stegun M Abramowitz. *Handbook of Mathematical Functions with Formulas, Graphs and Mathematical Tables*. 10th ed. National Bureau of Standard Applied Mathematics, 1972.

[31] M. Fortin D. Boffi F. Brezzi. *Mixed Finite Element Methods and Applications*. Springer, 2013.

[32] Leo C. Stein Char R. Galley David Tsang. "The principle of stationary nonconservative action for classical mechanics and field theories". In: *arXiv:1412.3082* (2014).

[33] John Safko Herbert Goldstein Charles Poole. *Classical Mechanics*. 3rd ed. Addison Wesley, 2001.

[34] Daniel Arovas. *Lecture Notes on Classical Mechanics, Department of Physics, University of California, San Diego*. 2013.

[35] Janet D. Finch Louis N. Hand. *Analytical Mechanics*. 1st ed. Cambridge University Press, 2001.

[36] David Morin. *Introduction to Classical Mechanics with Problems and Solutions*. 1st ed. Cambridge University Press, 2008.

[37] M. A. Tavel E. Noether. "Invariant Variational Problems". In: *Transport Theory and Statistical Mechanics* 1.3 (1971), pp. 183–207.

[38] Harry G. Kwatny Leon Y. Bahar. "Generalized Lagrangian and conservation law for the damped harmonic oscillator". In: *American Journal of Physics* 49 (1981), pp. 1062–1065.

[39] Eduardo Bayo Javier García de Jalón. *Kinematic and Dynamic Simulation of Multibody Systems*. 1st ed. Springer-Verlag, 1994.

[40] K. Schulten. *Notes on Quantum Mechanics*. CreateSpace Independent Publishing Platform, 2014.

[41] Herman Feshbach Philip M. Morse. *Methods of Theoretical Physics*. 1st ed. McGraw-Hill Book Company, Inc., 1953.

[42] Y. Yamanaka Y. Kuwahara Y. Nakamura. "From Classical Mechanics with Doubled Degrees of Freedom to Quantum Field Theory for Nonconservative System". In: *arXiv:1307.1235v2* (2013).

[43] Marcelo Janovitch B. Pereira. *Keldysh Field Theory*. Oct. 2019.

[44] Char R. Galley. "The classical mechanics of non-conservative systems". In: *arXiv:1210.2745* (2013).

[45] D. Hilbert R. Courant. *Methods of Mathematical Physics, Volume I*. WILEY☐VCH Verlag GmbH Co. KGaA, 1989.

[46] School of Mathematics University of Minnesota Peter J. Olver. *The Calculus of Variations*. 2021.

[47] Ricardo Cristoferi. *Calculus of Variations Lecture Notes*. May 2016.

[48] Taylor E. F. Gray C. G. "When action is not least". In: *American Journal of Physics* 75.5 (2007), pp. 434–458.

[49] JUHA KINNUNEN. *Sobolev Spaces*. 2023.

[50] JASPER KREEFT et al. "A PRIORI ERROR ESTIMATES FOR COMPATIBLE SPECTRAL DIS-CRETIZATION OF THE STOKES PROBLEM FOR ALL ADMISSIBLE BOUNDARY CONDITIONS". In: *arXiv:1206.2812* (2012).

[51] Ch. Schwab D. Schötzau. "Exponential Convergence for hp-Version and Spectral Finite Element Methods for Elliptic Problems in Polyhedra". In: *Seminar für Angewandte Mathematik Eidgenössische Technische Hochschule* 2014-38 (2014).

[52] Wessel Niek Weijers. *Energy-conserving spectral element schemes based on Lagrangian dynamics*. 2020.

[53] Tommaso Corridoni. "Damped mechanical oscillator: Experiment and detailed energy analysis". In: *The Physics Teacher* 52.3 (2014), p. 88.

A
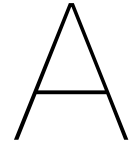
Analytical Solutions of the Damped Harmonic Oscillator

This appendix gives a detailed overview of the different solutions to the initial value problem of a damped harmonic oscillator and its integration constants.

A.1. Underdamped Solution

The velocity and acceleration of the mass are obtained through derivation in time and shown in equations (A.1) and (A.2) respectively. Inserting the initial conditions of location $x(0)$ and velocity $\dot{x}(0)$ in the general solution of location and its derivative yields the constants δ and X as is shown in equations (A.3) and (A.4).

$$\dot{x}(t) = -Xe^{-\beta t}\left(\beta cos(\omega_1 t - \delta) + \omega_1 sin(\omega_1 t - \delta)\right) \tag{A.1}$$

$$\ddot{x}(t) = -Xe^{-\beta t}\left((\beta^2 - \omega_1^2)cos(\omega_1 t - \delta) + 2\beta\omega_1 sin(\omega_1 t - \delta)\right) \tag{A.2}$$

$$tan(\delta) = \frac{\dot{x}(0) + \beta x(0)}{x(0)\omega_1} \tag{A.3}$$

$$X = \frac{x(0)}{cos(\delta)} \tag{A.4}$$

A.2. Critically damped Solution

The velocity and acceleration of the mass are obtained through derivation in time and shown in equations (A.5) and (A.6) respectively. Inserting the initial conditions of location $x(0)$ and velocity $\dot{x}(0)$ in the general solution of location and its derivative yields the constants X_1 and X_2 as is shown in equations (A.7) and (A.8).

$$\dot{x}(t) = e^{-\beta t}\left(X_2 - \beta(X_1 + X_2 t)\right) \tag{A.5}$$

$$\ddot{x}(t) = \beta e^{-\beta t}\left(\beta(X_1 + X_2 t) - X_2\right) \tag{A.6}$$

$$X_1 = x(0) \tag{A.7}$$

$$X_2 = \dot{x}(0) + \beta x(0) \tag{A.8}$$

A.3. Overdamped Solution

The velocity and acceleration of the mass are obtained through derivation in time and shown in equations (A.9) and (A.10) respectively. Inserting the initial conditions of location $x(0)$ and velocity $\dot{x}(0)$ in the general solution of location and its derivative yields the constants X_1 and X_2 as is shown in equations (A.11) and (A.12).

$$\dot{x}(t) = e^{-\beta t}\left(X_1(\omega_2 - \beta)e^{\omega_2 t} - X_2(\omega_2 + \beta)e^{-\omega_2 t}\right) \tag{A.9}$$

$$\ddot{x}(t) = \beta e^{-\beta t}\left(X_1(\omega_2 - \beta)^2 e^{\omega_2 t} + X_2(\omega_2 + \beta)^2 e^{-\omega_2 t}\right) \tag{A.10}$$

$$X_1 = \frac{\dot{x}(0) + \beta x(0)}{2\omega_2} + \frac{x(0)}{2} \tag{A.11}$$

$$X_2 = x(0) - X_1 \tag{A.12}$$

B

Lagrangian Mechanics and Energy of Doubled Degree of Freedom Systems

This section gives a discussion of the theory of Lagrangian mechanics for doubled systems of one degree of freedom physical systems. As briefly presented in the previous section these processes are applicable to multi degree of freedom physical systems. Furthermore it includes a discussion of energy and how it relates to the mimetic method.

First we write down the constituent terms of the total Lagrangian of the doubled system:

$$\Lambda' = L_{dc} + K + \frac{dG}{dt}$$

Here L_{dc} is defined as the conservative Lagrangian of the doubled system. That is kinetic energy minus potential energy that is derived from a scalar potential that is explicitly independent of time. Even though, the whole upcoming derivation for doubled systems could have worked with a (monogenic) generalized velocity potential in L_{dc} without any consequence to the formalism. This section however relies on this formulation of Lagrangians. To take velocity potentials of the physical system into account one can simply include the generalized forces from a velocity to the non-conservative ones. Obviously nothing than will change in the work presented in this section.

A conservative Lagrangian, as discussed in Section 2.6, can be written as as $L_c = T - U = T_0 + T_1 + T_2 - U_c$. For a holonomic system in the case of scleronomous constraints this reduces to $L_c = T_2 - U_c$. Here T_2 are quadratic homogeneous functions of generalized velocities. The conservative potential U_c depends only on generalized coordinates and not on their derivatives or time. The doubled conservative Lagrangian can than be written as below:

$$L_{dc} = L_c(\dot{x}_1, x_1) - L_c(\dot{x}_2, x_2) = T_2(\dot{x}_1) - U_c(x_1) - (T_2(\dot{x}_2) - U_c(x_2)) = T_2(\dot{x}_1) - T_2(\dot{x}_2) - (U_c(x_1) - U_c(x_2))$$

By the definition of a conservative Lagrangian of a system with the aforementioned scleronomous constraints we also know that:

$$L_{dc} = T_d(\dot{x}_1, \dot{x}_2) - U_{dc}(x_1, x_2)$$

This gives the kinetic energy, T_d, and conservative potential energy, U_{dc}, of the doubled system to be respectively as below:

$$T_d(\dot{x}_1, \dot{x}_2) = T_2(\dot{x}_1) - T_2(\dot{x}_2)$$

$$U_{dc}(x_1, x_2) = U_c(x_1) - U_c(x_2)$$

The second term, K, of the total monogenic Lagrangian, Λ', has the form of a generalized velocity potential that contributes to the total potential in the doubled system. In the physical limit with respect to the x_- Euler-Lagrange equation it generates the non-conservative forces (or also remaining monogenic forces as mentioned earlier) which was shown in the previous section 3.2.3. If we restrict it to this subclass of functions introduced in Section 2.6; i.e. functions that look like linear generalized velocity potentials, the potential contribution of K can than be written as below. Notice that this form of potentials is not merely academic but is also practical. It holds for instance for electromagnetic potentials [34, 33]. Also specifically for the coupling part of the potential, the source K, of the doubled damped harmonic oscillator has the same form. Notice that K is not on it self a generalized velocity potential but together with the other terms it forms a potential.

$$-K(\dot{x}_+, \dot{x}_-, x_+, x_-, t) = U_K = \overline{U}_{K,1}^+(x_+, x_-, t)\dot{x}_+ + \overline{U}_{K,1}^-(x_+, x_-, t)\dot{x}_- + U_{K,0}(x_+, x_-) = U_{K,1} + U_{K,0}$$

Next we analyse the contribution of the gauge term to the potentials in the total Lagrangian Λ'. This gives the gauge potential $U_G = -\frac{dG}{dt}$. The general formulation of the gauge term is $-\frac{d}{dt}(x_-\pi_+)$ where $\pi_+ = \frac{\partial \Lambda}{\partial \dot{x}_-}$ is the generalized momentum. It was shown in Section 2.7 that $\Lambda = L_{dc} + K = T_d - (U_{dc} + U_K)$. Since we declared for each term how it is a function of the degrees of freedom we get that:

$$\pi_+ = m\dot{x}_+ - \overline{U}_{k,1}^-$$

$$\dot{\pi}_+ = m\ddot{x}_+ - \dot{\overline{U}}_{k,1}^- = mf(\dot{x}_+, x_+) - \dot{\overline{U}}_{k,1}^-$$

Notice that $\ddot{x}_+$ can be obtained through the doubling procedure that gives the equation of motion through Euler-Lagrange which makes $\ddot{x}_+ = f(\dot{x}_+, x_+)$. This gives the formulation of the gauge potential to be:

$$U_G = m\dot{x}_+\dot{x}_- - \overline{U}_{k,1}^-\dot{x}_- - \dot{\overline{U}}_{k,1}^- x_- + mx_- f(\dot{x}_+, x_+)$$

Combining the above results gives a total Langrangian in terms of a doubled kinetic energy and doubled potential that has the:

$$\Lambda' = T_d - U_{dc} - U_{K,1} - U_{K,0} - U_G = T_d - (U_{dc} + U_{K,1} + U_{K,0} + U_G) = T_d - U_d$$

With:

$$U_d = U_{dc} + U_{K,1} + U_{K,0} + U_G$$

As shown in Section 2.6 the mechanical energy E_{mech} is the sum of kinetic energy and potential energy. Which gives:

$$E_{d,mech} = T_d + U_d = T_d + U_{dc} + U_{K,1} + U_{K,0} + U_G$$

Also the energy function E_d is defined in Section 3.2.3. First in this case, i.e. scleronomous systems, E_d contains only the homogeneous quadratic derivatives of degree of freedoms parts of the kinetic energy; which is all of T_d. It is also proved in that section that the terms of the complete potential U_d that look like linear generalized velocity potentials, only contribute with their scalar potential part. So the contribution of the coupling source K to the energy function, or Hamiltonian, is $U_{K,0}$. The contribution E_G of the gauge term of the potential U_G to the energy function E is shown below:

$$E_G = -\dot{x}_+ \frac{\partial U_G}{\partial \dot{x}_+} - \dot{x}_- \frac{\partial U_G}{\partial \dot{x}_-} + U_G$$

This is summarized as $E_G = E_{G,K} + U_G$, where $E_{G,K}$ can expanded as below in terms of the coefficients of the coupling potential and equation of motion descriptor $f(\dot{x}_+, x_+)$:

$$E_{G,K} = 2m\dot{x}_+\dot{x}_- - \overline{U}_{K,1}^-\dot{x}_- - \dot{x}_-x_-\frac{\partial \dot{\overline{U}}_{k,1}^-}{\partial \dot{x}_-} - \dot{x}_+x_-\left(\frac{\partial \dot{\overline{U}}_{k,1}^-}{\partial \dot{x}_+} - m\frac{\partial f(\dot{x}_+, x_+)}{\partial \dot{x}_+}\right)$$

Now we have a complete formulation of the doubled energy function E_d, or doubled Hamiltonian H_d, of the doubled system as:

$$E_d = T_d + U_{K,0} + U_G + U_{G,K} = H_d$$

Relating it with the doubled mechanical energy gives the equation below. This means that mechanical energy in the doubled system is not necessarily equal to the Hamiltonian.

$$E_{d,mech} = E_d + U_{K,1} - U_{G,K}$$

It is also shown in Section 2.6 that for totally closed monogenic systems, as is for totally closed doubled degree of freedom systems considered, that $\frac{dE_d}{dt} = 0$. The complete doubled system is monogenic since its Lagrangian Λ' satisfies Euler-Lagrange which makes it's generalized forces $Q_{d,j} = 0$. Furthermore if we work with a totally closed system which means that no external forces are working on the system and thus the total Lagrangian is explicitly independent of time [36]. Applying this to the derivative of the energy function, treated in Section 2.6, gives the relation below:

$$\frac{dE_d}{dt} = x_-Q_- + x_+Q_+ - \frac{\partial \Lambda'}{\partial t} = x_- \cdot 0 + x_+ \cdot 0 + 0 = 0$$

This means that the energy function E_d (or say Hamiltonian H_d) is a conserved property in the doubled setting. This gives the change in doubled mechanical energy as:

$$\frac{dE_{d,mech}}{dt} = \frac{dU_{K,1}}{dt} - \frac{dU_{G,K}}{dt}$$

With respect to the mimetic method it can be shown that the doubled Energy, E_d, is point wise conserved in the approximate projection. If we write the conservation of E_d in the exterior calculus formalism we get that:

$$d\tilde{E}_d^{(0)} = 0$$

To check the conservation of its projection -mimetic approximation- ,$\tilde{E}_d^h = \pi^h \tilde{E}_d^{(0)}$, we apply the commutation property of the exterior derivative with the projection operator in (2.20) of Section 2.4.2 and get that the mimicked doubled energy is point wise conserved as is shown below:

$$d \circ \tilde{E}_d^h = d \circ \pi^h \circ \tilde{E}_d^{(0)} = \pi^h \circ d \circ \tilde{E}_d^{(0)} = \mathcal{I} \circ \mathcal{R}\,(0) = 0$$

- **Verification and Application to the Damped Harmonic Oscillator**

In this subsection an idea will be formed about the the Lagrangian and energy of the doubled system of the damped harmonic oscillator and how they relate to each other. The former theory will be applied and this application of it is then verified for consistency with the system. The complete theory is applicable since

the double damped harmonic oscillator is a totally closed holonomic scleronomous monogenic system which has a coupling source that looks like a (linear) generalized velocity potential.

The double conservative potential U_c and doubled kinetic energy are:

$$U_{dc} = U_c(x_1) - U_c(x_2) = \frac{1}{2}kx_1^2 - \frac{1}{2}kx_2^2 = kx_+x_-$$

$$T_d = T_2(\dot{x}_1) - T_2(\dot{x}_2) = \frac{1}{2}m\dot{x}_1^2 - \frac{1}{2}m\dot{x}_2^2 = m\dot{x}_+\dot{x}_-$$

The coupling part of the potential U_K is below :

$$U_K = -K = \lambda x_-\dot{x}_+$$

Which makes $\overline{U}_{K,1}^+ = \lambda x_-$, $\overline{U}_{K,1}^- = 0$, $U_{K,1} = \lambda x_-\dot{x}_+$ and $U_{K,0} = 0$. We have also from the equation of motion that the discriptor $f(\dot{x}_+, x_+) = \ddot{x} = -\frac{1}{m}(\lambda\dot{x}_+ + kx_+)$, which could also be obtained during the doubling process. Evaluating the required derivatives in U_G and $E_{G,K}$ gives the doubled Energy:

$$E_d = 2m\dot{x}_+\dot{x}_- + 2kx_+x_- = H_d = \frac{2}{m}\pi_+\pi_- + 2x_+x_-$$

Next we remember that the derivative of E_d, and of the doubled Hamiltonian H_d, with respect to time is zero according to the presented theory earlier. To verify the correctness of the theory we evaluate this below:

$$\frac{d}{dt}E_d = 2m\ddot{x}_+\dot{x}_- + 2kx_+\dot{x}_- + 2m\dot{x}_+\ddot{x}_- + 2k\dot{x}_+x_-$$

This can be written as below where used Morse and Feshbach's [41] equation of motion in (2.51) for the virtual motion of the doubled damped harmonic oscillator is used:

$$\frac{d}{dt}E_d = -2\lambda\dot{x}_+\dot{x}_- + 2m\dot{x}_+\ddot{x}_- + 2k\dot{x}_+x_- = 2\dot{x}_+(m\ddot{x}_- - \lambda\dot{x}_- + kx_-) = 2\dot{x}_+ \cdot 0 = 0$$

In this appendix a methodology for working in the doubled setting is presented. It is very general in its application because it is applicable to all the systems of the classical holonomic sclerenomous totally closed non-monogenic class as long as the coupling source in the doubled setting is looks like a linear generalized velocity potential equation.